國立成功大學
資訊工程學系
博士論文

在可移動式無線通訊網路中，行動管理、繞送與能源控制機制之研究

Researches on Mobility Management, Routing and Power Control Mechanisms in Mobile Wireless Communication Networks

研 究 生: 李冠榮
指導教授: 郭耀煌
洪盟峰

中華民國九十五年六月

國立成功大學

博士論文

在可移動式無線通訊網路中，行動管理、繞送與能源控制機制之研究

Researches on Mobility Management, Routing and Power Control Mechanisms in Mobile Wireless Communication Networks

研究生：李冠榮

本論文業經審查及口試合格特此證明

論文考試委員

	鄭憲宗
黃仁誠	沈瑞峰
楊竹星	陳俊良
曾黎明	郭耀煌

指導教授：郭耀煌 沈瑞峰

系(所)主管：李泰

中華民國九十五年六月二十日

Researches on Mobility Management, Routing and Power Control Mechanisms in Mobile Wireless Communication Networks

by

Kuan-Rong Lee

A dissertation submitted to the graduate division in partial fulfillment of the requirement for the degree of
DOCTOR OF PHILOSOPHY

National Cheng Kung University
Tainan, Taiwam, Republic of China

June 20, 2006

Approved by

_____	Shong-Jay Cheng
Ren-Hung Hwang	Song-Mao Song
Chin-Sing Yang	Jiann-Liang Chen
J. M. Tseng	Kuo, Jau-Hwang

Advisor: Kuo, Jau-Hwang, Song Mao Song

Chairman: Cheng

在可移動式無線通訊網路中，行動管理、繞送與能源控制機制之研究

李冠榮*　　郭耀煌**　　洪盟峰**

國立成功大學資訊工程研究所

中文摘要

基於可移動式無線通訊網路的特性，發展低成本、低功率及高品質的傳輸技術已成為重要的議題。這本論文提出了一些新穎的方法論及演算法，能有效的降低能源耗損以延長可移動式無線網路之生命週期。

首先，我們提出了一個分散式動態註冊區域管理機制，稱之為行動導向區域註冊(Mobility Oriented Regional Registration, MORR)。此機制可依據個別的移動者行為模式以制訂其最佳之註冊區域。此外，我們發展了移動行為分析模組用以分析移動行為特性。模擬結果顯示我們的機制比現有的動態區域管理機制能有效節省 3 到 15 個百分比的訊號成本。

其次，我們制訂隨意網路 (Ad Hoc Network) 的能源耗損模組並發展能源控制機制(Adaptive Power Control Mechanism, APCM)。此機制能依據個別無線節點推測出其最佳的傳輸能源階層，以降低隨意網路的能源耗損。分析結果顯示，此方法能有效節省百分之 32 的能源耗損，降低百分之 6 的封包遺失率，以及提升百分之 22 的能源使用率。

再者，我們研究探索環境式的感測網路 (Probing Environment Sensor Network) 機制，並制訂數學模組以分析其特性。此外，我們發展了一個探索範圍調整機制（Probing

Radius Adjusting Mechanism, PRAM)。此機制能降低探索環境式的感測網路之能源耗損並符合被要求之感測率。

最後，我們亦針對感測網路提出了能源比例繞送演算法 (Energy-Proportional Routing Algorithm, EPR)。此演算法可適用於任何網路拓樸架構並能有效的提升感測網路生命週期，在叢聚式網路架構尤為明顯。我們透過實驗分析及數學證明，此演算法能有效滿足三項特性：降低能源耗損、提升網路節點存活率，以及提升資料傳輸量。

*作者　　**指導教授

Researches on Mobility Management, Routing and Power Control Mechanisms in Mobile Wireless Communication Networks

Kuan-Rong Lee* **Yau-Hwang Kuo**** **Mong-Fong Horng****

Department of Computer Science and Information Engineering
National Cheng Kung University

Abstract

On the basis of the inherently characteristics of mobile wireless networks, to develop the low-cost, low-power and high-quality communication technologies are important issues. This dissertation proposes some novel methodologies and algorithms in order to achieve objectives of reducing power consumption and life time extension in mobile wireless networks.

First, we propose a novel distributed dynamic regional location management scheme, called MORR (Mobility Oriented Regional Registration), to improve the signaling traffic cost of a mobile node. This improvement is achieved by adjusting each mobile node's optimal regional domains according to its mobility behavior. We also develop new analytical models to formulate the movement behavior and mathematically evaluate their characteristics. Simulation results show that anywhere from 3 to 15 percent of the signaling cost can be saved by our scheme in comparison with the previous distributed dynamic location management schemes.

Second, we formulate the energy consumption in Ad hoc network and propose a novel power control mechanism, Adaptive Power Control Mechanism (APCM), to evaluate the optimal transmission power level in each wireless node in order to minimize the total energy consumption in Ad hoc network. The analyses show that up to 32 percent energy can be

conserved, packet loss rate is reduced by 6 percent and the utilization of energy is enhanced to 22 percent.

Third, we explore the operations of probing environment sensor networks and force to define some mathematical models to describe the operations. By these models, a probing radius adjusting mechanism “PRAM” has been provided to control the trade-off between energy efficiency, network scalability and sensing rate. PRAM can estimate the desirable probing range to minimize the energy consumption based on the premise that the required sensing rate and scalability of WSNs can be satisfied. Simulation results show PRAM can adjust exactly the value of probing range to satisfy the required sensing rate and extend substantially the life time of sensor networks.

Finally, this dissertation proposes an energy-proportional routing (EPR) algorithm, which effectively extends the lifetimes of sensor networks. The algorithm makes no specific assumption on network topology and hence is suitable for improving sensor networks with clustering. In addition to experiments, the mathematical proofs of lifetime extension by the proposed routing algorithm are given in accordance with three widely accepted criteria – total energy dissipation, the number of live nodes in each round and the throughput.

*Author **Advisor

誌　　謝

首先，感謝我的指導教授郭耀煌博士多年來的悉心指導，並提供良好的研究環境與設備。除了學術上的收穫之外，更該感謝的是郭教授在日常生活上給與的關心與鼓勵。在求學過程中，郭教授給予我相當多的學習機會與處理一般事務的訓練。此外亦感謝曾黎明教授、楊竹星教授、鄭憲宗教授、黃仁竑教授、陳俊良教授、洪盟峰教授等博士學位論文考試委員對本論文的費心審查及提出的寶貴意見。

其次，感謝我的父親李進業先生、母親陳玉鳳女士及兄姐從小到大對我的教養與栽培。由於他們任勞任怨的付出與照顧，使我能夠專心的求學。同時亦感謝家人對我的愛護。在我成長的過程中，他們總是時時刻刻關心我，給我最好的資助。

再來，感謝實驗室內所有曾經與我相處過的學長、同學、學妹與學弟。在這段一起研究討論的日子中，讓我收穫充實不少。

最後，謹以本論文及所有成果獻給神。我的一生一世都將在祂的祝福與保守下，願將所有的榮耀歸與神!

2006 年 6 月

李冠榮 謹致於
成功大學資訊系
智慧型系統暨媒體處理實驗室
(ISMP Lab.)

Table of Contents

Figure Listing

Table Listing

Chapter 1

Introduction

In recent years, we have seen a proliferation of wireless devices including cellular phones, pagers, laptops, and personal digital assistants PDAs. Advances in energy-efficient design and wireless technologies have enabled portable devices to support several important wireless applications, including real-time multimedia communication, medical applications, surveillance using micro-sensor networks [JL00, Bult96, AR99, MK97], and home networking applications. Furthermore, the demand for ubiquitous personal communications is driving the development of new networking techniques that accommodate mobile users who move throughout buildings, cities, or countries. The wireless communication networks are responsible for providing service to mobile users.

Wireless transport of multimedia data presents several challenges due to the real-time requirements of the applications and the low bandwidth and error-prone nature of the wireless channel. These applications of wireless channels are becoming increasingly important. The introduction of the 3rd generation (3G) mobile systems based on the Global System for Mobile Communications (GSM) standard (being developed under a project called the "Third_Generation Partnership Project" or 3GPP) will offer each user rates between 144 and 384 kbps [MW00], enough bandwidth to support real-time video in addition to audio and data services. It is predicted that after its inception, there will be over 50 million subscribers to 3G services. Video cellular phones will enhance personal communications, entertainment, and

web browsing. However, several technological barriers need to be overcome before wireless multimedia devices become commonplace. The hardware must support the high bit-rates, memory, and data transfers required for video processing in an energy-efficient manner so as not to drain the portable device's battery. The compression algorithms need to minimize compression artifacts, such as blocking found in discrete cosine transform (DCT) based coders and jerkiness associated with low frame rates. Finally, the channel coding algorithms need to reduce the raw channel bit error rate to an acceptable level.

While there is a need to produce high-quality video under the low bit-rate and high error constraints of the wireless channel, there is a tradeoff in how many bits are allocated to the video compression versus how many are allocated to the channel coding. The user wants to achieve the highest quality possible given a limited bandwidth and (possibly) high bit error rates. The challenge thus becomes how to make best use of the overhead bits so as to achieve the highest reconstructed video quality.

Mobile multimedia terminals must be able to compress video for transmission over the low-bandwidth, error-prone wireless channel such that the decoder obtains high-quality reconstructed video. The standard video compression algorithms (e.g. H.263 [BM98], MPEG [DL91]) use predictive coding (where the difference between the current frame and a previous frame is encoded) and variable-length code-words to obtain a large amount of compression. This makes the compressed video bit-stream sensitive to channel errors, as predictive coding causes errors in the reconstructed video to propagate in time to future frames of video, and the variable-length code-words cause the decoder to easily lose synchronization with the encoder in the presence of bit errors. This results in an unacceptably low quality of the reconstructed video. To make the compressed bit-stream more robust to channel errors, the MPEG-4 video compression standard incorporates several error resilience tools to enable detection, containment, and concealment of errors. These tools include resynchronization markers,

header extension codes, data partitioning, and reversible variable-length coding [RT98, YM95]. These techniques are effective when the bit error rate is less than about 10^{-3}. However, wireless channels can have much higher bit error rates. In this case, a link-layer protocol that adds channel coding or forward error correction (FEC) can be used to bring the aggregate bit error rate down to less than 10^{-3}. The research presented in this dissertation on wireless multimedia networks focuses on ways in which application-level information can be exploited to create a link-layer protocol that achieves better performance than a general-purpose protocol for this application.

Application-specific information can be incorporated into the link-layer protocol for a wireless video system to improve reconstructed video quality for a given bandwidth. This dissertation describes our research in designing a link-layer protocol that exploits the inherent structure of an MPEG-4 compressed bit-stream. This protocol uses unequal error protection to adjust the amount of protection to the level of importance of the corresponding bits [WM99, CH99]. This ensures that there are fewer errors in the important portions of the bit-stream. While an unequal error protection scheme that uses the same number of overhead bits as an equal error protection scheme actually leaves more errors in the channel decoded bit-stream, these errors are in less important portions of the video bit-stream. Therefore, an unequal error protection scheme will provide better application-perceived quality than an equal error protection scheme.

1.1 Mobility Management in Wireless Networks

In recent years, computer users have demanded increasing mobility, with traditional desktop computing giving way to new and innovative mobile computing solutions. Notebook computers, personal digital assistants, and palmtop devices have facilitated the ability to be mobile within wireless network environment. Even through the portable computers are small

and mobile, their usefulness are somewhat limited if the network services that users have come to relay on are unavailable. Wireless networking adds the final piece to the puzzle. With wireless networking, mobile users are free to move about without restriction. Typically, wireless networks can be classified into two categories: cellular networks, and ad hoc networks. A cellular network has a set of fixed base stations connected to a common backbone. The end host is mobile and accesses the network by establishing a wireless connection to the base station. An ad hoc network is different from the cellular environment since it has no fixed infrastructure. In an ad hoc network, any host can act as a router to relay packets.

Wireless networks pose new challenges in protocol design. For example, conventional bandwidth reservation and routing schemes such as RSVP and RIP can no longer be used in the wireless environment since some of the network elements are mobile.

In a cellular network, a mobile user will travel from one access point to another. Therefore, the last top connection between a mobile terminal and its local base station is often rerouted. This rerouting process is called a handoff. When a mobile user travels to a new cell, it is important that the network can provide an uninterrupted handoff for the active connection. In the case for an ad hoc network, the connectivity between neighboring nodes is very dynamic. This is due to the fact that all nodes are non-stationary. It is crucial for the routing protocol to adapt quickly to such a fast changing environment in order to reduce the amount of disruptions suffered by the link disconnections. In such an environment, it is also desirable to educe transmission overhead and power consumption because the bandwidth for a wireless channel is limited.

Typically, a mobile user’s traveling pattern is not totally random. By exploiting a mobile user’s non-random traveling pattern, it is possible to predict the future state of a network topology and thus provide a continuous access during period of topology changes.

This dissertation covers the topic of using mobility prediction to minimize service

disruptions in cellular and ad hoc networks. Mobility prediction is used to lower the number of handoffs that are dropped in cellular networks. For ad hoc networks, routing protocols are enhanced by mobility prediction to perform path reconstruction prior the topology changes.

Many recent papers deal with mobility prediction in cellular networks. The shadow cluster concept is introduced in [LAN 95]. It targets wireless ATM (Asynchronous Transfer Mode) networks [AC96]. It aims to enhance connection quality by reducing the number of dropped calls during handoffs. The shadow cluster concept builds on the "virtual connection tree" idea. The "shadow cluster", or the leaves for a virtual connection tree, consists of base stations in cells within a neighborhood location of where a mobile terminal's initiating connection setup is situated. The shadow cluster can be used to estimate future resource requirements and to perform call admission decisions in the cellular network.

The tracking scheme proposed in [LH99] uses a Gauss-Markov model to predict a mobile's future location for efficient paging. Based on the Gauss-Markov model, a mobile's future location is predicted based on the information gathered from the last report of location and velocity. Simulations were performed to determine the cost reduction in mobility management when prediction is used. Another scheme that uses prediction to locate a mobile in a cellular network is presented in [AGG96]. Statistical search theory is used in this approach by maintaining a history of prior known mobility patterns of users. Based on this prior information, a vector of probability mass functions concerning the likely location of a target station is first computed. These probability mass functions are then used as input to a search strategy that specifies the manner in which a mobile terminal is to be paged. An extension of RSVP [ZED93] for cellular networks is proposed in [AA97]. The proposed scheme uses mobility prediction to reserve bandwidth and it is based on the same framework presented in [AGG96]. In this scheme, each datum of mobility history information consists of a tuple whose elements include the identity of the mobile station, the last location visited, and

a timestamp indicating the time at which the current cell was entered. Based on the historical data, a prediction can be made on the most likely location of the mobile station. This knowledge can then be used for intelligent pre-allocation of resources. In [CS98], a similar method to predict a mobile user's movements in cellular networks is used to reserve bandwidth, but the amount of bandwidth to be reserved is dynamically adjusted according to the time-varying traffic pattern and the observed handoff dropping events. An adaptive algorithm for controlling the mobility estimation time window to prevent over-reserving bandwidth is also used.

Although there has been no previous work done on mobility prediction in ad hoc networks, some routing protocols that use geographical information provided by Global Positioning Systems (GPS) have been proposed. They include Location-Aided Routing (LAR) [KV98] and Distance Routing Effect Algorithm for Mobility (DREAM) [BCS98]. For both protocols, all nodes exchange their location information with each other. In LAR, the geographical information is used to selectively flood route-request messages in the destination node's direction. In DREAM, the location information of the destination node is used to decide the direction that data packets are flooded.

Also, there are several multicast routing protocols proposed for Ad hoc network. They can be classified into two groups, namely three based and mesh based. Three based protocols include ODMRP [GPL98] and CAMP [GM99]. Tree based protocols use a shared tree for data delivery in the entire group, while mesh based protocols use a collection of nodes or a "mesh" to forward packets. Tree based protocols are more scalable in networks with a large number of senders, but they are more prone to disruptions caused by mobility. Mesh based protocols are more robust to node mobility because of redundant routes. However, mesh based protocols generate more network traffic since data packets are partially flooded.

1.2 Ad hoc Networks

An “Ad hoc” network in the context is defined to be a network without a predetermined physical distribution, or logical topology, of the nodes. Multi-hop, ad hoc networking has been the focus of many recent research and development efforts. Wireless networks and multi-hop routing have application in military, commercial, and educational environments including wireless office LAN connections, home networks of devices, and sensor networks.

A number of routing protocols have been proposed to provide multi-hop communication in wireless ad hoc networks [CP99, JB99, EB94, VS99]. Traditionally these protocols are evaluated in terms of packet loss rates, routing message overhead, and route length [JD98, PT99, RE00]. Since ad hoc networks will often be deployed using battery-powered nodes, comparison and optimization of protocol energy consumption is also important (as suggested for future work by some researchers [PT99]). Since many ad hoc networks will often be deployed using battery-powered nodes, another important question is how limited energy resources affect system lifetime and overall performance in ad hoc networks. For scenarios such as sensor networks where power use maps directly to lifetime and utility, power is *the* important metric. To understand energy efficiency we examined existing ad hoc routing protocols using models of Lucent WaveLAN direct sequence spread spectrum radio with the IEEE 802.11 protocol with representative models of energy consumption [MH97] and radio propagation [JD98]. We first only consider energy cost due to packet transmission or reception. Such costs may also include energy dissipation in MAC-level retransmissions, RTS/CTS etc. We studied energy consumption of four ad hoc routing protocols (AODV, DSR, DSDV, and TORA) with a simple traffic model where a few nodes send data over a multi-hop path [YJ00]. With this energy model we found that on-demand protocols such as AODV and

DSR consume much less energy than a priori protocols such as DSDV. A priori protocols are constantly expending energy pre-computing routes, even though there is no traffic passing on these routes. In other words, on demand protocols, by their very nature, are efficient in the energy consumed by routing overhead packets. As a result, energy use is dominated by routing protocol overhead. In fact, the major source of extraneous energy consumption was from *overhearing*, as previously observed in PAMAS [SC98]. Radios have a relatively large broadcast range. All nodes in that range must receive each packet to determine if it is to be forwarded or received locally. Although most of these packets are immediately discarded, they consume energy with this simple energy model. This observation motivates approaches that avoid overhearing. The PAMAS protocol suggests a MAC-layer approach to minimize this cost [SM98]; TDMA protocols would also be applicable (for example [JJ00]). Actual Radios consume power not only when sending and receiving, but also when *listening* or *idle* (the radio electronics must be powered and decoding to detect the presence of an incoming packet). Research [MH97] and product specifications show that idle energy dissipation can not be ignored in comparing to sending and receiving energy dissipation. Stemm and Katz show idle:receive:send ratios are 1:1.05:1.4 by measurement, while Digitan 2 Mbps Wireless LAN module (IEEE 802.11/2Mbps) specification shows idle:receive:send ratios is 1:2:2.5. In either case, energy dissipation in idle state can not be ignored. With such energy model, all ad hoc routing protocols considered consume roughly the same amount of energy (within a few percent). In the scenario with modest traffic, idle time completely dominates system energy consumption.

In general, ad hoc routing protocols can be categorized into three categories. On-demand based, distance-vector based, and location based. Each approach has its own strengths and weaknesses. We will describe each one of them in the following paragraphs.

1. On-demand routing protocols: these protocols only maintain routes for source/destination

pairs that have data to send. They include Lightweight Mobile Routing (LMR) [CE95], Temporally-Ordered Routing Algorithm (TORA) [PC97], Dynamic Source Routing (DSR) [JM96], Associativity-Based Routing (ABR) [Toh97], and Ad Hoc On-Demand Distance Vector (AODV) [RP99]. In these schemes, the source node finds routes to the destination by flooding the entire network with "route-request" messages. Intermediate nodes upon receiving a non-duplicate route-request message forward it. Also intermediate nodes learn about the route back to the particular source via backward learning. The destination node, upon receiving the route-request message, sends a "route-reply" packet back to the resource. The major advantage of on-demand protocols is that no route is maintained by a source-destination pair that doesn't have data to send. However, using flooding to construct routes can generate a large amount of overhead when the number of sources that have data to send is high.

2. Distance-vector protocols: these protocols such as DSDV (Destination Sequence Distance Vector) [PB94], WRP (Wireless Routing Protocol) [MG96] and ZRP (Zone Routing Protocol) [Has97] generally require every node in the network to maintain routing table entire for al other hosts. In DSDV, a nodes' routing table is broadcasted periodically to its neighbors. In WRP, only entire in the routing table that reflects a path change is broadcasted. ZRP uses a hybrid approach of maintaining routing table entire for all destinations within a certain zone, while paths outside the defined area are updated in an on demand basis. For distance-vector protocols, the routing table update interval is crucial to their performance. If the interval is too large, the protocol can not react quickly to topology changes. If the interval is too large, the protocol can not react quickly to topology changes. If the interval is too small, the network is congested with routing table updates. Distance-vector protocols are more efficient when the number of active source-destination pairs in the network is large since less routing overhead is wasted.

However, for network that have relatively light traffic, distance-vector protocols generate large amount of routing overhead which is not being used efficiently.

1.3 Wireless Sensor Networks

Applications in wireless sensor networks (WSNs) typically require network components with average power consumption that is substantially lower than currently provided in implementations of existing wireless networks. Applications involving the monitoring and control of industrial equipment require exceptionally long battery life so that the existing maintenance schedules of the monitored equipment are not compromised. Other applications, such as environmental monitoring over large areas, may require a very large number of devices that make frequent battery replacement impractical. Also, certain applications can not employ a battery at all; network nodes in these applications must get their energy by mining or scavenging energy from the environment. An example of this type is the wireless automobile tire pressure sensor, for which it is desirable to obtain energy from the mechanical or thermal energy present in the tire instead of a battery that may need to be replaced before the tire does.

As shown in Fig. 1.1, different form the infrastructure wireless network frequently be using presently. In the wireless sensor networks, sensors can communicate with every sensor under their communicating range. The communication topology of wireless sensor network becomes more complicated than infrastructure wireless network. So, how to routing data in the network is one of thorny problem of sensor network issue. The other thorny problem is how to effective using energy. Because the battery of sensor is un-replaceable, the energy of every sensor is limited. To extend lifetime of single sensor or whole sensor network is a great challenge.

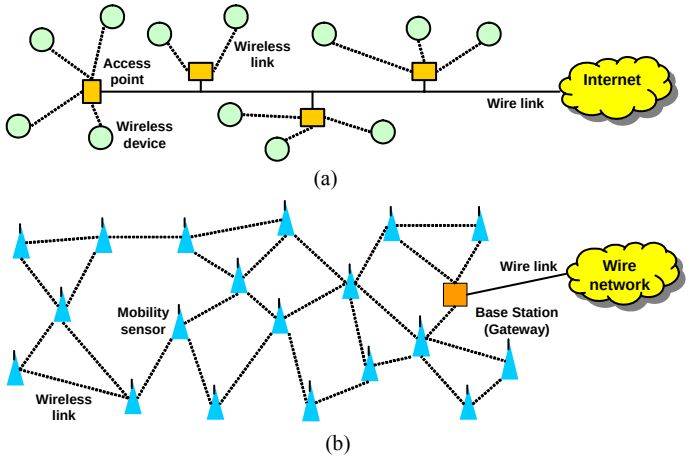

Figure 1.1. Difference between infrastructure wireless network and the sensor network. (a)The infrastructure wireless network; (b)The sensor network.

The wireless sensor network is a stretch of wireless ad hoc network (WANET) in the view of network form and data forwarding. But some characteristics are total different form MANET as following:

1. *Large scale*: In the MANET, it will be assumed that the number of network member should be tens or not greater than one hundred. However, many wireless sensor network applications involve large geographic domain such as vast deserts, oceans. The number required to cover the field can easily surpass thousand or even millions.
2. *Less hardware capability*: Sensor nodes usually have very limited computing, memory and energy resource. By this reason, they cannot perform complex operations. A large variety of them involves only simple processor, small memory and limited wireless communication capabilities. In contrast, nodes in MANETs are usually capable computers which have ample computing and memory resources and sustained power supplies.
3. *Data centric*: Unlike traditional networks, sensor nodes in wireless sensor networks may

not need a global identity (e.g., network address). Applications focus on the data generated by sensors. Data is named by attributes and applications request data matching certain attribute values. So, the communication primitive in this system is a request: Where are nodes whose temperatures recently exceeded 30 degrees? This approach decouples data from the sensor that produced it. This allows for more robust application design: even if sensor #27 dies, the data it generates can be cached in other (possibly neighboring) sensors for later retrieval.

4. *Application specific*: Traditional networks are designed to accommodate a wide variety of applications. We believe it is reasonable to assume that sensor networks can be tailored to the sensing task at hand. In particular, this means that intermediate nodes can perform application-specific data aggregation and caching, or informed forwarding of requests for data. This is in contrast to routers that facilitate node-to-node packet switching in traditional networks.

The above described features ensure a wide range of applications for sensor networks. Some of the applications areas are health, military and home… etc. For example:

1. *Environments sampling*: If the scientists want to get the information about a harsh environment such as the spheres beside earth or the volcanoes, them don't need to deep going to environment and risk their life to collect the data. They can drop a huge number of sensor nodes into the region they want to monitor. Then the sensor nodes will periodically sense information, generate data and forward data to a base station, which is located on a save place. The scientists will get all information them want thought the base station.
2. *Disaster prevention*: Put the sensor on everyone's body. Maybe the sensor is embedded in the watch or the waistband. It will do sensing some information, like body temperature, pulsation and respiratory rate. If any data it monitoring is unusual, it will send a warning

message to a health monitoring center, and indicate the location of this node. The health monitoring center will try to contact the owner of this sensor. If he has not responded, it will call the hospital, and dispatch the ambulance to rescue him.

3. *Object detection*: In the battlefield, a large number of sensor nodes are dropped on the enemy's territory form an airplane. Every sensor monitoring the activities around it. If the user wants to detect the tank, he sends a request to the sensor network. The sensor nodes, which had detected the tank, will response the related information. As shown in Fig. 1.2.

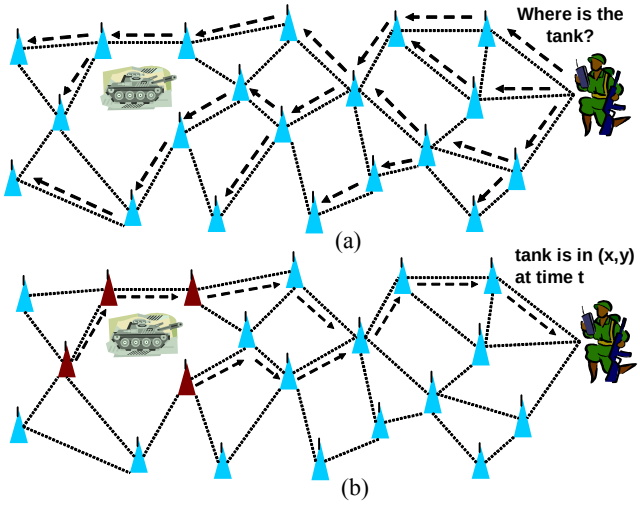

Figure 1.2 Military application of the sensor network. (a)Query the location of tank; (b) Sensors response data.

Communications in a wireless sensor network occur in different ways depending on the underlying application or mission of the network. In general, there are three types of communications: *clock-driven*, *event-driven* and *query-driven*.

1. *Clock-driven*: Clock-driven communication takes place where sensors gather and send data at constant periodic intervals. Such periodic transmission can be destined for a certain receiver or collector. Combining data from all sensors generates "snapshots" of the field that is being sensed. Over time these snapshots produce temporal and spatial

information about the field, e.g., acoustic, seismic, meteorological.

2. *Event-driven*: Event-driven communication is triggered by the certain event. The sensor after deployed is sensing some kind of data around it. If one of the data it monitoring occurred deviance, it sends the event message to the monitoring center.
3. *Query-driven*: Query-driven communication is triggered by the certain query. If the user of sensor network wants to acquire a specific data, e.g., where are the regions whose temperatures recently exceeded 40 degrees? The sensors whose temperatures recently exceeded 40 degrees will response their location to the user.

In order to meet the described requirement of the applications, a successful design of wireless sensor networks must have several unique features.

1. *Low Power Consumption*: Applications in wireless sensor networks typically require network components with average power consumption that is substantially lower than currently provided in implementations of existing wireless networks. Applications involving the monitoring and control of industrial equipment require exceptionally long battery life so that the existing maintenance schedules of the monitored equipment are not compromised. Other applications, such as environmental monitoring over large areas, may require a very large number of devices that make frequent battery replacement impractical. Also, certain applications can not employ a battery at all; network nodes in these applications must get their energy by mining or scavenging energy from the environment. An example of this type is the wireless automobile tire pressure sensor, for which it is desirable to obtain energy from the mechanical or thermal energy present in the tire instead of a battery that may need to be replaced before the tire does. In additional to average power consumption, primary power sources with limited average power sourcing capability often have limited peak power sourcing capabilities as well; this factor should also be considered in the system design.

2. *Low Cost*: Cost plays a fundamental role in applications adding wireless connectivity to inexpensive or disposable products, and for applications with a large number of nodes in the network. These potential applications require wireless links of low complexity that are low in cost relative to the total product cost. To meet the objective, the communication protocol and network design must avoid the need for high-cost components and minimize silicon area by minimizing protocol complexity and memory requirements. In additional, however, it should be recognized that one of the largest costs of many networks is administration and maintenance. To facilitate the volume production expected of such systems and devices, thereby minimizing the cost of the wireless network components, the development of a standardized communication protocol is necessary. Recently, the IEEE 802 Local Area Network/Metropolitan Area Network Standards Committee (LMSC) created Working Group 15 to develop a set of standards for WPANs. To address the need for low-power, low-cost wireless network, the IEEE network standards Committee officially sanctioned a network task group in Working Group 15 to being the development of a standard for Low-Rate WPANs (LR-WPANs), to be called 802.15.4. The goal of Task Group 4, as defined in its Project Authorization Request, was to provide a standard having ultra-low complexity, cost, and power for low-data-rate wireless connectivity among inexpensive, fixed, portable, and moving devices. Location awareness was considered a unique capability of the standard.
3. *Worldwide Availability*: Many of the proposed applications of wireless sensor network, such as wireless luggage tags and shipping container location systems, implicitly require that the network be capable of operation worldwide. Further, to maximize production, marketing, sales, and distribution efficiency of products that may have wireless sensor network devices embedded in them, and avoid the establishment of regional variants that must be individually monitored through (perhaps separate) distribution chains, it is

desirable to product devices capable of worldwide operation. Although, in theory, this capability may be obtained by employing Global Positioning System (GPS) or Global Navigation Satellite System (GLONASS) receivers in each network node and adjusting node behavior according to its location, the cost of adding a second receiver, plus the additional performance flexibility required to meet the varying worldwide requirements, makes this approach economically unviable. It is, therefore, desirable to employ a single band worldwide (one that has minimal variation in government regulatory requirements from country to country) to maximize the total available market for wireless sensor networks.

4. *Network Type*: A conventional star network employing a single master and one or more slave devices may satisfy many applications. Because the transmit power of the network devices is limited by battery life concerns, however, this network design limits the physical area a network may serve to the range of a single device (the master). When additional range is need, network types that support multi-hop routing (e.g. mesh or cluster types) must be employed; the additional memory and computational cost for routing tables or algorithms, in addition to network maintenance overhead, must be supported without excessive cost or power consumption. It should be recognized that for many applications, wireless sensor networks are of relatively large order; device density may also be high.

5. *Security*: The security of wireless sensor networks has two facets of equal importance: how secure the network actually is and how secure the network is perceived to be by users and potential users. The perception of security is important because users have a natural concern when their data is transmitted over the air for anyone to receive. The wireless application must work to regain that confidence to attain the lower costs. In many applications, encryption is not an important security goal of wireless networks.

Often, the most important security goals are to ensure that any message received has not been modified in any way. Wireless sensor networks have additional requirements, including the need for scalability to very large networks, fault tolerance, and the need to operate in a wide variety of possibly hostile environments.

6. *Data Throughput*: As already mentioned, wireless sensor networks have limited data throughput requirements when compared with Bluetooth (IEEE 802.15.1) and other WPANs and WLANs. For design purposes, the maximum desired data rate, when averaged over a one-hour period, may be set to be 512 bps. This low required amount of data throughput implies that with any practical amount of protocol overhead, the communications efficiency of the network will be very low. No matter what design is chosen, the efficiency will be very low, and the situation, therefore, may be viewed in a positive light: the protocol designer has the ability to design free of the consideration of communications efficiency, often a critical parameter in protocol design.
7. *Message Latency*: Wireless sensor networks have very liberal Quality of Service (QoS) requirements, because, in general, they do not support isochronous or synchronous communication, and have data throughput limitations that prohibit the transmission of real-time video and, in many applications, voice. The message latency requirement for wireless sensor networks is, therefore, very relaxed in comparison to that of other WPANs; in many applications, a latency of seconds or minutes is quite acceptable.
8. *Mobility*: Wireless sensor network applications, in general, do not require mobility. Because the network is therefore released from the burden of identifying open communication routes, wireless sensor networks suffer less control traffic overhead and may employ simpler routing methods than mobile ad hoc networks.

1.4 Background and Motivations

As compared with the local, fixed network, where all end-users and routers are static, a wireless communications system is extremely complex.

First, the wireless network requires an air interface between base stations and subscribes to provide communications under a wide range of propagation conditions and any possible user location. The wireless channels are inherently error-prone and their time-varying characteristics make it hard to consistently obtain good performance. Communication protocols must be designed to adapt to current conditions instead of being designed for worst-case conditions.

Second, the network topology may be non-administrated and variable. Such as mobile ad hoc networks (MANETs) and wireless sensor networks (WSNs), the networks should be capable of self-configuration and self-maintenance. “Self-configuration” is defined to be the ability of network nodes to detect the presence of other nodes and to organize into a structured, functioning network without human intervention. “Self-maintenance” is defined to be the ability of the network to detect, and recover from, faults appearing in either network nodes or communication links, again without human intervention.

Third, the power sourcing capabilities of these devices in wireless communication system often are more limited than in a tethered network environment. These restrictions require innovative communication techniques to increase the amount of bandwidth per user and innovative design techniques and protocols to use available energy efficiently.

Fourth, by the reason of computer users have demanded increasing mobility in wireless networks, many wireless mobile computing [DS91, RA93, JG93, BA93, GE94, CE02, GM94] have been extensively studied in recent years in both the computer and communication communities. However, most of the recent studies focus on the network layer

communication protocols and few of them on the mobility aspects caused by mobile user behavior. To make intelligent mobile-aware applications, it is important that a mobile terminal be more intelligent and can anticipate the change of the location of its user. On the other hand, service and resource mobility [GG95, AA94] introduce new requirements for mobility management. Mobility is an aspect of user behavior which impacts on wireless networks as well as on wired ones. The concepts of mobility management have been used in the cellular mobile networks for many years, but, it was primarily designed to support mobile voice communication. Traditionally, mobility management includes functions to passively keep track of the location of the users/terminals and to maintain connections to the terminals belonging to the system [SJ94, RS94]. How to adopt mobility management for efficiently supporting mobile computing is still an open question. Therefore, in order to meet the described requirement of the applications, there are some important challenges in the design of wireless and mobile systems.

This dissertation focuses on these issues that:

1. To reduce the signal traffic cost in wireless mobile systems. Because computer users (or hosts) have demanded increasing mobility in wireless networks, it results in the more signal traffic cost will be expended in registration and handoff. How to reduce this signal cost is the important issue in wireless mobile system.
2. To minimize the energy consumption in Ad hoc system. The popular medium access control technique in Ad hoc system is Carrier Sense Multiple Access (CSMA) protocols. These protocols suffer from both the hidden and exposed terminal problems to reduce channel capacity and increase more power consumption in retransmission. Therefore, it is important issue to control the transmission power level in each wireless node in order to achieve objectives of reducing power consumption and life time extension in an ad hoc network.

3. To extend the lifetime of the whole wireless sensor network. Some power control techniques and routing protocols were proposed to reduce the energy consumption in wireless sensor network. It is important subject to improve these techniques and protocols in order to minimize the energy consumption and extend the lifetime of wireless sensor network.

1.5 Contributions of Dissertation

The main contributions in this dissertation are:

1. A novel distributed dynamic regional location management scheme called MORR (Mobility Oriented Regional Registration) is proposed for Mobile IP to improve the signaling traffic cost of a mobile node. This improvement is achieved by adjusting each mobile node's optimal regional domains according to its mobility behavior. With Mobile IP, the capricious mobility and variable traffic load of a mobile node has an impact on its average signaling traffic cost. In this paper, the mobility of all mobile nodes is classified into two modes: random mobility mode and regular mobility mode. We develop new analytical models to formulate the movement behavior and mathematically evaluate their characteristics when applied to these two modes. MORR has the adaptability to manipulate various mobility modes of each mobile node in dedicated ways to determine an optimal regional domain of this mobile node. Simulation results show that anywhere from 3 to 15 percent of the signaling cost is saved by MORR in comparison with the previous distributed dynamic location management schemes for various scenarios.
2. This dissertation investigates the energy consumption of ad hoc networks and presents the optimal transmission power level in each wireless node in order to achieve objectives of quality of service (QoS) and life time extension in an ad hoc network. In general, the energy consumption in an ad hoc network is affected by three factors: the physical

property of wireless nodes, the topology of network and the interference degree in each message transmission. This thesis formulates the energy consumption in terms of these factors and performs experiments in various scenarios for proving effectiveness of these formulations. According to these formulae, we propose a novel power control mechanism, *Adaptive Power Control Mechanism* (APCM), to evaluate the optimal transmission power level in each wireless node in order to minimize the total energy consumption that satisfy the quality of service requirement in ad hoc networks. The analyses show that up to 32 percent energy can be conserved, packet loss rate is reduced by 6 percent and the utilization of energy is enhanced to 22 percent.

3. We explore the operations of probing environment sensor networks and force to define some mathematical models to describe the operations. By these models, a probing radius adjusting mechanism "PRAM" has been provided to control the trade-off between energy efficiency, network scalability and sensing rate. PRAM can estimate the desirable probing range to minimize the energy consumption based on the premise that the required sensing rate and scalability of WSNs can be satisfied. Simulation results show PRAM can adjust exactly the value of probing range to satisfy the required sensing rate and extend substantially the life time of sensor networks.
4. This dissertation proposes an energy-proportional routing (EPR) algorithm, which effectively extends the lifetimes of sensor networks. The algorithm makes no specific assumption on network topology and hence is suitable for improving sensor networks with clustering. To optimally utilize energy, light-load units -- nodes or clusters that conserve energy are ideal candidates as intermediate units for forwarding data from others. To balance the load, first, the proposed algorithm predicts energy consumption of each node in each round. Then the algorithm controls the energy consumption of each unit as close as possible to the threshold representing the energy utilization mean value among clusters.

Finally the algorithm checks satisfaction of the energy constraints in terms of distances and predicted data amounts. The proposed algorithm performs routing by determining whether a cluster head or a node should either undertake forwarding tasks or transmit data to intermediate hops. In this way, energy dissipation is evenly distributed to all units and the lifetime of the whole wireless sensor network is ultimately extended. The algorithm applies hierarchically to different levels of network topology. In addition to experiments, the mathematical proofs of lifetime extension by the proposed routing algorithm are given in accordance with three widely accepted criteria – total energy dissipation, the number of live nodes in each round and the throughput (data amount per round).

1.6 Organization of Dissertation

The content of this dissertation is partitioned into six chapters and is organized as follows. In Chapter 1, the overview of mobile wireless networks is introduced. Then, we describe the characteristics of mobile wireless networks including mobile management, ad hoc network and sensor network. Furthermore, the background, motivations and contributions of this dissertation are also mentioned. In Chapter 2, a novel distributed dynamic regional location management scheme is proposed. Furthermore, the modeling of mobile node mobility and the signaling cost analysis are presented. Chapter 3 investigates the energy consumption of ad hoc networks and propose a novel power control mechanism to evaluate the optimal transmission power level in each wireless node in order to minimize the total energy consumption that satisfy the quality of service requirement in ad hoc networks. In Chapter 4, we explore the operations of probing environment sensor networks and force to define some mathematical models to describe the operations. Furthermore, we also provide a probing radius adjusting mechanism to control the trade-off between energy efficiency,

network scalability and sensing rate. Chapter 5 proposes an energy-proportional routing (EPR) algorithm, which effectively extends the lifetimes of sensor networks. Finally, we give some conclusions in Chapter 6.

Chapter 2

Mobility Oriented Regional Registration (MORR)

Mobile IP [CE02] applies a connection reestablishment algorithm to solve the connection problem caused by host mobility on the Internet. This protocol is a simple and scalable global mobility solution, but it has a considerable setup cost for mobile communication. Several regional registration algorithms [EA02, RT01, AA98, SA00], therefore, have been proposed to avoid a large hand-off overhead by reducing the frequency of home registration and the cost of regional registration. Unfortunately, these algorithms still have some drawbacks in common. Firstly, the regional domains are decided in advance by administrators and fixed throughout the connection, so the domains cannot fully match the mobility ranges of all mobile nodes. Thus, when a mobile node hovers around the boundary between regional domains, the task of home registration is frequently invoked. Secondly, because the packets delivered to mobile nodes are routed by the foreign agent hierarchies in the visited domains, the hold cost on this hop-by-hop basis increases rapidly, and the hierarchy is sensitive to foreign agent failure. Moreover, controversial issues arise on how the foreign agent is supposed to be aware of which Gateway Foreign Agent (GFA) is to deal with its registrations [Niko03]. Thirdly, while a fixed GFA is required to function as an endpoint for all tunnels established with the home agents of mobile nodes roaming in a regional domain, a traffic bottleneck will inevitably occur on the GFA.

Some distributed dynamic regional location management schemes [XI02, WY03] have

been proposed to improve the system performance by overcoming these drawbacks. In these schemes, each foreign agent can function either as a foreign agent or a GFA depending on each mobile node. Thus, the traffic load in a regional network is evenly distributed to each foreign agent. Furthermore, in these dynamic systems, the regional domain boundary is flexible, i.e. it is able to adjust the number of foreign agents under a GFA for each mobile node. Therefore, a mobile node is able to decide when to perform a home location update according to its varying location and packet arrival pattern.

In this chapter, we propose a novel distributed dynamic location management scheme, called MORR. This scheme compels each mobile node to execute its location registration with its own "*Optimal Regional Domain*" (*ORD*) at all times. The *ORD* of a mobile node is dynamically adjusted according to its current mobility, and each *ORD* is organized by its *"optimal domain"* and *"optimal GFA"*. For a mobile node, the *optimal domain* of a GFA is formed by the foreign agents under this GFA in which this mobile node will have the minimum total signaling cost. The optimal GFA is one in which the mobile node moving within the *optimal domain* of this GFA has minimum signaling cost. Therefore, when a mobile node executes its regional registration in its *ORD*, the total signaling cost can be minimized.

Due to the great variation in the mobility behavior of each mobile node, it is difficult to formulate a strategy for all mobile nodes' mobility. In modeling practical movements of mobile nodes, Liu *et al.* [GY95] proposed using two modes: *Random Mobility* (RM) mode and *reGular Mobility* (GM) mode. The RM mode is based on the assumption that a mobile node randomly decides its irregular moving course, whereas the GM mode is based on the assumption that the movements of each mobile node are in accordance with its historical movement patterns. Both Liu *et. al* [GL95] and Chan *et. al.* [JA99] predicted the future locations of mobile nodes based on their historical patterns. In this paper, we formulate the

mobile node mobility and mathematically evaluate its characteristics for these two modes. According to these analytical models, MORR determines the *ORD* of this mobile node.

2.1. Modeling of Mobile Node Mobility and Signaling Cost Analysis

The mobility of a mobile node is measured by tracing both its movement and its speed. Tracing of movement is accomplished by identifying the change in mobile agents at which the mobile node arrives, and the speed of movement is defined by the duration of stay of the mobile node at these mobile agents. Data concerning the mobile agents visited and the duration of stay of the mobile node are recorded by this mobile node while it is active.

2.1.1 Network Model

The triangular graph model shown in Fig. 2.1 has been adopted here as the topological model for a mobile communication network in this paper; each hexagon and the dot in the center of each hexagon indicate the foreign agent domain and foreign agents respectively. Each foreign agent is placed in the vertices of the triangular grids and is assigned a two-dimensional coordinate according to the relative location of these foreign agents. The coordinates of a foreign agent must be filled in its advertisement extensions. While a mobile node is within a foreign agent domain, it will receive the foreign agent's advertised coordinates.

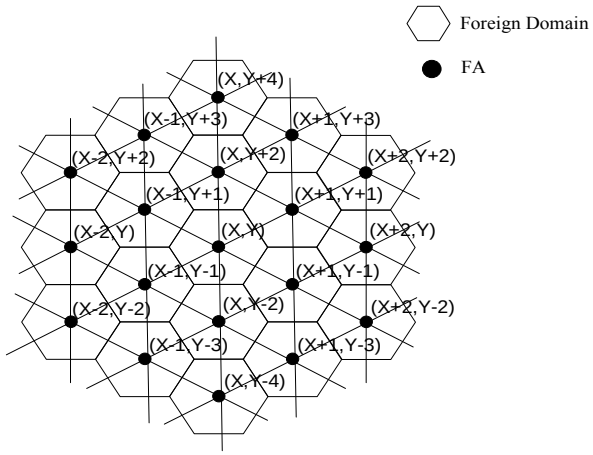

Figure 2.1. Network model and the relative coordinates of foreign agents.

Distance *D(u,v)* is defined by the number of links along the shortest path connecting foreign agents *u* and *v*. For instance, consider two foreign agents *u* and *v* with coordinates (x_u, y_u) and (x_v, y_v), respectively, where their distance *D(u,v)* is given by:

$$D(u,v) = \begin{cases} \dfrac{|x_u - x_v| + |y_u - y_v|}{2} & if\ |y_u - y_v| - |x_u - x_v| > 0, \\ |x_u - x_v| & otherwise. \end{cases} \tag{2-1}$$

2.1.2 Mobility Data Structures of a Mobile Node

There are 4 data structures stored at a mobile node as shown in Fig.2.2 in order to maintain its mobility characteristic values and to record movement patterns. These data structures include: *Mobility Behavior Table (MBT)*, *Movement Tracing Queue (MTQ)*, *Trace Pattern Base (TPB)* and *Direction Tendency Pattern Base (DPB)*. MBT records the mobility characteristic values of a mobile node in each foreign domain at which it arrives; MTQ records this mobile node movement. TPB and DPB extract movement patterns from MBT and MTQ. These data structures are discussed below.

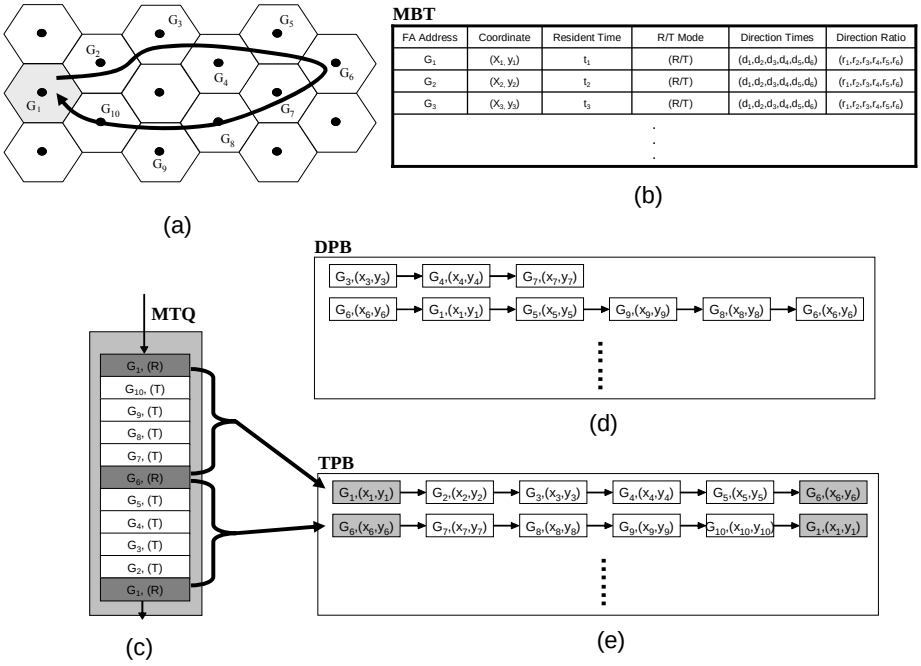

Figure 2.2. A Example of mobile node mobility data structures: (a) mobile node moving track; (b) MBT; (c) MTQ; (d) DPB; (e) TPB.

MBT includes six fields; *IP address*, *relative coordinate*, *residence time*, *residence/transient mode*, *direction times* and *direction ratios* of all foreign agents visited by the mobile node. The contents of local IP address and relative coordinate field are obtained from the advertisement extension of the visited foreign agent. If the relative coordinate of the foreign agent is the same as the home agent of a mobile node, this mobile node must perform home registration directly. The residence time of a foreign agent means the average time the mobile node stays in this foreign domain. When a mobile node leaves the visited foreign domain and registers with another foreign agent, the residence time of this foreign agent must be modified as follows

$$\mathrm{Re}\,sidenceTime = \alpha \times \mathrm{Re}\,sidenceTime + (1-\alpha) \times StayingTime \qquad (2\text{-}2)$$

where *Staying Time* is the period a mobile node stays in this foreign agent domain, and which it is measured by a timer or the number of advertisement extensions received from this

foreign agent; and α is the weighting value ranging in [0,1].

The residence/transient mode indicates whether this foreign agent is in residence mode or transient mode for this mobile node. The foreign agent is in residence mode when its residence time is more than a given threshold; otherwise, it is in transient mode. Those foreign agents in residence mode represent the starting and destination points of the mobile node trace paths.

The direction times of a foreign agent include six variables ($d_1, d_2, d_3, d_4, d_5, d_6$) to represent the time that the mobile node takes to move from a foreign agent to its six neighboring agents respectively. A mobile node is aware of which neighbor agent it moves to by the coordinate of the new foreign agent visited and that of the preceding foreign agent. The direction ratios of a foreign agent are represented by the ratios ($r_1, r_2, r_3, r_4, r_5, r_6$) of these direction times. For a mobile node, these ratios represent the tendencies of this mobile node towards different movement directions in this foreign agent. They are calculated as follows.

$$r_i = \frac{d_i}{\sum_{j=1}^{6} d_j} \qquad (2\text{-}3)$$

where d_j is the direction time of this foreign agent.

```
Procedure direction-tendency-pattern (MBT, DPB);
    begin
        var p1=p2=NULL: point;
        var pattern = NULL: foreign agent list;
        p1 = the first foreign agent in MBT;
        while p1 != END OF MBT
            p2 = p1;
            while (p2 is a directing foreign agent
                and p2 is not recorded in any pattern of DTPB
                and p2 is not recorded in pattern)
                add p2 to pattern;
                p2 = the arriving foreign agent of p2;
            endwhile
            if the length of pattern > threshold value θ then
                add pattern to DTPB;
            endif
```

```
            p1 = the next foreign agent of p1 in MBT;
        endwhile
    end
```

Figure 2.3. Algorithm for discovering direction tendency patterns.

MTQ is a FIFO queue kept by a mobile node to record those foreign agents visited by this mobile node in sequence according to this mobile node's movement track. When a mobile node visits a new foreign domain, the coordinate and residence/transient mode of this foreign agent will be added to the tail of this queue. A trace pattern is defined as a list of foreign agents that represent the moving path (or cycle) of a mobile node from one residence foreign agent to another residence foreign agent (or back to the original foreign agent). When a new residence foreign agent is added to the MTQ, the list of foreign agents in the MTQ from the preceding residence foreign agent to the new foreign agent is defined as a trace pattern, and is recorded in the TPB. For a mobile node, the direction ratios of a foreign agent in its MBT represent the tendency of this mobile node towards different directions in this foreign agent. If the greatest movement direction ratio of a foreign agent is more than a threshold ξ, this foreign agent is called the *directing foreign agent* of this mobile node, and the neighboring foreign agent in this direction of movement which has the maximum direction ratio is called the *arriving foreign agent* for this foreign agent. The *Directing Tendency Pattern* (DTP) for a mobile node is defined as a list (or a cycle) of foreign agents in which each foreign agent in this pattern is a directing foreign agent of this mobile node and the arrival foreign agent of its prior foreign agent. When a new foreign agent is added to the MBT of a mobile node, this mobile node tries to discover the DTP from this MBT by the algorithm shown in Fig. 2.3. If a new DTP is found, it will be recorded in the DPB.

2.1.3 Analysis of Signaling Cost in a Regional Registration

We estimate the total signaling cost of regional registration according to the cost function derived by Jiang [XI02]. In the cost function, the total signaling cost C_{TOT} consists of two metrics: the location update cost C_{LU} and packet delivery cost C_{PD}. That is

$$C_{TOT} = C_{LU} + C_{PD} \tag{2-4}$$

For the distributed dynamic scheme, the upper bound of the total location update costs per unit time is calculated as follows.

$$C_{LU} \le \frac{\tilde{C}_{Ur} + (E[M]-1) \times C_{Ur} + C_{Uh}}{E[M] \times T_f} \tag{2-5}$$

where the variables are defined as follows:

(1) $E[M]$: the expectation of performing a home registration at movement M.

(2) T_f : the average time a mobile node stays in each subnet.

(3) C_{Uh} : the home registration cost.

(4) C_{Ur} : the regional registration cost.

(5) $\tilde{C}_{Ur}$: the regional registration cost when the mobile node resides in the subnet of GFA.

These costs are given by

$$C_{Uh} = 2a_f + 2a_g + a_h + 2(l_{hg} + l_{gf} + \rho)\delta_U \tag{2-6}$$

$$C_{Ur} = 2a_f + a_g + 2(l_{gf} + \rho)\delta_U \tag{2-7}$$

$$\tilde{C}_{Ur} = a_g + 2\rho\delta_U \tag{2-8}$$

where a_h, a_g and a_f are the processing costs of location update at the home agent, GFA

and foreign agent, respectively; l_{hg} and l_{gf} are the distances between the home agent and GFA, and between the GFA and foreign agent, respectively. The transmission cost is proportional to the distance and the proportionality constant is δ_U. The transmission cost over the wireless link is assumed to be ρ times the wired line transmission cost.

$$C_{PD} = \eta\lambda_a + \xi w\lambda_a(\alpha w + \beta\log(k)) + (l_{hg} + l_{gf})\delta_D \quad (2\text{-}9)$$

The packet delivery cost is derived from Eq. 2-9. It includes three metrics: the processing cost at the home agent, the processing cost at the GFA and the transmission cost to route packets from the home agent via the GFA to the visited foreign agent:

1) The processing cost at the home agent is $\eta\lambda_a$, where η is a packet delivery constant cost and λ_a is the packet arrival rate for each mobile node.

2) In a distributed system, the processing cost function at the GFA is defined as $\xi w\lambda_a(\alpha w + \beta\log(k))$, where w is the average number of mobile nodes in a subnet. Because a mobile node selects one of all foreign agents as its GFA, the average number of mobile nodes under a GFA is w. k is the number of foreign agents under a GFA domain, and it is also the length of the routing table in GFA. The complexity of IP address lookup is proportional to **log(*k*)** [HT99]. The values α and β are weighting factors for visitor lists and routing table lookups; ξ is a constant which captures the bandwidth allocation cost at the GFA.

3) The transmission cost, defined as $(l_{hg} + l_{gf})\delta_D$, is proportional to the distances l_{hg} and l_{gf}, and the proportional constant is δ_D.

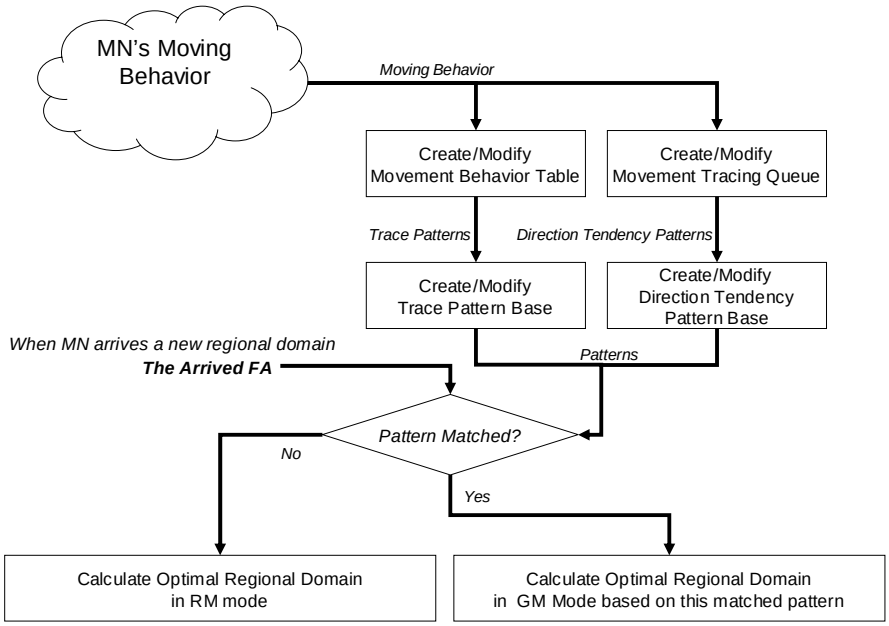

Figure 2.4. Flowchart of MORR.

2.2. The Proposed Scheme for Mobility Oriented Regional Registration (MORR)

In the proposed MORR, the regional domain of a GFA is composed of those foreign agents whose distances to the GFA are not more than the threshold r , denoted as the radius of this regional domain. When a mobile node leaves its visited regional domain, *i.e*. the distance between its GFA and the visited foreign agent is more than *r*, this mobile node should execute home registration.

The flowchart for MORR is shown in Fig. 2.4. When a mobile node leaves its regional domain and arrives at a new foreign agent domain, it examines the trace patterns in its TPB and the direction tendency patterns in its DPB to check whether or not the new foreign agent has been maintained in these patterns. If a pattern is found, this mobile node is regarded as being in GM mode and the mobile node moving track is predicted to match this pattern.

Otherwise, this mobile node is regarded as being in RM mode. Two algorithms are proposed for mobile nodes to calculate the optimal regional domain in these two modes. The details of these algorithms are described below.

2.2.1 Optimal Regional Domain in Random Mobility Mode

In this mode, there are two main steps to acquire the optimal regional domain of a mobile node: 1) to calculate the *optimal domain* of a GFA, and 2) to calculate the *optimal GFA* for this mobile node. Before describing this algorithm, we formulate the mobile node moving behavior in this mode. First, we define two parameters as follows.

(1) Equidistant set $E_S(x)$: the set of foreign agents whose distances to the foreign agent *S* are *x*, i.e., $\forall m \in E_S(x)$, $D(S,m) = x$.

(2) Moving probability $P_{i,j}^{k}(S)$: the probability that a mobile node moves directly from a foreign agent domain belonging to $E_S(i)$ to any of the foreign agent domains belonging to $E_S(j)$ in k movements.

In our network model, a mobile node leaves its visited domain in one movement and moves to any of the six neighboring domains with equal probability of $\frac{1}{6}$. Therefore, the moving probability $P_{i,j}^{1}(S)$ is obtained as:

$$P_{i,j}^{1}(S) = \begin{cases} 0 & i = j = 0 \\ 1 & j = i+1, i = 0 \\ \frac{1}{3} & i = j \geq 1 \\ \frac{2i+1}{6i} & j = i+1, i \geq 1 \\ \frac{2i-1}{6i} & j = i-1, i \geq 1 \\ 0 & otherwise \end{cases} \quad (2\text{-}10)$$

An $n \times n$ *mobility matrix* $A_n(S)$ is defined to denote the moving probabilities, where each element $[A_n(S)]_{i+1,j+1}$ is equal to the moving probability $P_{i,j}^1(S)$ and n denotes the coverage radius of the mobile network. Because the movement of mobile nodes in this network model follows a Markov process [GY95], the moving probability is as follows.

$$P_{i,j}^k(S) = [A_n(S)^k]_{i+1,j+1} \quad for\ k \geq 2 \tag{2-11}$$

The stability probability $R_d^k(S,x)$ is defined as the probability that a mobile node visiting the foreign agent $\in E_S(x)$ remains within a regional domain with a radius d ($d > x$) and the foreign agent S after the next k movements. This stability probability is calculated as follows.

$$R_d^k(S,x) = \sum_{p=1}^{d+1} [A_n(S)^k]_{x+1,p} \tag{2-12}$$

Let $\overline{D}_d^k(S,x)$ denote the average distance between a mobile node visiting the foreign agent $\in E_S(x)$ and the GFA S in the regional domain with radius d, during the period of k movement. Then, the average distance is calculated as follows.

$$\overline{D}_d^k(x) = \frac{\sum_{p=0}^{d} \{p \times [A_n(S)^k]_{x+1,p+1}\}}{\sum_{p=0}^{d} [A_n(S)^k]_{x+1,p+1}} \tag{2-13}$$

In the following, we derive the relationship between the radius and total cost. Based on that, the radius with minimal cost is regarded as the *ORD* boundary of a GFA. Consider that a foreign agent is selected as a GFA of a mobile node, d is the distance between the foreign agent visited and this GFA, and r is the radius of this regional domain ($d \leq r$). The expectation of the moment M at which the mobile node moves out of this regional network is

calculated by Eq. 2-14. The value of the expectation is determined by the radius *r* and the distance *d*.

$$E[M](d,r) = \sum_{k=0}^{\infty} (k+1) \times P_{d,r}^{k}(visitedFA) \times P_{r,r+1}^{1}(visitedFA) \tag{2-14}$$

The average distance between the visited foreign agent and the GFA is given by Eq. 2-15. The home registration cost and the regional registration cost for each location update are shown by Eqs. 2-16 and 2-17.

$$l_{gf}(d,r) = \overline{D}_{r}^{E[M](d,r)}(d) \tag{2-15}$$

$$C_{Ur}(d,r) = 2a_f + a_g + 2(l_{gf}(d,r) + \rho)\delta_U \tag{2-16}$$

$$C_{Uh}(d,r) = 2a_f + 2a_g + a_h + 2(l_{hg} + l_{gf}(d,r) + \rho)\delta_U \tag{2-17}$$

The upper boundary of the total location update costs per unit time in this operation is calculated by

$$C_{LU}(d,r,T_f) \le \frac{E[M](d,r) \times C_{Ur}(d,r) + C_{Uh}(d,r)}{E[M](d,r) \times T_f} \tag{2-18}$$

In our network model, the number of foreign agents in a regional domain whose radius is r is $1 + 3r \times (r+1)$. Therefore, the packet delivery cost per unit time is represented by Eq. 2-19. It is determined by the radius *r*, the distance *d* and the packet arrival rate λ_a.

$$C_{PD}(d,r,\lambda_a) = \eta\lambda_a + \xi w\lambda_a(\alpha w + \beta \log(1 + 3r \times (r+1))) + \lambda_a(l_{hg} + l_{gf}(d,r))\delta_D \tag{2-19}$$

Based on this analysis, the overall signaling cost function is formulated as in Eq. 2-20. Because the foreign agent visited by a mobile node at this moment is fixed, the distance *d* is determined by the location of the GFA as in Eq. 2-1. This function is determined by the location of the GFA, the radius *r* , the packet arrival rate λ_a, and the residence time T_f.

$$C_{TOT}(GFA,r,\lambda_a,T_f) = C_{LU}(d,r,T_f) + C_{PD}(d,r,\lambda_a) \tag{2-20}$$

As discussed in [XI02], an iterative algorithm has been used to give the optimal radius, r_{opt}, which is defined as the value of a radius that results in the minimum local signaling cost function [JI95]. Similar to the algorithm proposed in [HS93], the cost difference function between systems with a radius *r* and *r*-1 is obtained by

$$\Delta(GFA, r, \lambda_a, T_f) = C_{TOT}(GFA, r, \lambda_a, T_f) - C_{TOT}(GFA, r-1, \lambda_a, T_f) \tag{2-21}$$

Then, the optimal radius is given by

$$r_{opt}(GFA, \lambda_a, T_f) = \begin{cases} 1, & if\ \Delta(GFA, r, \lambda_a, T_f) > 0 \\ \max\{r : \Delta(GFA, r, \lambda_a, T_f) \le 0\}, & otherwise \end{cases} \tag{2-22}$$

The optimal radius depends on the packet arrival rate of the visiting mobile node, the average time a mobile node stays in this regional domain and the location of the GFA. The packet arrival rate can be estimated by the algorithm in [HS93]. The average time is calculated by the residence times of the foreign agents kept in the visiting mobile node's MBT under this regional domain by Eq. 2-23. It is determined by the location of the GFA and the radius *r*.

$$T_f(GFA, r) = \sum_{i=0}^{r} \left(\sum_{FA \in E_{GFA}(i)} (FA's \quad residentTime) \right) \tag{2-23}$$

With distributed regional location management, any one of the foreign agents can function as either a GFA or a foreign agent. When a foreign agent functions as the GFA of a mobile node, its optimal radius is derived from Eq. 2-22. The optimal GFA is defined as one in which the mobile node moving within the *ORD* boundary of this GFA is able to minimize its total signaling costs. In the distributed dynamic location management schemes [XI02, WY03], the first foreign agent visited by the mobile node when this node enters a new regional domain will function as the GFA of this regional network. Obviously, this first foreign agent is not necessarily the optimal GFA.

In MORR, when a mobile node leaves its regional domain and it is in RM mode, it

attempts to find its optimal GFA from the *search area*. The search area includes those foreign agents whose distances from the visited foreign agent do not exceed the search radius *k*, i.e. $FA^* \in \bigcup_{r=0}^{k} E_{visitedFA}(r)$. The criterion to find the local optimal GFA is given by

$$GFA_{opt}(\lambda_a, T_f, k) = \left\{ FA_m, \begin{array}{l} C_{TOT}(FA_m, r_{opt}(FA_m, \lambda_a, T_f), \lambda_a, T_f) \\ = \underset{FA^*}{Min}(C_{TOT}(FA, r_{opt}(FA, \lambda_a, T_f), \lambda_a, T_f)) \end{array} \right\} \quad (2\text{-}24)$$

The optimal GFA depends on the packet arrival rate λ_a, the residence time T_f and the search radius *k*. Because the search area does not cover the total network, this algorithm will find only the local optimal solution for a GFA.

With reference to the local optimal GFA and its local optimal radius, the local optimal signal cost is calculated by Eq. 2-25. It also depends on the packet arrival rate, residence time and the search radius *k*.

$$C_{opt}(\lambda_a, T_f, k) = C_{TOT}(GFA_{opt}(\lambda_a, T_f, k), r_{opt}(GFA_{opt}(\lambda_a, T_f, k), \lambda_a, T_f), \lambda_a, T_f) \quad (2\text{-}25)$$

2.2.2 Optimal Regional Domain in GM Model

In GM mode, the *ORD* of a mobile node is determined by its matched pattern. Let a pattern P_n be the list of foreign agents that includes *n* foreign agents $a_1, a_2, ..., a_n$ with coordinates $(x_1, y_1), (x_2, y_2), ..., (x_n, y_n)$. And $P_{i,j}$ is the sub-pattern of P_n including those foreign agents $a_i, a_{i+1}, ..., a_j$, where $1 \le i \le j \le n$. $R_{i,j}$ is defined as a regional domain that includes only the foreign agents of $P_{i,j}$. $GFA_{i,j}$ is defined as the GFA of $R_{i,j}$ and its coordinate value is $(\left\lfloor \frac{1}{(j-i+1)} \sum_{k=i}^{j} x_k \right\rfloor, \left\lfloor \frac{1}{(j-i+1)} \sum_{k=i}^{j} y_k \right\rfloor)$. The average distance and average residence time from $a_i, a_{i+1}, ..., a_j$ to $GFA_{i,j}$ is shown as

$$l_{gf}(a_i,a_j)=\frac{\sum_{k=i}^{j} d(GFA_{i,j},a_k)\times FA_k.rt}{\sum_{k=i}^{j} FA_k.rt} \tag{2-26}$$

$$T_f(a_i,a_j)=\frac{\sum_{k=i}^{j} FA_k.rt}{j-i+1} \tag{2-27}$$

Similar to the equations in RM mode, a mobile node home registration cost, regional registration cost and packet delivery cost in $R_{i,j}$ are depicted in Eqs. 2-28 and 2-29. And the total signaling cost function in $R_{i,j}$ is formulated in Eq. 2-30.

$$\overline{C_{Ur}}(a_i,a_j)=2a_f+a_g+2(l_{gf}(a_i,a_j)+\rho)\delta_U \tag{2-28}$$

$$\overline{C_{PD}}(\lambda_a,a_i,a_j)=\eta\lambda_a+\xi w\lambda_a(\alpha w+\beta\log(j-i+1))+(l_{hg}+l_{gf}(a_i,a_j))\delta_D \tag{2-29}$$

$$C_{TOT}(\lambda_a,T_f,a_i,a_j)=\frac{(j-i+1)\times\overline{C_{Ur}}(i,j)}{T_f(a_i,a_j)}+\overline{C_{PD}}(\lambda_a,a_i,a_j) \tag{2-30}$$

For a trace pattern $P_{i,j}$, a cutting point *k*, where $1\le k\le j-i$, is selected to partition this pattern into two sub-patterns $P_{i,i+k-1}$: $a_i,a_{i+1},...,a_{i+k-1}$ and $P_{i+k,j}$: $a_{i+k},a_{i+k+1},...,a_j$. In addition, $P_{i,i+k-1}$ and $P_{i+k,j}$ are also considered as two regional domains, i.e. $R_{i,j}$ is partitioned into $R_{i,i+k-1}$ and $R_{i+k,j}$. In this condition, the total signaling cost when a mobile node moving in $P_{i,j}$ is calculated is as follows:

$$P(\lambda_a,T_f,a_i,a_j,k)=\begin{cases} C_{TOT}(\lambda_a,T_f,i,j) & k=0 \\ C_{TOT}(\lambda_a,T_f,a_i,a_{i+k-1})\times\dfrac{T_f(a_i,a_{i+k-1})}{T_f(a_i,a_j)} & \\ +C_{TOT}(\lambda_a,T_f,a_{i+k},a_j)\times\dfrac{T_f(a_{i+k},a_j)}{T_f(a_i,a_j)} & 0<k<j-i \\ +C^*_{Uh}(a_{i+k},a_j)+C^*_{Ur}(a_{i+k},a_j) & \end{cases} \tag{2-31}$$

where $C^*_{Uh}(a_{i+k}, a_j)$ and $C^*_{Ur}(a_{i+k}, a_j)$ are the home and regional registration costs while this mobile node hands off from $R_{i,i+k-1}$ to $R_{i+k,j}$, and they are calculated by

$$C_{Uh}{}^*(a_i, a_j) = 2a_f + 2a_g + a_h + 2(l_{hg} + d(GFA_{i,j}, a_i) + \rho)\delta_U \quad (2\text{-}32)$$

$$C_{Ur}{}^*(a_i, a_j) = 2a_f + a_g + 2(d(GFA_{i,j}, a_i) + \rho)\delta_U \quad (2\text{-}33)$$

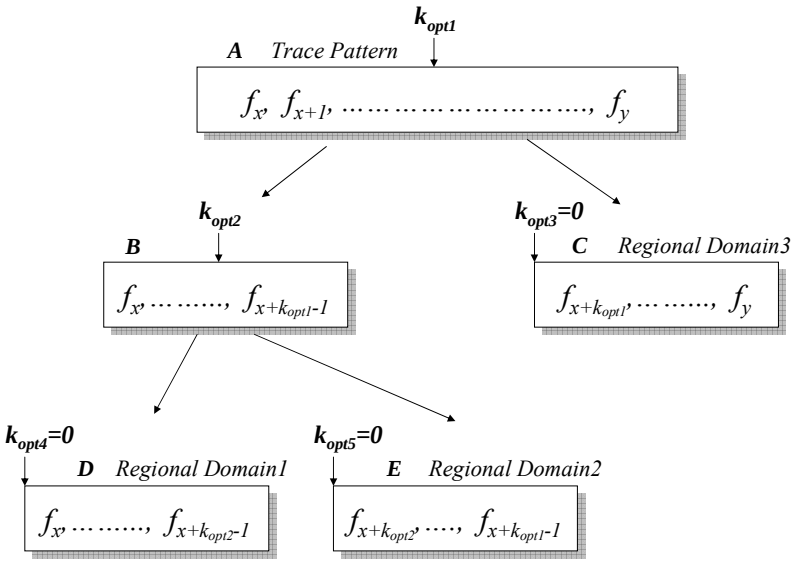

Figure 2.5. Optimal partition binary tree of a trace pattern.

The *optimal cutting point* of a trace pattern is defined as a cutting point in this pattern that minimizes the total signaling costs of the two sub-patterns. The optimal cutting point is calculated by Eq. 2-34.

$$k_{opt} : P(\lambda_a, T_f, a_i, a_j, k_{opt}) = \min_{k=0}^{j-i}(P(\lambda_a, T_f, a_i, a_j, k)) \quad (2\text{-}34)$$

When a trace pattern optimal cutting point is greater than 0, this trace pattern can be partitioned into two sub-patterns by this cutting point in order to minimize the mobile node signaling cost. Similarly, these sub-patterns are further partitioned by their optimal cutting

points recursively until their optimal cutting points equal 0. A sub-pattern whose optimal cutting point equals 0 is called an optimal sub-pattern, and the foreign agents in this sub-pattern comprise a regional domain. By repeating these steps, a binary tree pattern can be created, as shown in Fig. 2.5, and the external nodes of this tree are this pattern's regional domains. The recursive program is illustrated in Fig. 2.6.

```
Procedure optimal-partiton(TracePattern);
    begin
    var k:integer;
    k = the optimal cutting point of TracePattern;
    if k > 0 then
        partition TracePattern into sub-pattern1 and sub-pattern2 by k;
        optimal-partiton(sub-pattern1);
        optimal-partition(sub-pattern2);
    endif
    end
```

Figure 2.6. Recursive optimal partition program.

2.3. Simulation Results and Performance Evaluation

In this section, we demonstrate how MORR improves the performance of the distributed dynamic scheme proposed by Xie and Akyildiz [XI02]. In [XI02], each mobile node keeps a buffer for storing the addresses of its arrived foreign agents in a regional network. If the number of addresses kept in this buffer is greater than a threshold value k, the visited foreign agent will function as the GFA and the mobile node performs home registration through the new GFA, i.e. the mobile node will exit a regional network only after it has visited k different subnets. This scheme is able to dynamically optimize the regional network size of each mobile node according to its current traffic and mobility by adjusting the threshold value k.

2.3.1. Foreign Agent Domain Types in Evaluation

As evident from the analysis in Section 2.2, the total signaling cost functions of a mobile node are influenced by its packet arrival rates and the duration of its residence in each arrived foreign agent. Therefore, similarly to [HS93], we define six types of foreign agent domains to formulate the various mobility behaviors of mobile nodes by different probability density functions (pdf) of packet arrival rates and residing times. Type 1, 2 and 3 foreign agent domains explore the impact of variant packet arrival rates, with residence time as a constant; in contrast, Type 4, 5 and 6 foreign agent domains explore the impact of variant residence times, and assume packet arrival rates are constant. We evaluate the performance of MORR and Jiang's scheme under these six types of foreign agent domains.

Type 1 foreign agent domain: mobile nodes in this domain possess a higher average packet arrival rate ($\overline{\lambda}_{a_1} = 10.0$), and the pdf of packet arrival rates follows a Gaussian distribution:

$$f_1(\lambda_a) = \frac{1}{\sqrt{2\pi\sigma}} e^{-(\lambda_a - \overline{\lambda_{a_1}})^2 / 2\sigma^2}, \quad \lambda_a \geq 0, \quad where \quad \sigma = 4.0 \tag{2-35}$$

Type 2 foreign agent domain: mobile nodes in this domain possess a lower average packet arrival rate ($\overline{\lambda}_{a_2} = 0.1$), and the pdf of packet arrival rates follows an exponential distribution:

$$f_2(\lambda_a) = \frac{1}{\overline{\lambda_{a_2}}} e^{-\lambda_a / \overline{\lambda_{a_2}}}, \quad \lambda_a \geq 0 \tag{2-36}$$

Type 3 foreign agent domain: mobile nodes in this domain possess both higher and lower packet arrival rates at 50 percent probability respectively, and the packet arrival rates have the following pdf:

$$f_3(\lambda_a) = 0.5(f_1(\lambda_a) + f_2(\lambda_a)) \tag{2-37}$$

Type 4 foreign agent domain: mobile nodes in this domain possess a higher average residing time ($\overline{T}_{f_1} = 100$), and the pdf of residing times follows a Gaussian distribution:

$$f_4(T_f) = \frac{1}{\sqrt{2\pi}\sigma} e^{-(T_f - \overline{T}_{f1})^2 / 2\sigma^2}, \quad T_f \geq 0, \quad where \quad \sigma = 10 \tag{2-38}$$

Type 5 foreign agent domain: mobile nodes in this domain possess a lower average residing time ($\overline{T}_{f_2} = 1.0$), and the pdf of residence times follows an exponential distribution:

$$f_5(T_f) = \frac{1}{\overline{T}_{f_2}} e^{-T_f / \overline{T}_{f2}}, \quad T_f \geq 0 \tag{2-39}$$

Type 6 foreign agent domain: mobile nodes in this domain possess both higher and lower residence times at 50 percent probability respectively, and the residence times have a pdf as follows:

$$f_6(T_f) = 0.5(f_1(T_f) + f_2(T_f)) \tag{2-40}$$

Table 2.1. Parameters of signaling cost function.

Pkt Process Cost			Distance Cost Unit		Wireless Multiple	
a_h 25.0	a_g 15.0	a_f 10.0	δ_U 0.1	δ_D 0.05	ρ 10	
# of MNs/subnet	Distance		Weight		Pkt Process Const.	
w 15	l_{hg} 25	l_{gf} 10	α 0.3	β 0.7	ξ 0.01	η 10.0

We use the same parameters as [XI02] in our performance analysis. By using the parameters listed in Table1, measurements of the total signaling costs of MORR and of Jiang's scheme are possible. In this section, we show the performance improvement of MORR in numerical evaluations.

2.3.2 Cost Performance in Random-Mobility Mode

We compare the total signaling cost of Jiang's scheme with MORR when the visiting mobile node is in RM mode. In MORR, the total signaling cost function of a mobile node in RM mode is shown as Eq. 2-25. And in Jiang's scheme, the total signaling cost function is obtained by

$$C_{TOT\_dd}(k_{opt\_dd}(\lambda_a, T_f), \lambda_a, T_f), \tag{2-41}$$

where $k_{opt\_dd}(\lambda_a, T_f) = \begin{cases} 1 & if \Delta_{dd}(2, \lambda_a, T_f) > 0 \\ \max(k : \Delta_{dd}(k, \lambda_a, T_f) \le 0) & otherwise \end{cases}$, and

$\Delta_{dd}(k, \lambda_a, T_f) = C_{TOT\_dd}(k, \lambda_a, T_f) - C_{TOT\_dd}(k-1, \lambda_a, T_f)$.

First, we investigate the impact of a time-variant packet arrival rate. For this, we apply Type 1, 2 and 3 foreign agent domains to display variant packet arrival rates by different probability density functions. In these three types of foreign agent domains, the overall signaling cost of MORR is given by Eq. 2-42, and the total signaling cost of Jiang's scheme is given by Eq. 2-43.

$$C_{MORR\_RM\_Type1-3} = \int_0^\infty f_{1-3}(\lambda_a) C_{opt}(\lambda_a, T_f, k) d\lambda_a \tag{2-42}$$

$$C_{dd\_RM\_Type1-3} = \int_0^\infty f_{1-3}(\lambda_a) C_{TOT\_dd}(k_{opt\_dd}(\lambda_a, T_f), \lambda_a, T_f) d\lambda_a \tag{2-43}$$

The total signaling costs of MORR and Jiang's scheme with a time-variant packet arrival rate are shown in Fig. 2.7. There is can be a 3 percent cost reduction by using MORR in Type1 and Type 2 foreign agent domains, but there is a more than 10 percent cost reduction in a Type 3 foreign agent domain. This indicates there is a better performance for MORR when the mobile node packet arrival rate consists of both higher and lower packet arrival rates.

We also define Type 4, 5 and 6 foreign agent domains to display variant residence time by different probability density functions. In these three types of foreign agent domain, the overall signaling cost of MORR is given by Eq. 2-44, and the total signaling cost of Jiang's scheme is given by Eq. 2-45.

$$C_{MORR\_RM\_Type4-6} = \int_0^\infty f_{4-6}(T_f) C_{opt}(\lambda_a, T_f, k) dT_f \tag{2-44}$$

$$C_{dd\_RM\_Type4-6} = \int_0^\infty f_{4-6}(T_f) C_{TOT\_dd}(k_{opt\_dd}(\lambda_a, T_f), \lambda_a, T_f) dT_f \tag{2-45}$$

The comparison between MORR and Jaing's schemes under conditions of variant residence time are shown in Fig. 2.8, which indicates a cost improvement of up to 5 percent. MORR is slightly better than Jiang's scheme in Type 4, 5 foreign agent domains, but more than 10 percent of the cost can be reduced in a Type 6 foreign agent domain. It can also be seen that there is a better performance for MORR when the mobile node packet arrival rate consists of both higher and lower residence times.

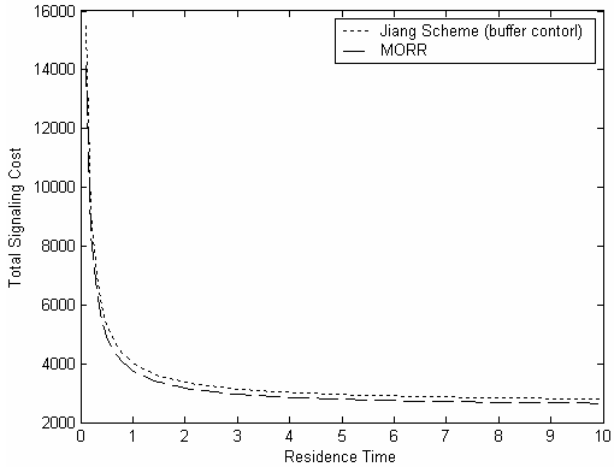

(a)

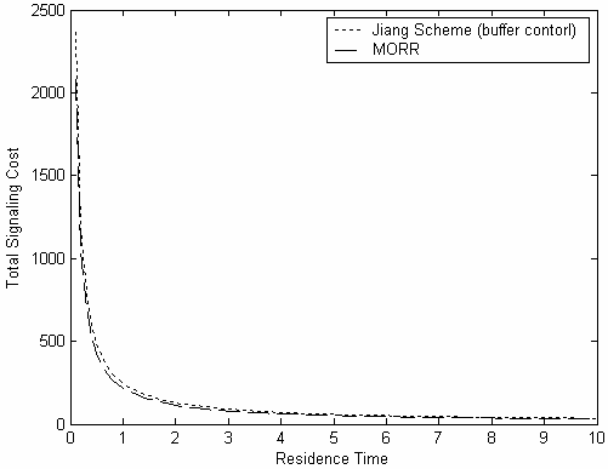

(b)

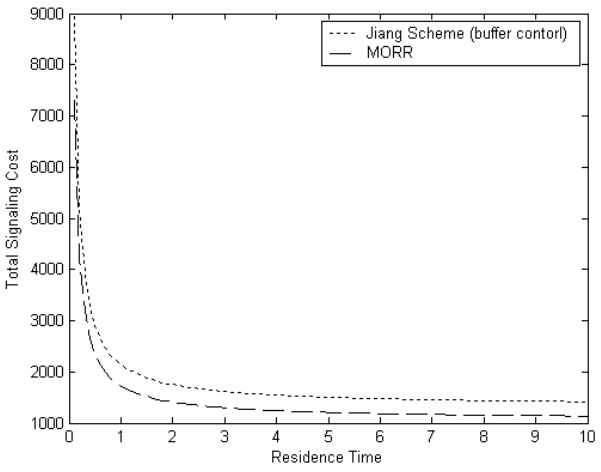

(c)

Figure 2.7. Comparison of total signaling cost under time-variant packet arrival rate. (a) In Type 1 foreign agent domain. (b) In Type 2 foreign agent domain. (c) In Type 3 foreign agent domain.

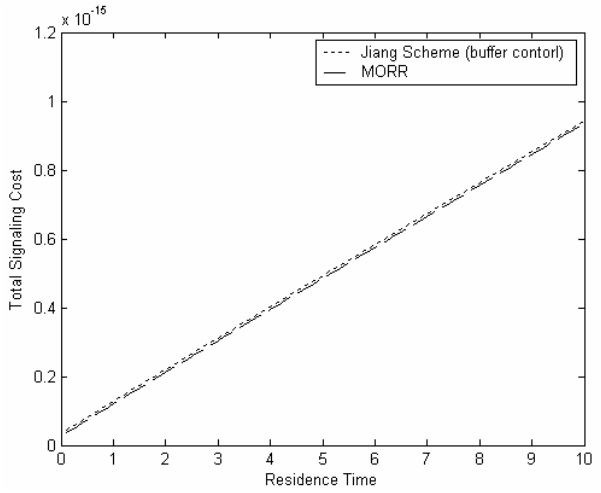

(a)

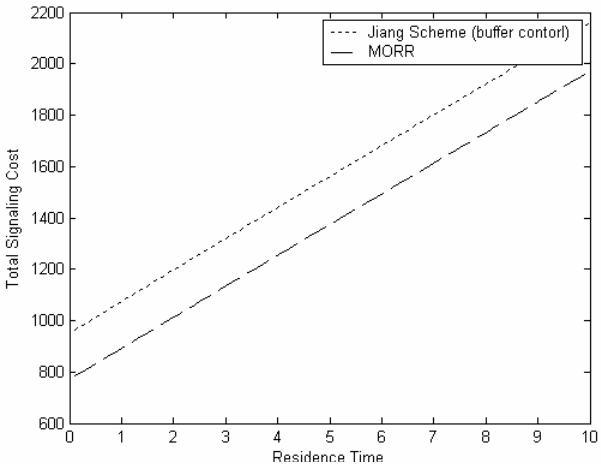

(b)

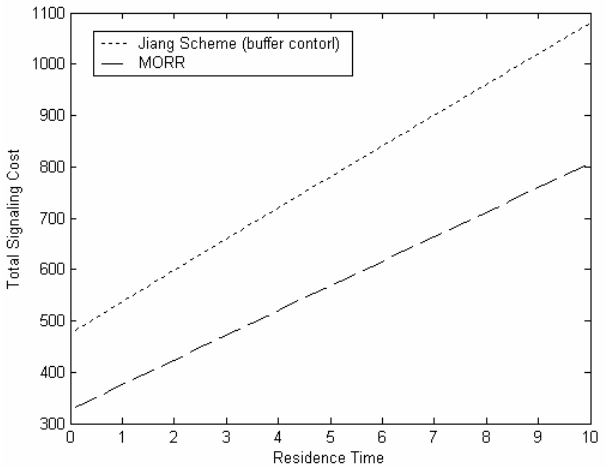

(c)

Figure 2.8. Comparison of total signaling cost in conditions of varying residence time: (a) In Type 4 foreign agent domain; (b) In Type 5 foreign agent domain; (c) In Type 6 foreign agent domain.

2.3.3 Cost Performance in Regular-Mobility Mode

We here compare the total signaling cost of Jiang's scheme with MORR when the mobile node is in GM mode. In this mode, we suppose the moving path of a mobile node is in accordance with a trace pattern $a_i, a_{i+1}, ..., a_j$, where $j > i$. The total signaling cost function of a mobile node using MORR can be obtained by the recursive optimal partition program, as shown in Fig. 2.6. In Jiang's scheme, because the mobile node moves across different foreign agent domains according to the trace pattern, the expectation of performing a home registration at movement M is:

$$E[M] = M / k \tag{2-46}$$

where k is the optimal buffer size of the mobile node. The distance l_{gf} is nearly $\frac{k}{2}$, and the total signaling cost function can be obtained by Eq. 2-4.

We now investigate the impact of a time-variant packet arrival rate. The overall signaling cost of MORR in three types of foreign agent domain (Types 1-3) is given by Eq. 2-47, and

the total signaling cost of Jiang's scheme is given by Eq. 2-48.

$$C_{MORR\_GM\_Type1-3} = \int_0^\infty f_{1-3}(\lambda_a) P(\lambda_a, T_f, a_i, a_j, k_{opt}) d\lambda_a \tag{2-47}$$

$$C_{dd\_GM\_Type1-3} = \int_0^\infty f_{1-3}(\lambda_a) C_{TOT\_dd}(k_{opt\_dd}(\lambda_a, T_f), \lambda_a, T_f) d\lambda_a \tag{2-48}$$

The total signaling costs of MORR and Jiang's scheme given a time-variant packet arrival rate are shown in Fig. 2.9. There is a more than 5 percent cost reduction using MORR in Type 1 and Type 2 foreign agent domains, and a more than 10 percent cost reduction in a Type 3 foreign agent domain.

Next, we investigate the impact of variant residence time. The overall signaling cost of MORR in three types of foreign agent domains (Types 4, 5 and 6) is given by Eq. 2-49, and the total signaling cost of Jiang's scheme is given by Eq. 2-50.

$$C_{MORR\_GM\_Type4-6} = \int_0^\infty f_{4-6}(T_f) P(\lambda_a, T_f, a_i, a_j, k_{opt}) dT_f \tag{2-49}$$

$$C_{dd\_GM\_Type4-6} = \int_0^\infty f_{4-6}(T_f) C_{TOT\_dd}(k_{opt\_dd}(\lambda_a, T_f), \lambda_a, T_f) dT_f \tag{2-50}$$

The total signaling costs of MORR and Jiang's schemes under variant residence time are shown in Fig. 2.10, which indicates that more than 10 percent of the cost can be reduced in these types of foreign agent domains.

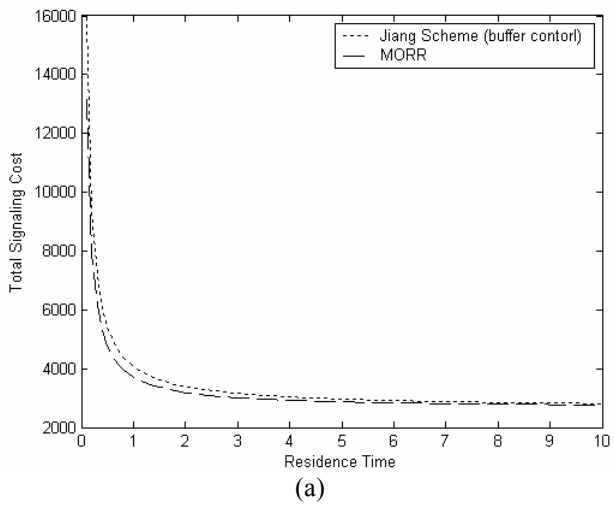

(a)

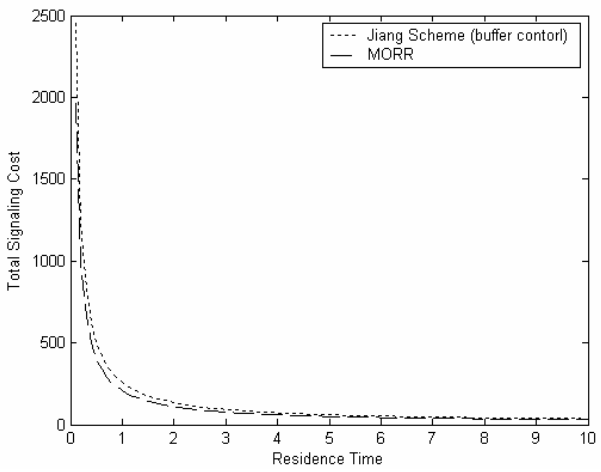

(b)

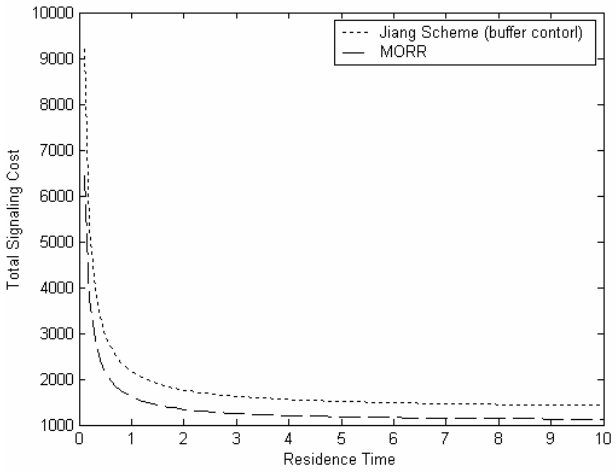

(c)

Figure 2.9. Comparison of total signaling cost with a time-variant packet arrival rate: (a) In Type 1 foreign agent domain; (b) In Type 2 foreign agent domain; (c) In Type 3 foreign agent domain.

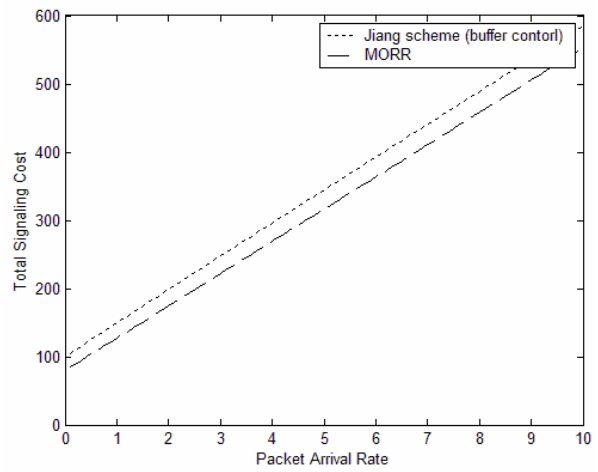

(a)

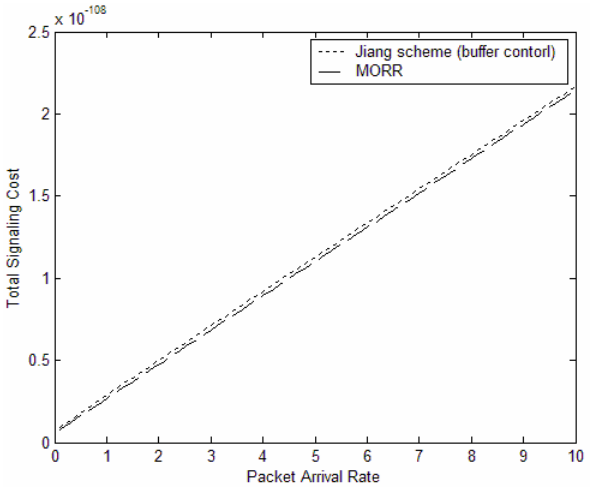

(b)

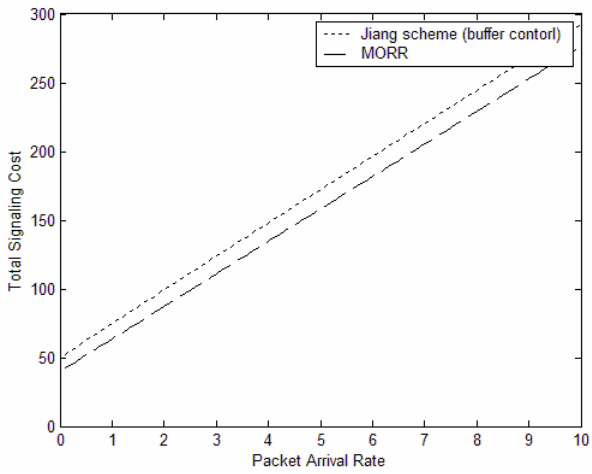

(c)

Figure 2.10. Comparison of total signaling cost under varying residence time: (a) In Type 4 foreign agent domain; (b) In Type 5 foreign agent domain; (c) In Type 6 foreign agent domain.

Chapter 3

Adaptive Power Control Approach in Ad Hoc Networks

Ad hoc networks have witnessed an explosion of interest in the last few years as they are expected to have a significant impact on the efficiency of many military and civilian applications, such as combat field surveillance, security and disaster management, data gathering, and conferences. Most of wireless devices are usually powered by batteries which provide a limited amount of energy. The capacity of electric power in batteries does not grow rapidly in a short period time in the future. Therefore, how to reduce energy consumption in ad hoc networks is an important issue. The energy consumption in transmission is affected by wireless MAC layer protocols. Therefore, several mechanisms used to save energy consumption are proposed in the MAC design. One way is to use power saving mechanism which allows a node to enter a doze state by powering off its wireless network interface [EN02, SS98]. Another alternative mechanism is to use power control mechanism which suitably varies transmission power to reduce transmission energy consumption [JV01, ES02].

In wireless communication, the condition that digital signals will be received correctly is depended on the signal-to-noise ratio (SNR). In other word, the stronger signal will be more possible to be received correctly. The signal strength depends on two factors: One is transmission power of transmitters; and the other is the distance between a transmitter and a receiver. However, transmitters consume more energy when they radiate stronger signal. In order to save energy, transmitters reduce their transmission power. But, it will result in weak signal strength of received data. There is more possibility that receivers identify data

incorrectly in this situation. When receivers identify data wrong, transmitters have to retransmit it. It costs more energy. Hence, there is a tradeoff between transmission power and energy saving.

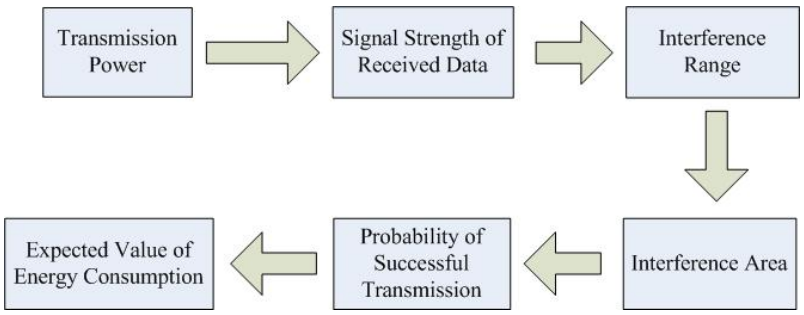

Figure 3.1. The relationship between transmission power and energy consumption.

As shown in figure 3.2, the transmission power of transmitters decides the signal strength of received data. In this chapter, we evaluate the signal strength of interfering nodes which can result in the transmission fails. This signal strength decides the interference range and interference area. The scope of interference area decides the probability of successful transmission. By this probability, the expected value of energy consumption can be estimated. When transmitters consume less energy to transmit stronger signal, the interference area will be large. It will increase the probability of unsuccessful transmission. The transmitters will cost more energy to retransmit these failed data. This chapter will investigate the optimal transmission power to minimize the energy consumption.

The main contributions of this chapter are three-fold: First to present the relationship between transmission power level and the probability of interference by mathematical models; Second to formulate the energy consumption in terms of these factors: transmission power levels, propagation models and wireless network topology; and Third proposing a novel

power control mechanism, *Adaptive Power Control Mechanism* (*APCM*), to evaluate the optimal transmission power level in each wireless node in order to minimize the whole of energy consumption and satisfy the quality of service in ad hoc wireless networks.

3.1. The Investigations of Energy Consumption in Ad Hoc Networks

In ad hoc networks, interference is based on the locations of wireless nodes. The position of wireless nodes affects the relationship between each other. The transmission of one node could affect the transmission of other nodes depending on the distance between each other. This interference problem is called the hidden terminal problem [ZJ02, ZB02, PK90, FL75]. Resolving hidden terminal problem becomes one of the major challenges in MAC protocols. IEEE 802.11 DCF is the most popular MAC protocol used in both wireless LANs and mobile ad hoc networks (MANETs). Its RTS/CTS (Request/Clear To Send) handshake is mainly designed for resolving hidden terminal problem. However, it has an underlying assumption that all hidden nodes are within the transmission range of receivers (e.g. to receive the CTS packet successfully), but some nodes which are out of the transmission ranges of both a transmitter and its receiver may still interfere with this receiver. This situation happens rarely in a wireless LAN environment since most nodes are in the transmission range of either transmitters or receivers. However, in ad hoc networks, it becomes a serious problem due to the large distribution of mobile nodes and the multi-hop operation.

In this chapter, we propose some mathematical models to analyze interference in 802.11 MAC. These models are based on the observation that there is a tradeoff between transmission power and power consumption. When a transmitter reduces its transmission power, it spends little energy to transmit data. The signal strength which the receiver senses is weak. The weak signal is easy to be interfered. When the transmission is interfered, the transmitter has to retransmit the data. Retransmission costs additional energy. Therefore,

minimal transmission power is not exactly optimal transmission power. On the contrary, strong signal is not easy to be interfered and the transmitter spends little energy on retransmission, but more energy is expended on transmissions. In this thesis, we present some mathematical models to formulate the relationship between power level and the probability of successful transmission, this relationship is based on the *Power Control Medium Access Control* (*PCM*) mechanism.

3.1.1. Wireless Network Models

In this section, we propose our wireless interference model depending on 802.11 MAC protocols in Ad hoc networks. We formulate the relationship between transmission power and the probability of successful transmission in the wireless interference model. There are three radio ranges defined on our network models:

Transmission Range (Rtx): Transmission range represents the range of the sender's transmission within which a packet can be successfully received if there is no interference from other radios. The transmission range is mainly determined by transmission power and radio propagation properties (i.e., attenuation).

Carrier Sensing Range (R_{cs}): Nodes in the carrier sensing range can sense the sender's transmission. The carrier sensing range is depended on the transmission power level and antenna sensitivity. In IEEE 802.11 MAC, a transmitter only starts transmission when it senses the channel free. However, in the IEEE 802.11 specification, there is no well-defined carrier sensing range. From the recent literatures [JL99, ST02], we find that in typically employed IEEE 802.11 radio modules, such as WaveLAN cards, the carrier sensing

range is about twice longer than the successful transmission range. In A. Kamerman and L. Monteban [AL97], carrier sensing range is two times larger than the transmission range.

Interference Range (R_i): Interference range of a node is the range within which transmission of the nodes will result in interfering with this node. The interference range depends on transmission power level of transmitter and interferer.

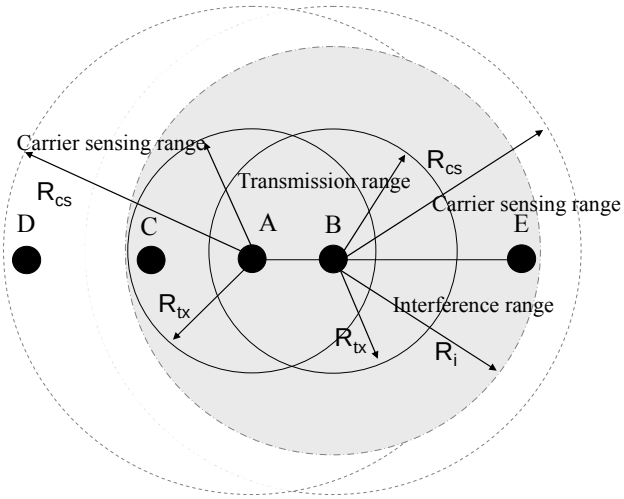

Figure 3.2. The transmission range, carrier sensing range, and interference range

The transmission range, carrier sensing range, and interference range are illustrated in Fig. 3.2. Node A is a transmitter and node B is a receiver. When A transmits data to B, this real circle is indicated the transmission range. The nodes within this circle are able to receive the frames successfully if there is no interference from other nodes. The receiver B has to be within this real circle. The length of radius of the real circle depends on the transmission power level of transmitter. At this condition, node C also receives the data which node A transmits. The dotted circle is the carrier sensing range. When A is transmitting data, the

nodes within this range are able to sense the transmission of node A. In this figure, when A transmits data to B, D is able to sense the transmission of A but can not decode the data correctly.

The shadow dotted circle is the interference range. Nodes within the interference range are called hidden nodes. When a receiver receives a frame, and a hidden node also tries to start its own transmission concurrently, the interference will be arisen. It will result in the wrong messages in this receiver. When A transmits data to B, and E transmits data to another receiver at the same time it will lead to the wrong messages in B. Node A has to retransmit these messages to B. The scope of interference range depends on these transmission power levels of transmitters and interferers.

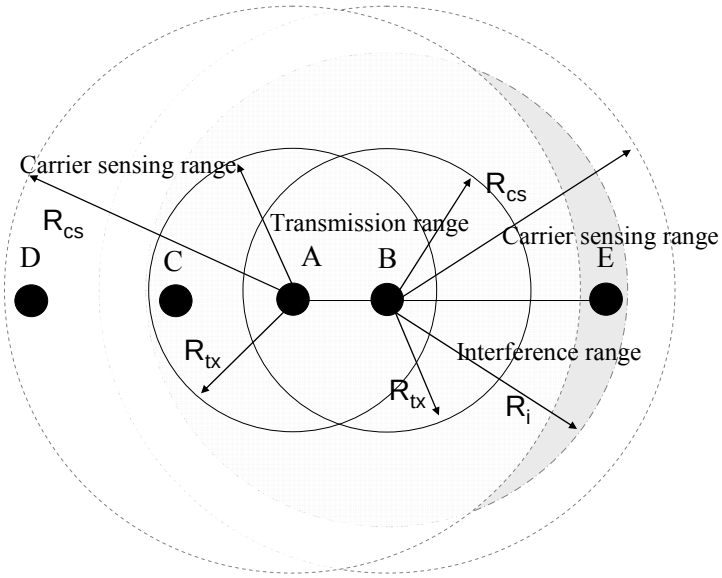

Figure 3.3. Wireless Interference Model

The wireless interference model is presented in Fig. 3.3, the shadow area is the

interference area. This area is composed from the area which is inside the interference range of the receiver and outside the carrier sensing range of the transmitter. In CSMA/CA model, when a node wants to transmit data, it shall sense the channel to determine if another node is transmitting. If the channel is not determined to be busy, the transmission proceeds. The CSMA/CA distributed algorithm mandates that a gap of a minimum specified duration exists between contiguous frame sequences. A transmitter shall ensure that the channel is idle for this required duration before attempting to transmit. If the channel is determined to be busy, the transmitter shall defer until the end of the current transmission. Hence, if a transmitter senses signal which another node radiates, the transmitter defers the transmission.

When one transmitter transmits data to the receiver, the nodes within the carrier sensing range of the transmitter do not transmit data. These nodes do not result in collision unless two or more nodes transmit data at the same time. This situation happens rarely. In the wireless interference model which we propose the nodes within the transmitter's carrier sensing range are able to sense the transmission of this transmitter and defer their own transmissions. Hence, the interference area of the receiver is the area which is composed from the area inside the interference range of the receiver and outside the carrier sensing range of the transmitter.

The signal strength depends on transmission power of transmitter. If a transmitter is in the carrier sensing range of another node, the transmitter will sense the signal. The carrier sensing range of another node depends on its transmission power. The value of transmission power depends on the kind of frame transmitter transmits. Nodes form maximum carrier sensing range by using maximum transmission power. We define the value of carrier sensing range to be maximum carrier sensing range because our model is based on PCM [ES02]. Transmitter transmits data at the power level P_{tmax} periodically, for just enough time so that nodes in the carrier sensing range can sense it. Hence, in our model we use maximum carrier sensing range whenever transmitter transmits RTS/CTS or data. When the transmitter is in the

carrier sensing range of another node, that node is certain in the carrier sensing range of the transmitter because the value of carrier sensing range is all the same for each node in the networks. In other words, there are no nodes which transmit data in carrier sensing range of transmitter when transmitter transmits data. If there is such one node, transmitter will defer the transmission.

3.1.2. Power Control and Interference Area

A signal received by the receiver is assumed to be valid when the signal to noise ratio (SNR) is above a certain threshold (SNR_THRESHOLD). Let P_r is denoted the received power of signal from the transmitter and P_i denote the power of interference signal at this receiver. Then, SNR is given as SNR=P_r /P_i. We ignore the thermal noise since it is ignorable comparing to interference signal. When the signal of a transmitter arriving at the receiver is not valid, the formula is derived in [TS02] as shown.

$$\frac{P_r}{P_i} \leq SNR\_THRESHOLD \tag{3-1}$$

$$P_i \geq \frac{P_r}{SNR\_THRESHOLD} \tag{3-2}$$

If a transmitter reduces its transmission power, the signal strength arriving at the receiver becomes weak. The value of P_r becomes smaller, and the value of P_i which conforms to Eq. 3-2 also becomes smaller. It means that weak interference signal is able to affect the transmission. Therefore, the transmission fails more easily. Although using little transmission power is able to save the energy consumption in transmission, the probability of unsuccessful transmission is also raised. It is possible that the transmitter spends more energy in retransmitting data. Hence, by using little transmission power to transmit data does not really save energy consumption.

3.1.3. Interference Area Models

In this section, we formulate the relationship between transmission power and interference area. We derive the interference signal strength which affects the transmission of a transmitter from Eq. 3-2 and calculate interference range by the interference signal strength. We continue to derive the scope of interference area from the interference range.

When a signal is propagated from a transmitter to a receiver, whether the signal is valid at the receiver almost depends on the strength of receiving power at the receiver. Given transmission power, the receiving power is almost decided by path loss over the transmitter-receiver distance, which models the signal attenuation over the distance. Here we ignore multi-path fading and shadowing since they are minor factors in the open space environment.

Propagation models that predict the mean signal strength for an arbitrary transmitter-receiver (T-R) distance are useful in estimating the radio coverage area of a transmitter. These models are called large-scale propagation models, since they characterize signal strength over large T-R distances (several hundreds or thousands of meters). There are two large-scale propagation models which are commonly used. One is free space propagation model. The other is two-ray ground model. The free space propagation model is used to predict received signal strength when the transmitter and receiver have a clear, unobstructed line-of-sight path between them. The free space power received by a receiver antenna which is separated from a radiating transmitter antenna by a distance d, is given by the Friis free space equation,

$$P_r(d) = \frac{P_t G_t G_r \lambda^2}{(4\pi d)^2 L} \tag{3-3}$$

where P_t is the transmitted power, $P_r(d)$ is the received power which is a function of the T-R separation, G_t is the transmitter antenna gain, G_r is the receiver antenna gain, d is the T-R

separation distance in meters, L is the system loss factor not related to propagation ($L \geqq 1$), and λ is the wavelength in meters.

The other is two-ray ground model. This model considers both the direct path and a ground reflection path. According to [TS02] the received power at distance d can be modeled as Eq. 3-4.

$$P_r = P_t G_t G_r \frac{h_t^2 h_r^2}{d^4 L} \tag{3-4}$$

where P_t is the transmission power. G_t and G_r are antenna gains of transmitter and receiver respectively. h_t and h_r are the heights of the transmit and receive antennas respectively. d is the distance between the transmitter and receiver. L is the system loss factor. However, the two-ray model does not give a good result for a short distance due to the oscillation caused by the constructive and destructive combination of the two rays. Instead, the free space model is still used when d is small. When the transmitter is close to the receiver (e.g. within the Freznel zone [TS02]), the receiving signal power is inverse proportional to d^2. When their distance is larger (e.g. outside of Freznel zone), the receiving signal power is inverse proportional to d^4 [TS02]. Therefore, a cross-over distance d_c is calculated in this model. When $d < d_c$, Equation (3-3) is used. When $d > d_c$, Eq. 3-4 is used. At the cross-over distance, there are the same results in Eqs. 3-3 and 3-4. Hence, d_c can be calculated as

$$d_c = \frac{4\pi h_t h_r}{\lambda} \tag{3-5}$$

We assume that the nodes in the ad hoc network are homogeneous. All the radio parameters are the same. We use a constant to replace the same parameters. The equations 3-3 and 3-4 can be simplified as Eqs. 3-6 and 3-7.

$$P_r(d) = \frac{P_t \times K}{d^2} \tag{3-5}$$

$$P_r = \frac{P_t \times K}{d^4} \tag{3-6}$$

where the value of K are obtained Eqs. 3-8 and 3-9 in free space propagation model and two-ray propagation model respectively.

$$K = \frac{G_t G_r \lambda^2}{(4\pi)^2 L} \tag{3-7}$$

$$K = G_t G_r \frac{h_t^2 h_r^2}{L} \tag{3-8}$$

By propagation models, we use the transmission power of transmitter and interferer to substitute P_i and P_r in Eqs. 3-10 and 3-11. By the equation 3-2, we can get Eq. 3-12.

$$P_i = \frac{P_{t\_i} \times K}{d(i,r)^{\alpha_i}} \tag{3-9}$$

$$P_r = \frac{P_{t\_t} \times K}{d(t,r)^{\alpha_t}} \tag{3-10}$$

$$\frac{P_{t\_i} \times K}{d(i,r)^{\alpha_i}} \geq \frac{P_{t\_t} \times K}{d(t,r)^{\alpha_t}} \times \frac{1}{SNR\_THRESHOLD} \tag{3-11}$$

where P_{t_t} denotes the transmission power at transmitter and P_{t_i} denotes the interference power at interferer. $d(i,r)$ is the distance between the interferer and receiver. $d(t,r)$ is the distance between the transmitter and receiver. The value of α_i and α_t depends on $d(i,r)$ and $d(t,r)$. If the interferer and transmitter are close to the receiver within the Freznel zone, the receiving signal power is inverse proportional to d^2. The value of α_i and α_t is 2. When their distance is larger (e.g. outside of Freznel zone), the receiving signal power is inverse proportional to d^4 [TS02]. The value of α_i and α_t is 4.

Hence, we derive the value of interference range (R_i). When the nodes outside the interference range transmit data, the transmission of the transmitter will be successful. When the nodes inside the interference range transmit data, the transmission of the transmitter fails.

The formula of interference range is derived from the Eq. 3-12, where $d(i,r)$ is the interference range. The formula of interference range is obtained in the Eq. 3-13.

$$d(i,r) \le \left(\frac{P_{t\_i} \times K}{P_{t\_t} \times K} \times SNR\_THRESHOLD \times d(t,r)^{\alpha_t} \right)^{\frac{1}{\alpha_i}}$$
$$= \left(\frac{P_{t\_i}}{P_{t\_t}} \times SNR\_THRESHOLD \times d(t,r)^{\alpha_t} \right)^{\frac{1}{\alpha_i}} \quad (3\text{-}12)$$

However, the value of P_{t_i} depends on the kind of frame interferer transmits. If interferer transmits data frame, it uses little transmission power. The value of P_{t_i} is smaller. If interferer transmits RTS/CTS frame, it uses maximum available transmission power. The value of P_{t_i} is P_{tmax}. P_{tmax} is maximum transmission power. Our model is based on PCM. Node periodically transmits data frame at the maximum power. So we use P_{tmax} to replace P_{t_i}. We do not consider the kind of frame interferer transmits. The equation 3-13 will be transferred to Eq. 3-14.

$$R_i = \left(\frac{P_{t\max}}{P_{t\_t}} \times SNR\_THRESHOLD \times d(t,r)^{\alpha_t} \right)^{\frac{1}{\alpha_i}} \quad (3\text{-}13)$$

We derive the relationship among the transmission power of transmitter, the distance between the transmitter and receiver and interference range. The value of interference range depends on two factors. One is the transmission power of transmitter. The other is the distance between the transmitter and receiver. P_{tmax} and SNR_THRESHOLD are fix values which depend on the kind of antenna. We derive the size of interference area (A_i) from the value of R_i.

We derive the formulas of interference area on four scope of interference range: $R_i \le R_{CS} - d$, $R_{CS} - d < R_i \le R_{CS}$, $R_{CS} < R_i \le R_{CS} + d$, and $R_i > R_{CS} + d$.

1. $R_i \leqq R_{cs} - d$

When the value of R_i is smaller than the value of R_{cs}–d, we show the relationship between the carrier sensing range and the interference range in Fig. 3.4.

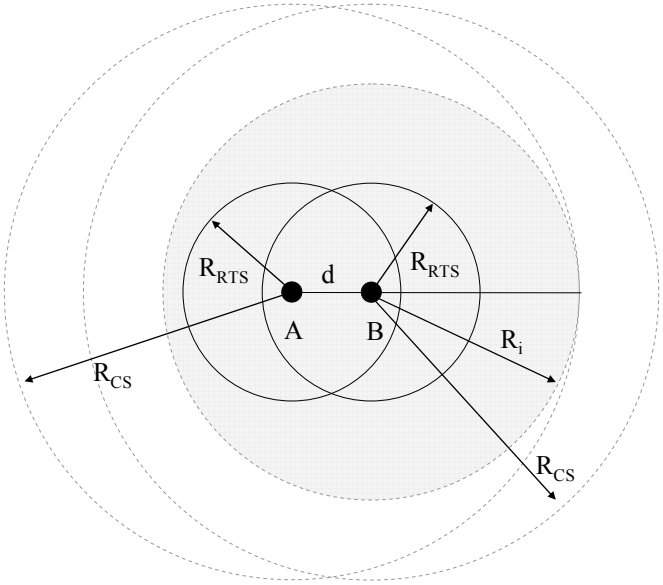

Figure 3.4. The interference area when $R_i \leqq R_{cs} - d$

In Fig. 3.4, the node A is transmitter and B is receiver. d is the distance between the transmitter and receiver. R_{RTS} is the transmission range of the RTS and CTS frame. It is maximum transmission range. R_{cs} is maximum carrier sensing range. R_i is the interference range. As shown in Fig. 3.4, we see that the interference range of B is all covered by the carrier sensing range of A. In the carrier sensing range of A there are no nodes transmitting when A transmits frame. Therefore, there are no nodes transmitting in the interference area. The transmission of A is not interfered in this situation. We derive that interference area is zero in this situation.

2. Rcs – d < Ri ≦ Rcs

When the value of R_i is bigger than the value of R_{cs}–d and smaller than the value of R_{cs}, we show the relationship between the carrier sensing range and the interference range in Fig. 3.5.

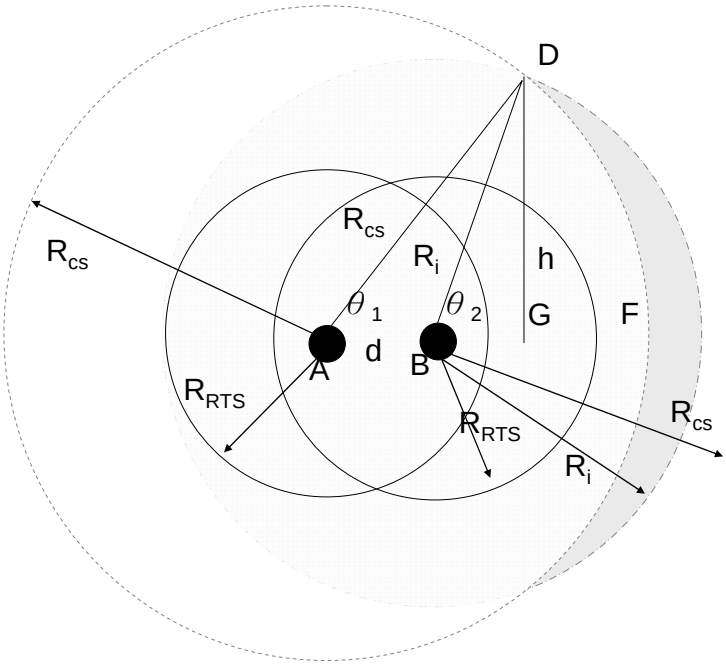

Figure 3.5. The interference area when $R_{cs} - d < R_i \leqq R_{cs}$

The node A is transmitter and B is receiver. d is the distance between the transmitter and receiver. R_{RTS} is the transmission range of the RTS and CTS frame. It is maximum transmission range. R_{cs} is maximum carrier sensing range. R_i is the interference range. As shown in Fig. 3.5, we see that interference area is the area of moon shape. Interference area is the shadow area. In the carrier sensing range of A it is the same that there are no nodes transmitting when A transmits frame. Hence, we deduce that interference area is outside the carrier sensing range of A and inside the interference range of B. We derive the formula of interference area below.

The size of interference area (Ai) is equal to the area of shadow. The size of shadow area is equal to 2 × (∠BDE+△ABD-∠ADF). The size of ∠BDE, △ABD, and ∠ADF

area is the Eqs. 3-15, 3-16, and 3-17.

$$\text{BDE} = \frac{\theta_2}{2\pi}\pi R_i^2 \tag{3-14}$$

$$\Delta ABD = \frac{1}{2} \times d \times h \tag{3-15}$$

$$\text{ADF} = \frac{\theta_1}{2\pi}\pi R_{cs}^2 \tag{3-16}$$

The value of *h* can be obtained by the Eq. 3-18. By the Eqs. 3-15, 3-16, 3-17, and 3-18, the formula of interference area is shown in Eq. 3-19.

$$h = R_{cs} \times \sin\theta_1 = R_i \times \sin\theta_2 \tag{3-17}$$

$$\begin{aligned} A_i &= 2 \times \left(\frac{\theta_2}{2\pi}\pi R_i^2 + \frac{1}{2} \times d \times h - \frac{\theta_1}{2\pi}\pi R_{cs}^2 \right) \\ &= \theta_2 R_i^2 + d \times h - \theta_1 R_{cs}^2 \\ &= \theta_2 R_i^2 + d \times R_i \sin\theta_2 - \theta_1 R_{cs}^2 \end{aligned} \tag{3-18}$$

We could calculate the size of interference area from the Eq. 3-19 as long as we know the value of variables. From the Eq. 3-18 and $\overline{AB} + \overline{BG} = \overline{AG}$, we derive the value of ϑ_1, ϑ_2. And we can get Eqs. 3-20, 3-21, and 3-22.

$$R_{cs} \cdot \cos\theta_1 = R_i \cdot \cos\theta_2 + d \tag{3-19}$$

$$\sin\theta_1 = \sin\theta_2 \cdot \frac{R_i}{R_{cs}} \tag{3-20}$$

$$\cos\theta_1 = \cos\theta_2 \cdot \frac{R_i}{R_{cs}} + \frac{d}{R_{cs}} \tag{3-21}$$

The equations 3-23, 3-24 and 3-25 are derived from the sum of the square of the Eq. 3-21 and the square of the Eq. 3-22.

$$1 = \frac{R_i^2}{R_{cs}^2} + 2\cos\theta_2 \frac{R_i \cdot d}{R_{cs}^2} + \frac{d^2}{R_{cs}^2} \tag{3-22}$$

$$2R_i \cdot d\cos\theta_2 = R_{cs}^2 - R_i^2 - d^2$$

$$\cos\theta_2 = \frac{R_{cs}^2 - R_i^2 - d^2}{2R_i \cdot d} \tag{3-23}$$

$$\theta_2 = \cos^{-1}\left(\frac{R_{cs}^2 - R_i^2 - d^2}{2R_i \cdot d}\right) \tag{3-24}$$

By the equations 3-20 and 3-24, we can get the result shown in Eqs 3-26, and 3-27.

$$R_{cs} \cdot \cos\theta_1 = \frac{R_{cs}^2 - R_i^2 - d^2}{2d} + d = \frac{R_{cs}^2 - R_i^2 + d^2}{2d} \tag{3-25}$$

$$\theta_1 = \cos^{-1}\left(\frac{R_{cs}^2 - R_i^2 + d^2}{2R_{cs} \cdot d}\right) \tag{3-26}$$

By the Equations 3-25 and 3-27, we are able to calculate the value of θ_1 and θ_2 if the values of R_{cs}, R_i, and d can be obtained. In this condition, the interference area can be obtain by Eq. 3-19.

3. **Rcs < Ri < Rcs + d**

In this condition, the relationship between the carrier sensing range and the interference range is shown in Fig. 3.6. The node A is transmitter and B is receiver, d is the distance between the transmitter and receiver. R_{RTS} is the transmission range of the RTS and CTS frame, it is maximum transmission range. R_{CS} is maximum carrier sensing range. R_i is the interference range.

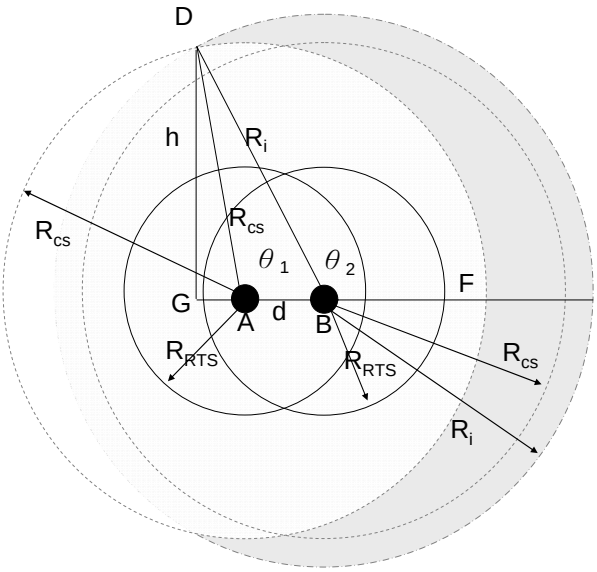

Figure 3.6. The interference area when $R_{cs} < R_i < R_{cs} + d$

The size of interference area (*Ai*) is equal to the area of shadow. The size of shadow area is equal to 2 × (∠BDE+△ABD-∠ADF). The size of ∠BDE, △ABD, and ∠ADF area can be obtained by Eqs. 3-15, 3-16, and 3-17. The value of *h* can be obtained by Eq. 3-28. And by these equations, the formula of interference area can be obtained in Eq. 3-29.

$$\begin{aligned} h &= R_{cs} \times \sin(\pi - \theta_1) = R_i \times \sin(\pi - \theta_2) \\ &= R_{cs} \times \sin\theta_1 = R_i \times \sin\theta_2 \end{aligned} \tag{3-27}$$

$$\begin{aligned} A_i &= 2 \times \left(\frac{\theta_2}{2\pi} \pi R_i^2 + \frac{1}{2} \times d \times h - \frac{\theta_1}{2\pi} \pi R_{cs}^2 \right) \\ &= \theta_2 R_i^2 + d \times h - \theta_1 R_{cs}^2 \\ &= \theta_2 R_i^2 + d \times R_i \sin(\pi - \theta_2) - \theta_1 R_{cs}^2 \\ &= \theta_2 R_i^2 + d \times R_i \sin\theta_2 - \theta_1 R_{cs}^2 \end{aligned} \tag{3-28}$$

Because $\overline{AB} + \overline{BG} = \overline{AG}$, we can obtain Eqs 3-30 and 3-31.

$$R_i \cdot \cos(\pi - \theta_2) = R_{cs} \cdot \cos(\pi - \theta_1) + d \tag{3-29}$$

$$R_{cs} \cdot \cos\theta_1 = R_i \cdot \cos\theta_2 + d \tag{3-30}$$

The equations 3-28 and 3-31 are the same as Eqs. 3-18 and 3-20, so we derive the value of ϑ_1, ϑ_2 is the same as that in session 3.3.2. The formula of ϑ_1, ϑ_2 are shown in Eqs 3-25 and 3-27.

4. Ri ≧ Rcs + d

In this condition, the relationship between the carrier sensing range and the interference range is shown as Fig. 3.6. The node A is transmitter and B is receiver, *d* is the distance between the transmitter and receiver. R_{RTS} is the transmission range of the RTS and CTS frame. It is maximum transmission range. R_{cs} is maximum carrier sensing range. R_i is the interference range. The interference area is the area which is the area of the circle whose radius is the interference range minus that of the circle whose radius is carrier sensing range. The size of interference area (*Ai*) is equal to the area of shadow. The formula of A_i is the Eq. 3-32.

$$A_i = \pi R_i^2 - \pi R_{cs}^2 \tag{3-31}$$

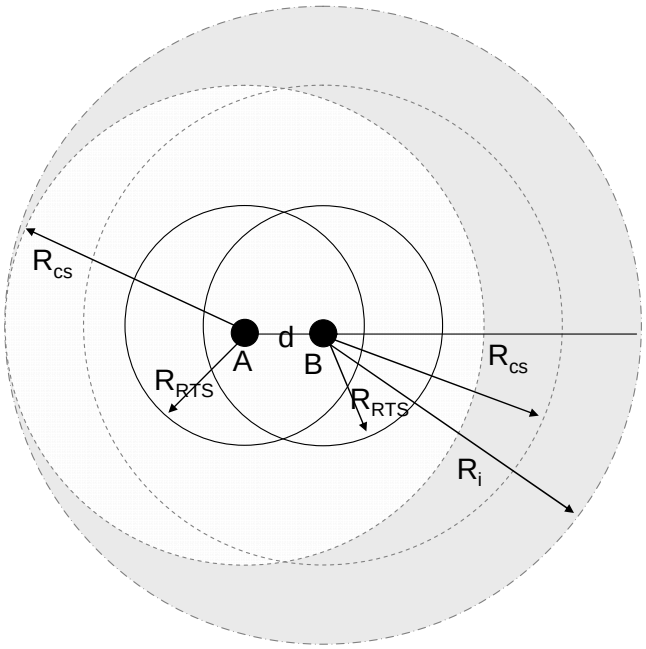

Figure 3.7. The interference area when $R_i \geqq R_{cs} + d$

We are able to conclude the relationship between the interference range and the interference area in Table 3.1.

Table 3.1 The relationship between the interference range and the interference area

The interference range (R_i)	The interference area (A_i)
$Ri \leqq R_{cs} - d$	0
$R_{cs} - d < R_i \leqq R_{cs}$	$A_i = \theta_2 R_i^2 + d \times R_i \sin\theta_2 - \theta_1 R_{cs}^2$
$R_{cs} < R_i < R_{cs} + d$	$A_i = \theta_2 R_i^2 + d \times R_i \sin\theta_2 - \theta_1 R_{cs}^2$
$R_i \geqq R_{cs} + d$	$A_i = \pi R_i^2 - \pi R_{cs}^2$

3.1.4. Transmission Power and Probability of Successful Transmission

We derived the formula of the interference area in Session 3.3. In this section we derive a formula to present the relationship between transmission power and the probability of successful transmission.

We define the probability that a node want to transmit data at time i as $P_T(i)$ and the

probability that a node does not want to transmit data at time i as $P_I(i)$. In addition, we define $P_{TT}(i)$ which is the probability of transforming from $P_T(i)$ to $P_T(i+1)$, $P_{TI}(i)$ which is the probability transforming from $P_T(i)$ to $P_I(i+1)$, $P_{IT}(i)$ which is the probability transforming from $P_I(i)$ to $P_T(i+1)$ and P_{II}(i) which is the probability from $P_I(i)$ to $P_I(i+1)$. We conclude these probabilities in the Table 3.2.

Table 1.2. The probability which is used in APCM

$P_T(i)$	The probability that a node wants to transmit data at time i
$P_I(i)$	The probability which a node does not want to transmit data at time i
$P_{TT}(i)$	The probability that a node wants to transmit data at time i and wants to transmit data at time i+1
$P_{TI}(i)$	The probability which a node wants to transmit data at time i but does not want to transmit data at time i+1
$P_{IT}(i)$	The probability which a node does not want to transmit data at time i but wants to transmit data at time i+1
$P_{II}(i)$	The probability which a node does not want to transmit data at time i and does not want to transmit data at time i+1

We derive $P_T(i)$ from $P_T(i-1)$, $P_I(i-1)$, $P_{TT}(i-1)$ and $P_{IT}(i-1)$. The probability which a node wants to transmit data at time *i* is derived from the probability of the status of nodes at time *i-1* and the probability of status transformation. The general formula of $P_T(i)$ is the Eq. 3-33.

$$\begin{aligned} P_T(i) &= P_T(i-1)\times P_{TT}(i-1) + P_I(i-1)\times P_{IT}(i-1) \\ &= P_T(i-1)\times P_{TT}(i-1) + (1-P_T(i-1))\times P_{IT}(i-1) \\ &= (P_{TT}(i-1) - P_{IT}(i-1))\times P_T(i-1) + P_{IT}(i-1) \\ &= c\times P_T(i-1) + d \end{aligned} \tag{3-32}$$

where $c = P_{TT}(i\text{-}1) - P_{IT}(i\text{-}1)$, $d = P_{IT}(i\text{-}1)$.

We assume that $P_{TT}(i)$, $P_{TI}(i)$, $P_{IT}(i)$ and $P_{II}(i)$ are equal for any time *i*. These values are changing at any time and we cannot model the behavior of nodes at any time. Therefore, we are able to gather these values by statistics during finite time and we assume that these values are the same during the finite time.

The relationship between $P_T(1)$ and $P_T(i)$ is shown in Eq.3-34.

$$P_T(i) = c^{i-1} P_T(1) + d\frac{1-c^{i-1}}{1-c}$$
$$\lim_{t\to\infty} P_T(i) = \frac{d}{1-c} = \frac{P_{IT}}{1-(P_{TT}-P_{IT})} \quad (3\text{-}33)$$

where the values of P_{TT} and P_{IT} are equal or less than one. $c = P_{TT}$-P_{IT}. The value of c ranges from -1 to 1. When wireless networks have started for a long time, the value of i tends to infinity. The value of c^{i-1} tends to zero. The value of $P_T(i)$ tends to Eq. 3-34. This means that when wireless network have started for a long time, the value of $P_T(i)$ tends to a fixed value. We simply $P_T(i)$ to P_T because the value of it is a fixed value when the value of i tends to infinity.

We define A as the size of the wireless network area and there are N nodes in this wireless network area. Therefore, there are $N*P_T$ nodes which want to transmit data in the wireless network area. Transmission of one node covers $\pi*R_{cs}*R_{cs}$ area. We define A_{cs} as $\pi*R_{cs}*R_{cs}$. When one node transmits data, the transmission will make the nodes in the carrier sensing range of the node delay their transmission. Here, we assume that $N*P_T$ nodes are all able to transmit data. It causes that there are $N*P_T*A_{cs}$ carrier sensing area in the wireless network area A. We assume that the node distribution in our model is uniform distribution. Therefore, these transmission nodes are averagely distributed in the wireless network area A. It causes that the $N*P_T*A_{cs}$ carrier sensing area is averagely distributed in the wireless network area A. So unit area are covered by the carrier sensing area of $N*P_T*A_{cs}/A$ nodes. It means that when one node wants to transmit data, the node has to compete the channel with other $N*P_T*A_{cs}/A - 1$ nodes. The probability of one node can use the channel is $A/(N*P_T*A_{cs})$. Furthermore, there are $N*A_i/A$ nodes in the interference area. There are $N*P_T*A_i/A$ transmission nodes in the interference area. So the probability of nodes transmitting data in the interference area is the Eq. 3-35.

$$N \times P_T \times \frac{A_i}{A} \times \frac{A}{N \times P_T \times A_{cs}} = \frac{A_i}{A_{cs}} \tag{3-34}$$

When there are nodes transmitting data in the interference area of the transmitter, it causes the transmission of the transmitter fail. The transmitter needs to retransmit data and spends additional energy. So we define $P(F_{data})$ as A_i / A_{cs}. It represents the failure probability of transmitting data. The equation 3-36 is the successful probability of transmitting data.

$$P(S_{data}) = 1 - P(F_{data}) = 1 - \frac{A_i}{A_{cs}} \tag{3-35}$$

From the Equation (3-14), Table 3.1, and the Equation (3-36) we derive the formula between transmission power of the transmitter and the probability of successful transmission of the transmitter in Table 3.3.

Table 3.3. The relationship between transmission power and the probability of successful transmission

Transmission power (P_{t_t})	The probability of successful transmission ($P(S_{data})$)
$P_{t\_t} \geq P_{t\max} \times SNR\_THRESHOLD \times \frac{d(t,r)^{\alpha_t}}{(R_{cs}-d)^{\alpha_i}}$	1
$P_{t\max} \times SNR\_THRESHOLD \times \frac{d(t,r)^{\alpha_t}}{(R_{cs}+d)^{\alpha_i}} < P_{t\_t}$, $P_{t\_t} < P_{t\max} \times SNR\_THRESHOLD \times \frac{d(t,r)^{\alpha_t}}{(R_{cs}-d)^{\alpha_i}}$	$1 - \frac{\theta_2 R_i^2 + dR_i \sin\vartheta_2 - \theta_1 R_{cs}^2}{A_{CS}}$
$P_{t\_t} \leq P_{t\max} \times SNR\_THRESHOLD \times \frac{d(t,r)^{\alpha_t}}{(R_{cs}+d)^{\alpha_i}}$	$1 - \frac{\pi R_i^2 - \pi R_{cs}^2}{A_{CS}}$

3.2. The Power Control Mechanism to Minimize Energy Consumption

The probability of successful transmission has been derived in session 3.1. By this

probability, we derive the expected value of transmission energy which is a criterion to select power level in our thesis. This session describes the expected value of energy consumption and proposes the power control mechanism (Adaptive Power Control Mechanism, APCM) to evaluate the adaptive transmission power in order to minimize the whole of energy consumption and satisfy the quality of service in ad hoc wireless networks.

3. 2. 1. Estimated Energy Consumption in 802.11 MAC Layer Protocol

In order to analyze energy consumption in 802.11 MAC layer protocol, we divide the period time of the DCF process in 802.11 MAC protocol into nine sub-periods. Period I is the duration that a transmitter transmits the RTS packet. Period II is the SIFS time between the RTS packet and CTS packet. Period III is the duration that a receiver transmits the CTS packet. Period IV is the SIFS time between the CTS packet and data packet. Periods V, VI, and VII are the durations that a transmitter transmits data message. Periods II, III, IV, and V are the EIFS time of the RTS packet. The nodes in the carrier sensing range of transmitter sense the RTS packets and set their NAVs for EIFS duration. Periods IV, V, and VI are the EIFS time of the CTS messages. The nodes in the carrier sensing range of receiver sense the CTS packet and set their NAVs for EIFS duration. Period VII is the duration which a transmitter transmits the remainder of data packet. Period VIII is the SIFS time between the data packet and ACK packet. Period IX is the duration that a receiver transmits the ACK packet. Figure 3.8 shows these nine parts in the flowchart of 802.11 packet transmission.

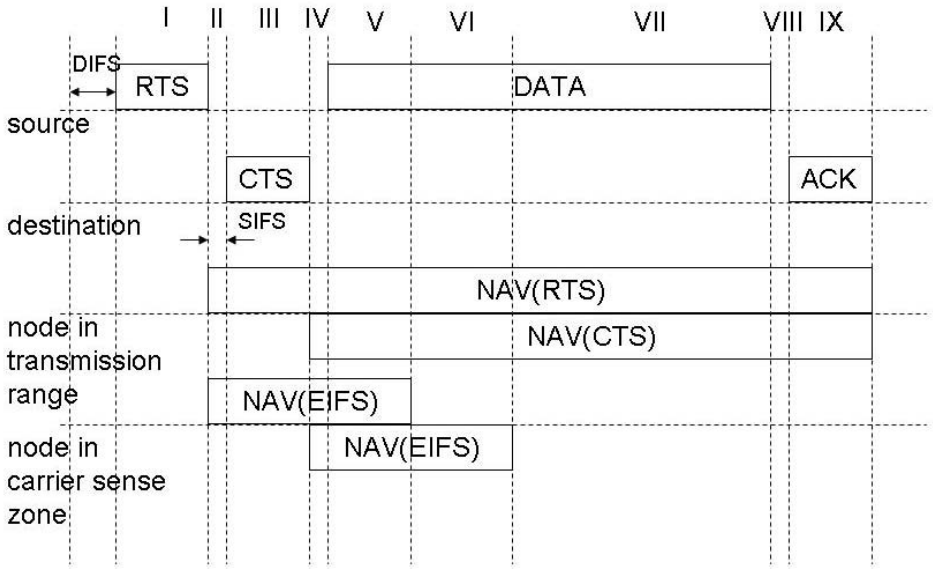

Figure 3.8. The flowchart of 802.11 packet transmission

We deduce reasonably that the interference area only appears in periods I and VII. In period I, when a transmitter sends the RTS packet to a receiver, the interfering nodes inside the interference range of the receiver interfere with the RTS transmission. In periods II, IV, and VIII, there is no transmission, hence there is no interference. In period III, when the receiver sends the CTS packet back to the transmitter, the nodes inside the carrier sensing range of the transmitter do not interfere with the CTS packet transmission because they sense the RTS packet and defer their own transmission. In periods V and VI, there is no interference because the nodes inside the carrier sensing range of the transmitter and receiver sense the RTS/CTS packet and defer their transmission. Our model is based on PCM. Transmitters periodically use P_{max} to transmit data and the signal arrives to the carrier sensing range of the transmitter. The interfering nodes inside the carrier sensing range of the transmitter periodically sense the signal which the transmitter radiates. Hence, there are no interfering nodes inside the carrier sensing range of the transmitter during the time which the transmitter transmits data. In period VII, when a transmitter sends data packet to a receiver, the

interfering nodes inside the interference range of the receiver interfere with the data transmission. In period IX, when the receiver sends the ACK packet back to the transmitter, the nodes inside the interference range of the transmitter do not interfere with the ACK packet because they sense the signal of data packet and defer their own transmission. Therefore, there is no interference in period IX.

If interference occurs in period I, the receiver does not receive the RTS frame correctly. The CTS frame is not returned. The additional energy cost is the energy of retransmitting the RTS frame. It is less because the length of RTS frame is shorter. If interference occurs in period VII, the receiver does not receive data correctly. The ACK frame is not returned. The additional energy cost is the energy of retransmitting data frame. It is more because the length of data frame is longer. Therefore, the transmission power of data frame affects energy consumption so much.

We divide transmission energy cost into two parts. One is the energy cost in retransmission. The other is the retransmission energy cost. When nodes use strong transmission power to transmit data frame, receivers sense the strong signal. It leads to less possibility that data frame is interfered. In this condition, the retransmission energy cost is less but it consumes more energy in transmission. Besides, when nodes use small transmission power to transmit data frame, receivers sense the weak signal. It leads to more possibility that data frame is interfered. There is higher possibility to retransmit data. The retransmission energy cost is higher but it consumes less energy in transmission.

From the successful transmission probability which we derive in Chapter 3, we derive the expected value of transmission energy. When transmission fails, the transmitter retransmits several times. It leads to spend more energy in transmitting the same data frame. This situation results in energy waste. We want to let the transmission energy cost per byte minimum and enhance the utilization of energy.

When the transmission of data packet of the transmitter fails, the transmitter will retransmit data packet. First, the transmitter retransmits RTS packet and expects reception of CTS packet of the receiver. If the transmitter receives CTS packet successfully, it will retransmit the data packet which fails before. The retransmission of RTS packet and data packet costs additional energy. In order to calculate the expected value of energy consumption which results from transmitting data packet, we have to consider the successful probability and the energy cost of transmitting RTS and data packet.

First, we need to know the successful probability and the energy cost of retransmitting RTS packet.

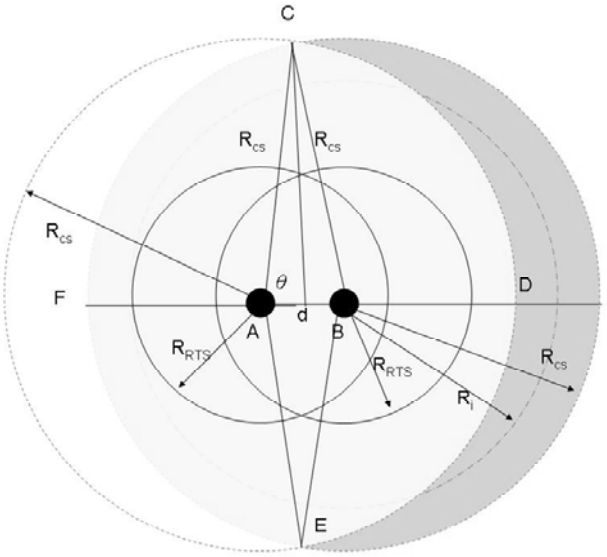

Figure 3.9. The RTS interference area (ARTS_i)

As shown in Fig. 3.9, the node A is transmitter and B is receiver. d is the distance between the transmitter and receiver. R_{RTS} is the transmission range of the RTS and CTS frame. It is maximum transmission range. R_{cs} is maximum carrier sensing range. R_i is the interference range. When the transmitter A transmits RTS packet, the nodes inside the carrier sensing range of A will delay their transmission. The transmission of RTS packet of A is not

affected by the nodes inside the carrier sensing range of A. The transmission of RTS packet of A is only affected by the nodes in the shadow area. We define this shadow area as A_{RTS_i}. It represents the interference area of RTS packet. The nodes in A_{RTS_i} can transmit packets when A transmits RTS packet. The transmission of the nodes in A_{RTS_i} is able to affect the RTS transmission of A. When the RTS transmission of A and the transmission of the nodes in A_{RTS_i} occur at the same time, node B will sense these two transmissions. However, node B does not know the signal which it senses from one node or two nodes. Node B considers the signal which it senses from one node. When node B receives the signal of node A first, it will think the signal of the nodes in A_{RTS_i} as the signal of node A. When node B receives the signal of the nodes in A_{RTS_i} first, it will think the signal of node A as the signal of the nodes in A_{RTS_i}. When the first situation occurs, node B correctly identifies the signal of node A. The signal of the nodes in A_{RTS_i} does not affect that of node A because node A is closer to node B than the nodes in A_{RTS_i} and the signal strength of node A is stronger than that of the nodes in A_{RTS_i}. The transmission of node A are not affected. When the second situation occurs, node B does not correctly identify the signal of the nodes in A_{RTS_i}. The signal of node A affects that of the nodes in A_{RTS_i} because node A is closer to node B than the nodes in A_{RTS_i} and the signal strength of node A is stronger than that of the nodes in A_{RTS_i}. So we first derive the size of A_{RTS_i}, and then calculate the successful probability of transmitting RTS packet.

From Fig. 3.9, we can obtain Eqs. 3-37, and 3-38.

$$\cos\theta = \frac{d/2}{R_{cs}} \quad \theta = \cos^{-1}\frac{d/2}{R_{cs}}$$

$$\begin{aligned} CDEF &= ACDE + BCFE - ACBE \\ &= 2\times\pi R_{cs}^2 \times \frac{2\theta}{2\pi} - dR_{cs}\sin\theta \\ &= 2\theta\times R_{cs}^2 - dR_{cs}\sin\theta \end{aligned} \tag{3-36}$$

$$A_{RTS\_i} = \pi R_{cs}^2 - CDEF = (\pi - 2\theta)R_{cs}^2 + dR_{cs}\sin\theta \tag{3-37}$$

In session 3.4, we define A as the size of the wireless network area, P_T as the probability that a node wants to transmit data and there are N nodes in this wireless network area. Hence, There are $N*P_T*A_{RTS\_i}/A$ nodes which want to transmit data in A_{RTS_i}. We derive that the probability of one node can use the channel is $A/(N*P_T*A_{cs})$, so when the transmitter A transmits RTS packet, the probability of nodes transmitting data in A_{RTS_i} is the Eq. 3-39.

$$N \times P_T \times \frac{A_{RTS\_i}}{A} \times \frac{A}{A_{cs} \times N \times P_T} = \frac{A_{RTS\_i}}{A_{cs}} \tag{3-38}$$

Here we define the probability of node B receiving the signal of node A first as $P(RTS_{T\_First})$, the successful probability of node A transmitting RTS packet as $P(S_{RTS})$ and the failure probability of node A transmitting RTS packet as $P(F_{RTS})$. The formula of $P(RTS_{T\_First})$ is Eq. 3-40.

$$P(RTS_{T\_First}) = \frac{A_{RTS\_i}}{A_{cs}} \times \frac{1}{N \times P_T \times {A_{RTS\_i}}/{A} + 1} \tag{3-39}$$

There are $N*P_T*A_{RTS\_i}/A$ nodes which want to transmit data in A_{RTS_i}, and the transmitter A has to compete with these nodes to make its signal arrive in node B first. So $P(RTS_{T\_First})$ is the probability of nodes transmitting data in A_{RTS_i} multiplied by $1/(N*P_T*A_{RTS\_i}/A+1)$. However, the formula of $P(S_{RTS})$ and $P(F_{RTS})$ are shown as:

$$P(F_{RTS}) = \frac{A_{RTS\_i}}{A_{cs}} - P(RTS_{T\_First}) = \frac{A_{RTS\_i}}{A_{cs}} \times \left(1 - \frac{1}{N \times P_T \times {A_{RTS\_i}}/{A} + 1}\right) \tag{3-40}$$

$$P(S_{RTS}) = 1 - \frac{A_{RTS\_i}}{A_{cs}} + P(S_{T\_First}) \tag{3-41}$$

.

When the transmitter A transmits RTS packet, it will expect reception of CTS packet of

the receiver B. If the transmitter A does not receive CTS packet of the receiver B during specific expiration time, A will retransmit RTS packet and the STA short retry count (SSRC) of A will be increased. The value of SSRC at most reaches the value of dot11ShortRetryLimit. When transmitter sends RTS packet dotllShortRetryLimit times but it does not receive CTS packet of receiver, it will consider this transmission error. We define the expected value of energy consumption of transmitting RTS packet as $\overline{E_{RTS}}$. The formula of $\overline{E_{RTS}}$ is

$$\begin{aligned}\overline{E_{RTS}} &= \sum_{k=1}^{ShortRetryLimit} k \times E_{RTS} \times P(F_{RTS})^{k-1} \times P(S_{RTS}) + ShortRetryLimit \times E_{RTS} \times P(F_{RTS})^{ShortRetryLimit} \\ &= \sum_{k=1}^{ShortRetryLimit-1} k \times E_{RTS} \times P(F_{RTS})^{k-1} \times P(S_{RTS}) + ShortRetryLimit \times E_{RTS} \times P(F_{RTS})^{ShortRetryLimit-1}\end{aligned} \quad . \quad (3\text{-}42)$$

where ShortRetryLimit is the value of dotllShortRetryLimit, and E_{RTS} is the energy cost of transmitting a RTS packet.

We are able to simplify Eq. 3-43 to the Eq.3-45 by Eq.3-44.

$$f = \sum_{k=1}^{a} k \times x^{k-1} = 1 + 2x + \ldots + ax^{a-1} = \frac{1-(a+1)x^{a} + ax^{a+1}}{(1-x)^2} \quad (3\text{-}43)$$

$$\begin{aligned}\overline{E_{RTS}} = E_{RTS} \times P(S_{RTS}) \times \frac{1 - ShortRetryLimit \times P(F_{RTS})^{ShortRetryLimit-1} + (ShortRetryLimit - 1) \times P(F_{RTS})^{ShortRetryLimit}}{(1-P(F_{RTS}))^2} \\ + ShortRetryLimit \times E_{RTS} \times P(F_{RTS})^{ShortRetryLimit-1}\end{aligned} \quad (3\text{-}44)$$

Now, we can use $\overline{E_{RTS}}$ to calculate the expected value of energy consumption of transmitting data packet. First, we define the expected value of energy consumption of transmitting data packet as $\overline{E_{data}}$. When a transmitter transmits data packets, it will expect reception of the ACK packet of the receiver. If the transmitter does not receive the ACK packet of the receiver during specific expiration time, it will retransmit RTS packet and the STA long retry count (SLRC) of the transmitter will be increased. The value of SLRC at most reaches the value of dot11LongRetryLimit. When the transmitter sends data packet dot11LongRetryLimit times but it does not receive the ACK packet of the receiver, it will

consider this data transmission error. The formula of $\overline{E_{data}}$ is below.

$\overline{E_{data}}$ = the energy cost of transmitting data first time + the energy cost of retransmitting RTS first time * the failure probability of transmitting data packet first time + the energy cost of transmitting data second time * the failure probability of transmitting data packet first time * the successful probability of retransmitting RTS first time + ……

Hence, we derive the Eq. 3-46.

$$\begin{aligned}
\overline{E_{data}} &= E_{data} + \overline{E_{RTS}} \times P(F_{data}) \\
&+ E_{data} \times P(F_{data}) \times \left(1 - P(F_{RTS})^{LongRetryLimit}\right) + \overline{E_{RTS}} \times P(F_{data})^2 \times \left(1 - P(F_{RTS})^{LongRetryLimit}\right) \\
&+ E_{data} \times P(F_{data})^2 \times \left(1 - P(F_{RTS})^{LongRetryLimit}\right)^2 + \overline{E_{RTS}} \times P(F_{data})^3 \times \left(1 - P(F_{RTS})^{LongRetryLimit}\right)^2 + \ldots \\
&+ E_{data} \times P(F_{data})^{LongRetryLimit-1} \times \left(1 - P(F_{RTS})^{LongRetryLimit}\right)^{LongRetryLimit-1} \\
&+ \overline{E_{RTS}} \times P(F_{data})^{LongRetryLimit-1} \times \left(1 - P(F_{RTS})^{LongRetryLimit}\right)^{LongRetryLimit-2} \\
&= E_{data} \times \sum_{k=1}^{LongRetryLimit} \left[P(F_{data}) \times \left(1 - P(F_{RTS})^{LongRetryLimit}\right)\right]^{k-1} \\
&+ \overline{E_{RTS}} \times \sum_{k=1}^{LongRetryLimit-1} P(F_{data})^k \times \left(1 - P(F_{RTS})^{LongRetryLimit}\right)^{k-1}
\end{aligned} \tag{3-45}$$

Where E_{data} is the energy cost of transmitting a data packet, and LongRetryLimit is the value of dotllLongRetryLimit. The additional energy cost of retransmitting RTS packet is $\overline{E_{RTS}}$. Only when the data transmission of the transmitter fails, the transmitter needs to retransmit RTS packet. The probability which the data transmission of the transmitter fails is $P(F_{data})$. The second data retransmission occurs when the RTS retransmission of the transmitter successes. If the RTS retransmission of the transmitter fails, the transmitter does not retransmit data packet. Hence, the probability of second data retransmission is the failure probability of first data transmission multiplied by the successful probability of first RTS retransmission. The failure probability of first data transmission is $P(F_{data})$. The successful probability of RTS retransmission is $\left(1 - P(F_{RTS})^{LongRetryLimit}\right)$. The probability of second data retransmission is $P(F_{data}) \times \left(1 - P(F_{RTS})^{LongRetryLimit}\right)$. We derive the formula of $\overline{E_{data}}$ by the

same step. In the following session, we use the formula of $\overline{E_{data}}$ to count the adaptive power level to transmit data.

3. 2. 2. The Optimal Transmission Power to Reduce Energy Consumption

This session introduces APCM (Adaptive Power Control Mechanism) proposed to choose adaptive power level. APCM includes the method to estimate the distance between a transmitter and a receiver and the method to calculate adaptive transmission power.

There are five steps in the APCM.

Step 1: Receivers sense the signal strength of RTS frame and record it in CTS frame.

Step 2: Transmitters estimate the distance between the transmitter and the receiver from the signal strength information of step 1.

Step 3: Transmitters compute the minimum transmission power level (P_{t_min}) which is able to transmit data to the receiver.

Step 4: Transmitters compute the enough transmission power level (P_{t_enough}) which makes interference range equal to zero.

Step 5: Transmitters estimate the adaptive power level by computing the expected value of energy consumption of each different power level between P_{t_min} and P_{t_enough}

The step 1 is the mechanism in order to obtain the necessary information which is used to estimate the expected value of energy consumption. When a receiver receives the RTS frame from a transmitter, it is able to sense the signal strength of the RTS frame and records the signal strength in the CTS frame. The transmitter knows the quality of channel between the transmitter and receiver from this step. The transmitter is able to derive the distance between the transmitter and receiver from this information. We derive the equation of the distance between the transmitter and receiver from the two-ray propagation model. The equation 3-50 is the formula of the distance.

$$d = \left(P_t G_t G_r \frac{h_t^2 h_r^2}{P_r L} \right)^{1/4} \quad (3\text{-}46)$$

Transmitters transmit the RTS frame by maximum available power level, so P_t is P_{t_max}. Transmitters get P_r from the CTS frame. From the Eq. 3-50, transmitters calculate the distance d between the transmitter and receiver in step 2. Steps 3, 4, and 5 are the mechanisms to estimate the expected value of energy consumption. From the distance d between the transmitter and receiver, we calculate the value of P_{t_min}. P_{t_min} is the minimum transmission power level which is able to transmit data across the distance between the transmitter and receiver. This value is obtained from the formula of the two-ray propagation model. We get the formula of P_t from the two-ray propagation model. The Equation 3-51 is the formula of P_t.

$$P_t = P_r \frac{d^4 L}{G_t G_r h_t^2 h_r^2} \quad (3\text{-}47)$$

where P_r is the receiving threshold. It is the minimum signal strength which receivers are able to identify data correctly. We assume that the nodes in the networks are homogeneous. The receiving threshold is the same for the all nodes in the networks. Hence, P_r has been known. d is derived in step 2, so we can calculate the value of P_{t_min}. by Eq. 3-51.

Step 4 is the mechanism which calculates the enough transmission power level (P_{t_enough}). P_{t_enough} is the transmission power level which makes the interference range equal to zero. When transmitters transmit data frame by P_{t_enough}, the interference range is equal to zero. If transmitters use stronger transmission power to transmit data frame, the interference range also equals to zero. There is no effect in enhancing transmission power. Transmitters waste energy when they use stronger transmission power than P_{t_enough} because the interference range has been zero since transmission power level reaches P_{t_enough}. We derive the formula of the interference range R_i by Eq. 3-14.

We assume that the nodes in the networks are homogeneous. Hence, P_{tmax}, and

SNR_TRHESHOLD have been known. The distance between the transmitter and receiver is derived in step 2. This is the value of $d(t,r)$. α_t and α_i could be derived from the distance $d(t,r)$. By the equation 3-14, we calculate the value of P_{t_enough} when we set R_i equal to zero. The expected value of energy consumption is calculated in step 5. Transmitters estimate the adaptive power level by computing the expected value of energy consumption of each different transmission power level between P_{t_min} and P_{t_enough}. The formula of computing the expected value of energy consumption is derived in Session 3.2.1.

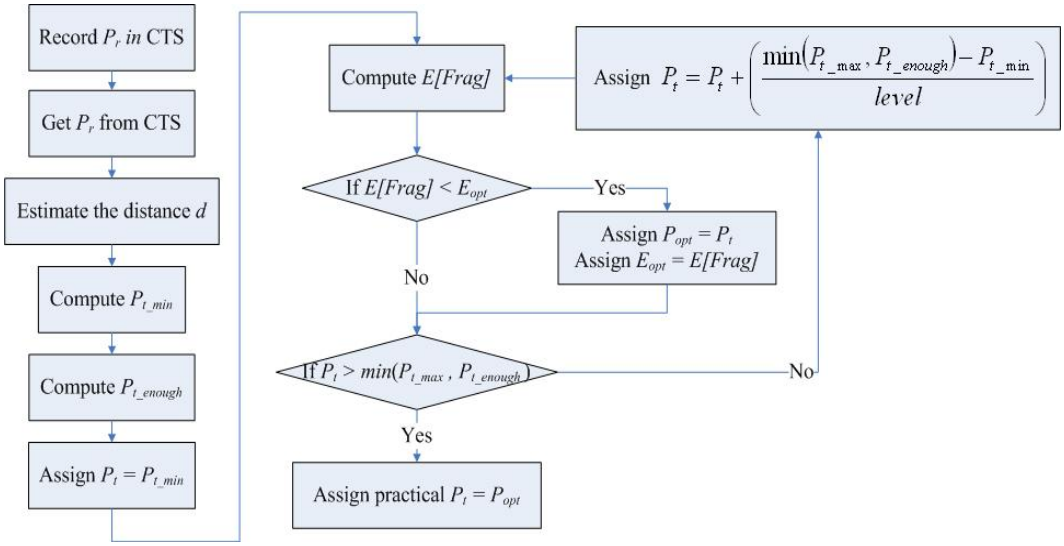

Figure 3.10. Flowchart of APCM to choose the adaptive transmission power

Figure 3.10 is the flow chart of APCM. The *level* is the delicate degree between adjacent power levels. When the value of *level* is big, it represents that there are many power levels which transmitters are able to choose to transmit data. In this situation, transmitters are able to select more precise adaptive transmission power level and the effect of APCM is better.

3.3. Simulation Results and Performance Evaluation

This session introduces the simulation environment, the parameters of the simulation network, the simulation results and analysis of these results.

3.3.1 Simulation Environment

We use ns-2 with the CMU wireless extension to validate the performance of APCM. The network size is 1000x1000 square meters. The channel bit rate is 11 Mbps. Packet size is 2k bytes. Each flow in the network transmits CBR (Constant Bit Rate) traffic. Radio propagation model is two-ray ground model. The two-ray ground model considers both direct path and ground reflection path. It is shown in [TS02] that this model gives more accurate prediction at a long distance than the free space model. We do not consider multi-path fading and shadowing in our simulations since they are minor factors in the open space environment. We set maximum transmission power P_{max} 15dbm.This value depends on ORiNOCO 802.11b client PC card specifications and the specification of the 802.11g USB card of ZyXEL, G-220. Their maximum transmission power is close to this value. The maximum transmission range is 80 meters. This value depends on the specification of the 802.11g USB card of ZyXEL. It also depends on our measurement experience in the playground. We measure the maximum transmission distance in the playground to be almost 80 meters. In addition, we set the minimum signal power needed for carrier sensing is -74.9dbm. The maximum carrier sensing range is 265 meters when transmitters transmit frame by P_{tmax}. The default values of the maximum transmission range and maximum carrier sensing range are 250m and 550m in ns2. Nevertheless, we think that the two default values in ns2 are too big to conform to the reality situation. We think that it is more reasonable that the maximum transmission range is set 80 meters. That is the reason that we set the value of the maximum transmission range and maximum carrier sensing range 80m and 265m. These values result in that the minimum signal power needed for successful reception is -63.36dbm and the minimum signal power needed for carrier sensing is -74.9dbm. These values approximately equal to those in [JV01]. The value of *SNR_Threshold* is 10. This value is the same as [KM02] and [JB04]. Table 3.4

lists all simulation parameters.

Table 3.4. The parameters of simulation network

Description	Parameter	Value
Maximum transmission Power	P_{max}	0.031622777 (W) = 15dbm
Receive Power	P_r	$P_r = P_t G_t G_r \frac{h_t^2 h_r^2}{d^4 L}$
Minimum signal power needed for successful reception	$P_{RXThresh\_}$	4.60835e-10 (W) = -63.36dbm
Minimum signal power needed for carrier sensing	$P_{CSThresh\_}$	3.24625e-11 (W) = -74.9dbm
Maximum transmission range	R_{tx}	80m
Maximum carrier sensing range	R_{cs}	265m
SNR threshold	*SNR_Threshold*	10
Antenna gain factor	G_t, G_r	1
Antenna height above the ground	h_t, h_r	1.5m
Frequency	*Freq*	2.472e9
Signal wavelength	λ	0.121m
Cross-over distance for Friss and two-ray ground models	$d_{crossover}$	233.67m
The probability from transmitting status to transmitting status	P_{TT}	0.1
The probability from transmitting status to idle status	P_{TI}	0.9
The probability from idle status to transmitting status	P_{IT}	0.1
The probability from idle status to idle status	P_{II}	0.9
System loss	*L*	1
Max retransmissions	*R*	4
Nodes	N	100
Network size	A	1000m × 1000m
Radio propagation speed	A	3×10^8 m/s
Radio speed	C	11Mbps
Data size		2000 bytes
Data rate		10kbps

3.3.2. Simulation Results

We set the distance between the transmitter and the receiver 10m, 20m, 30m, 40m, 50m, 60m, and 70m to measure the performance of APCM. There are 98 nodes exclusive of the

transmitter and the receiver distributed randomly in the simulation network. The positions of these 98 nodes are chosen randomly and they are not changed during the simulation time. The transmission between the transmitter and the receiver is always transmitting and it is not changed by the probability P_{TT}, and P_{IT}. The behavior of other nodes is changed by the probability P_{TT}, and P_{IT}. We observe the interference relationship between the transmitter and other nodes.

Depending on the parameters listed in Table 5, we run the simulation 100 times and each simulation time is 500 seconds. We measure the transmission between the transmitter and the receiver. The measurement metrics are energy consumption of the transmitter, throughput between the transmitter and the receiver, and energy consumption per byte of the transmitter.

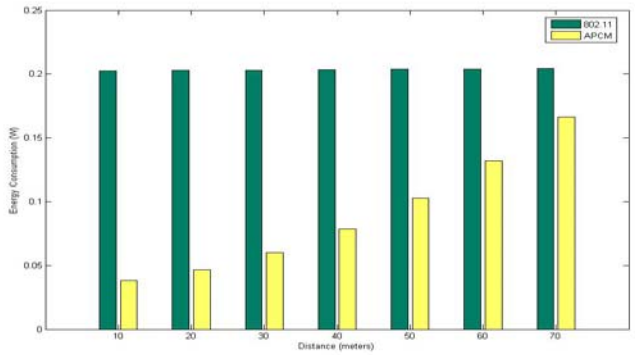

Figure 3.11. Energy consumption of the transmitter

Figure 3.11 is energy consumption of the transmitter of 802.11 and APCM in different distances. We are able to observe that when the distance between the transmitter and the receiver is small, APCM can save a great quantity of energy. When the distance between the transmitter and the receiver is bigger, the ratio of energy saving is lower. This phenomenon represents that when the distance between the transmitter and the receiver is small, 802.11 wastes a lot of energy in using stronger power level to transmit data. APCM can save up to 81.02 percent energy in this case.

Table 3.5. The result of energy consumption of the transmitter

	10m	20m	30m	40m	50m	60m	70m
802.11	0.20224	0.20264	0.203	0.20322	0.20365	0.20391	0.20425
APCM	0.03838	0.04669	0.06008	0.0786	0.10284	0.13162	0.16593
The ratio of energy saving	81.02%	76.96%	70.40%	61.32%	49.50%	35.45%	18.76%

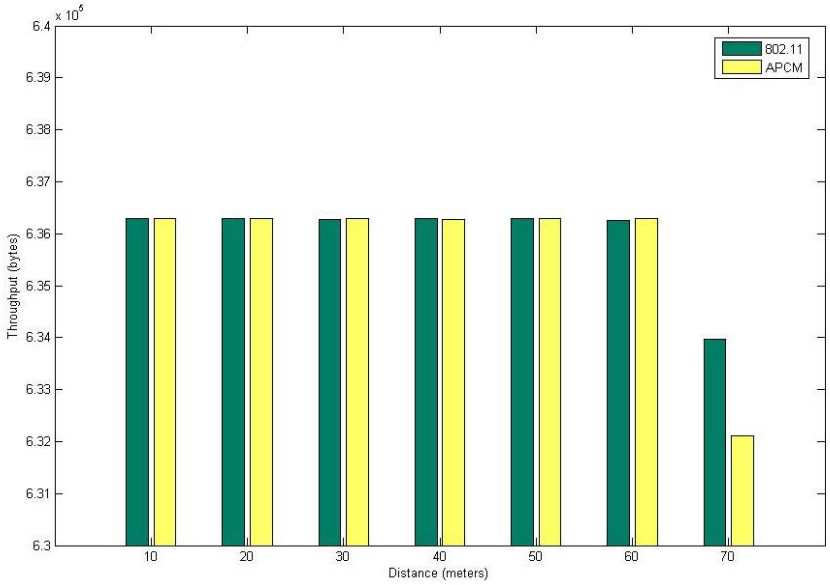

Figure 3.12. Throughput between the transmitter and the receiver

Figure 3.12 is the throughput between the transmitter and the receiver. We observe that when the distance between the transmitter and the receiver is big, the throughput of APCM is lower than that of 802.11 by 0.32 percent. This throughput loss is the cost of energy saving. The throughput loss is a small quantity and affects the performance of the wireless network a little.

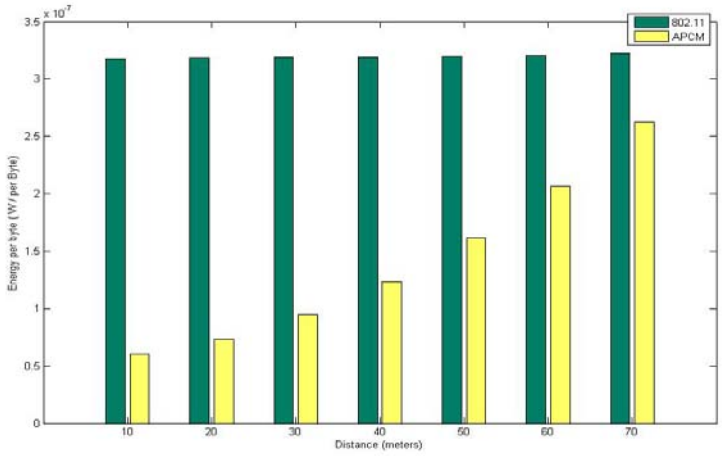

Figure 3.13. Energy consumption per byte of the transmitter

Figure 3.13 is energy consumption per byte of the transmitter of 802.11 and APCM in different distances. We are able to observe that when the distance between the transmitter and the receiver is small, APCM can save a great quantity of energy consumption per byte. When the distance between the transmitter and the receiver is bigger, the ratio of energy saving is lower. It represents that when the distance between the transmitter and the receiver is bigger, adjustable power level is almost the same P_{max}. The saving energy is littler than that of small distance.

Table 3.6. The result of energy consumption per byte of the transmitter

	10m	20m	30m	40m	50m	60m	70m
802.11	3.18*10^-7	3.18*10^-7	3.19*10^-7	3.19*10^-7	3.20*10^-7	3.20*10^-7	3.22*10^-7
APCM	6.03*10^-8	7.34*10^-8	9.44*10^-8	1.24*10^-7	1.62*10^-7	2.07*10^-7	2.63*10^-7
The ratio of energy consumption per byte	81.04%	76.92%	70.41%	61.13%	49.375%	35.31%	18.32%

3.4. Discussion

In this thesis, we have derived the relationship between transmission power and interference range by mathematical models. We derive the scope of interference area from the value of interference range. We also propose some mathematical models to present the relationships between transmission power and interference area. By these models, we estimate

the probability of transmission success and calculate the expected value of energy consumption. In addition, we propose APCM mechanism to evaluate the optimal transmission power level to minimize the whole of energy consumption and satisfy the quality of service in Ad hoc wireless networks. As shown in the simulations, up to 32 percent energy can be conserved, packet loss rate will be reduced 6 percent and enhances the utilization of energy to 22 percent.

There are some issues in this thesis that we can improve in the future:

1. In this thesis, we model the relationship between the transmission power and interference area. We discuss the influence of interference on transmission. In addition, there are still some other reasons to result in unsuccessful transmission. For example, collision also results in failure of transmission. We should add the influence of collision on transmission into our model.
2. We discuss the energy consumption of transmitters in this thesis. Transmitters use the adaptive power level to transmit data in order to save energy. Nodes consume energy not only on transmitting data, but also on receiving data. We do not model the energy consumption on receiving data. We should add this energy consumption into our estimated energy consumption. This lets our model more close to reality.
3. In this thesis we discuss transmission energy consumption between two adjacent nodes. In fact, energy consumption of nodes also depends on the routing path. We also should consider the method of choosing routing path into our model.

Chapter 4

Power Control by Probing Radius Adjustment in Probing Environment Sensor Networks

Micro-sensors and low-power wireless communications techniques have enabled dense deployment of distributed sensor nodes in large-scale wireless sensor networks (WSNs). With limited memory, constrained computing power and short battery lifetime, the sensor nodes perform significant signal processing, network self-configuration and certain computations to achieve objectives of robustness, scalability, and lifetime extension [AD02]. Therefore, the most challenging issue in WSNs is limited and un-rechargeable energy provision, many researches effort aim at improving the energy efficiency from different aspects. It is desirable to develop energy-efficient processing techniques that minimize power requirements across all levels of the protocol stack and, at the same time, minimize message passing for network control and coordination. In general, the energy efficiency challenges encountered in building WSNs can be categorized under four classes:

1. *Hardware design*: This category includes the entire range of design activities related to the hardware platforms that comprise WSNs. MEMS sensor technology is an important aspect of this category. Digital circuit design and system integration for low power consumption are also important issues [GM98] as well as design of a low power sophisticated RF front end and associated control circuitry.
2. *Applications*: WSNs are always required to satisfy applications' requirements.

Unfortunately, to improve the qualities of these requirements usually lead to the heavy burden in energy consumption. Therefore, some algorithms designed for WSNs often sacrifice application-desired qualities to save energy in order to prolong the operational lifetime of these networks.

3. *Routing Protocols*: Several energy-aware routing protocols have been proposed to capture the requirement of reducing route cost in terms of energy consumption. Some protocols [WA02, SN02, JW02, AT99] use clustering schemes to save energy for static sensor networks by reducing data redundancy and balancing energy consumption. Moreover, protocols proposed by Manjeshwar and Agarwal [AD01, AM02] try to reduce the number of transmissions by using threshold- sensitive schemes.

4. *Network deployments*: Deployment of WSNs can be in random fashion or planted manually. Regular grids (square, triangle, hexagon) and uniformly random distributions are widely used analytically tractable models. Regular grids overlaid with Gaussian variations in the positions may be more accurate. In general, uniformly random distributions with equilibrium density of sensor nodes will avoid heavy data redundancy in high density of sensor nodes and weak network topology in low density of sensor nodes.

The exploitation of sleeping modes [CS99, CT01] is imperative to prevent sensor nodes from wasting energy in receiving packets unintended for them. Combined with efficient medium access protocols, the “sleeping” approach could reach optimal energy efficiency. F. Ye, et al. [FJ03] propose the probing environment sensor network (PEAS) to maintain a necessary set of working nodes and turning off redundant ones. Each sensor node has three operation modes: Sleeping, Probing and Working. Each sleeping node wakes up in a while to

probe its neighborhood and to find out whether there already exists a working neighbor within a local probing range. Then, the node decides whether itself should start working or go back to sleep. Therefore, sleeping nodes can replace any failed working nodes as needed. The probing environment technique extends a sensor network's lifetime linearly proportion to the number of deployed sensor nodes since this technique consumes only slight energy and withstands a large number of sensor node failures.

Base on the operation of probing environment sensor networks, the deployment of working nodes will be uniformly random distribution on condition that these nodes own equivalent probing range. The density of working nodes is adapted to their probing range, and the probing range can be adjustable by signal power of the probing messages. To settle appropriate probing range is a significant factor in these dimensions of power consumption, sensing rate and scalability of WSNs:

1. *Power consumption*: to increase sensor nodes' probing range will lead to the fewer working nodes. In this condition, more sensing nodes in sleeping mode can save their energy power, but working nodes will spend larger energy to process and transmit the sensing data. Fewer working nodes can avoid data redundancy and mutual interference. In this paper, we use mathematical analyses and simulation results to prove the whole power consumption of WSNs will reduce exponentially while the probing range is enlarged.
2. *Scalability*: to increase sensor nodes' probing range will lead to the longer distance between working nodes. If the distance between working nodes is larger than the transmission range of these working nodes, the scalability of WSNs will be disintegrated because working nodes can not forward their sensing data to the base station by their neighbor working nodes. In this paper, we will prove that if the radius of probing range is larger than $1/\sqrt{3}$ radius of transmission range, the scalability of WSNs will be

disintegrated.

3. *Sensing Rate*: If the probing range is more than the sensing range, these sensing ranges of all working nodes can not cover all sensing area. It will lead to parts of sensing area in where the data will not be sensed called *dead areas*. The *sensing rate* (*SR*) of WSNs is defined as the ratio of the data can be sensed to the sensing data in the sensing area of WSNs. The requirement of WSNs' *SR* is application specific, i.e., the *SR* must be sufficient to satisfy applications' requirement. For example, the *SR* requirement of precision tactical surveillance is different from that required for a periodic weather-monitoring task. When the sensing data is distributed uniformly over the sensing region, the *SR* of WSNs can be obtained by

$$SR = 1 - \frac{dead\ areas}{sensing\ area} \quad (4\text{-}1)$$

To enlarge the probing range in WSNs is efficient in reducing the power consumption, but it is unfavorable to the network scalability and sensing rate. In this paper, we formulate the influences of sensor nodes' probing range upon energy consumption and sensing rate of WSNs by mathematical models. According to these formulae, a probing radius adjusting mechanism "PRAM" is proposed to control the trade-off between energy efficiency, network scalability and sensing rate. By this mechanism, the desirable probing range can be presented to minimize the energy consumption based on the premise that the required sensing rate and scalability of WSNs can be satisfied.

4.1. Assumptions and Network Models

In order to explicitly formulate the features in terms of *SR* and energy consumption in PEAS, we assume reasonably that WSNs conform to these conditions:

1. Sensor nodes are positioned randomly in a two-dimensional sensing area, and all of them are stationary.
2. Sensor nodes are equipped with wireless transmitters and receivers using antennas that are omni-directional (i.e., isotropic radiation).
3. All sensor nodes are homogeneous, i.e., they have same physical property, transmitting range, sensing range, probing range and power capacity.
4. The sensing data is distributed uniformly over the sensing area (i.e., there is same quantity of sensing data in each unit of sensing area).
5. The density of sensor nodes is enough such that the whole sensing area can be covered by the sensing rages of these nodes.
6. The density of sensor nodes is enough such that sensing data of each sensor node can be either directly transmitted to the base station or forwarded by its neighbor sensor nodes within its transmission range.

Consider the WSN composed by a set V of sensor nodes, with $|V| = n$. Nodes are deployed in a 2-dimensional square sensing area R with each side measuring l, i.e., $R = l^2$. The *working range* of a working node is defined as the range around this working node, such that all the points in the range are closer to this working node than any other working node. The *neighbors* of a working node are these working nodes which working ranges are neighbor with this working node's working range. Because all sensor nodes own same probing range, working nodes are distributed uniformly. Therefore, by Voronoi diagram [FR00], the working range of each working node is either a hexagon or a square grid. In this paper, we characterize the essential features of sensor network by the hexagon working range; there are same features in the square grid working range.

Some property parameters are defined in our model:

1. R_P is the radius of sensor node's probing range.

2. R_T is the radius of sensor node's transmission range.

3. R_S is the radius of sensor node's sensing range.

4. N_W is the number of working nodes in the WSN.

5. A_W is the working range.

6. D_N is the distances from a working node to its neighbors.

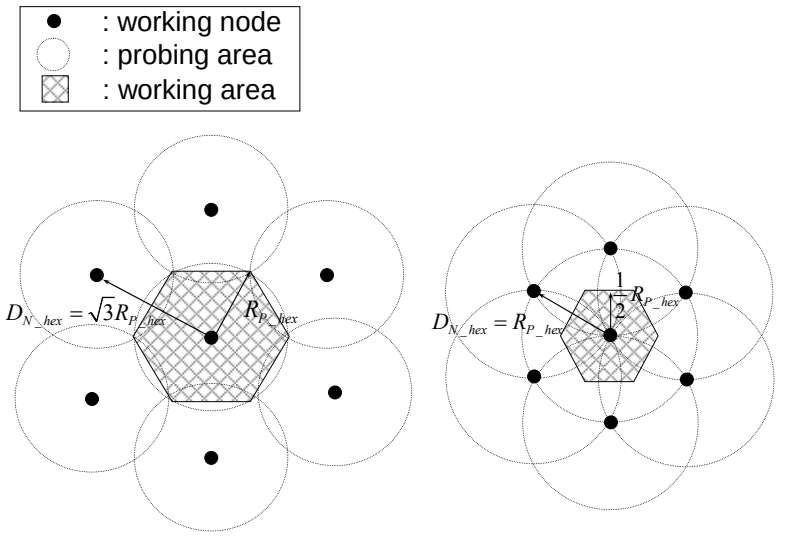

(a) Maximum working area in hexagon (b) Minimum working area in hexagon

Figure 4.1. The working area in a hexagon.

As shown in Fig. 4.1, the length of each edge in the hexagonal working range is $\frac{\sqrt{3}}{3} D_N$.

Therefore, the working range is

$$A_W = \frac{\sqrt{3}}{2} {D_N}^2 . \qquad (4\text{-}2)$$

Base on the operation of PEAS, D_N is maximum when its neighbor nodes are located

on the edge of its probing range, as Fig.4.1(a), and the value is $\sqrt{3}R_P$. Whereas D_N is minimum when its neighbor nodes are located on the edge of its working range, as shown in Fig. 4.1(b), and the value is R_P. Therefore, the boundary of D_N is

$$R_P \le D_N \le \sqrt{3}R_P \tag{4-3}$$

Since the neighboring working nodes are randomly distributed inside the area according to the boundary of D_N, the probability density function (PDF) of D_N is

$$f(D_N) = \frac{2D_N\pi}{(3R_P{}^2 - R_P{}^2)\pi} = \frac{D_N}{R_P{}^2}. \tag{4-4}$$

Therefore, the expectations of D_N and A_W can be obtained by Eq. 4-5 and 4-6.

$$E[D_N] = \int_{R_P}^{\sqrt{3}R_P} D_N \frac{D_N}{R_P{}^2} d(D_N) = \frac{3\sqrt{3}-1}{3} R_P. \tag{4-5}$$

$$E[A_W] = \int_{R_P}^{\sqrt{3}R_P} \frac{\sqrt{3}}{2} D_N{}^2 \frac{D_N}{R_P{}^2} d(D_N) = \sqrt{3}R_P{}^2. \tag{4-6}$$

When the sensing area R is hugely more than A_W, the approximate value of N_W is

$$N_W \approx \frac{R}{A_W} = \frac{2R}{\sqrt{3}D_N{}^2}. \tag{4-7}$$

Therefore, the approximate expectation of N_W can be obtained by

$$E[N_W] \approx \int_{R_P}^{\sqrt{3}R_P} \frac{2R}{\sqrt{3}D_N{}^2} \frac{D_N}{R_P{}^2} d(D_N) = \frac{2R}{\sqrt{3}R_P{}^2} (\ln(\frac{\sqrt{3}}{3R_P}) - \ln(\frac{1}{R_P})). \tag{4-8}$$

Moreover, in order to meet the assumption 6 (i.e., for each working node, at least one working node or base station must be located in the transmission range of this node), D_N must be less than R_T. By Eq. 4-3, R_P has an upper boundary as

$$R_P \le \frac{1}{\sqrt{3}} R_T. \tag{4-9}$$

4.2. The Power Consumption Analyses and Formulae

We use the radio model proposed in [WA00, SC02] to formulate the power consumption in the sensor node's physical property. Let E_p is the power consumption of receiving and transmitting a bit of message. It can be expended:

$$E_p(D_T,k) = E_t(D_T,k) + E_r = (\alpha_{amp} D_T{}^k + \alpha_t + \alpha_r), \quad (4\text{-}10)$$

where D_T is the reliable distance of radio propagation, α_t and α_r are per bit energy dissipation (in pico-Joule, pJ) in the transmitting and receiving modes respectively, α_{amp} is the per bit energy consumption (in pico-Joule, pJ) for the transmitting amplifier. The values of these parameters depend on the physical property of sensor nodes.

In WSNs, let E_n is the power consumption of a bit sensed data sensed and transmitted to the base station. It can be expended by:

$$E_n = E_p \times W_{SN} \times W_{TN}, \quad (4\text{-}11)$$

where W_{SN} is the number of working nodes sensed this bit data. Because sensing data and working nodes are distributed uniformly over the sensing area. The expectation value of W_{SN} is estimated as Eq. 4-12. W_{TN} is the number of working nodes along the routing paths from the sensing node which sensed this bit data to the base station. The approximated value of W_{TN} is as Eq. 4-13, where D_B is the distance from this bit data to the base station.

$$W_{SN} = \frac{N_W \times \pi R_S{}^2}{R} \quad (4\text{-}12)$$

$$W_{TN} \approx \frac{D_B}{D_N} \quad (4\text{-}13)$$

Therefore, by Eqs. 4-7, 4-10, 4-11, 4-12, and 4-13, the energy consumption is expended

as

$$E_{n\_hex} \approx (\alpha_{amp} {D_T}^k + \alpha_t + \alpha_r) \times \frac{2\pi D_B {R_S}^2}{\sqrt{3} {D_{N\_hex}}^3} \tag{4-14}$$

By Eq. 4-14, the energy consumption depends on the parameter quadruplet (D_T, k, D_B, R_p). The optimal R_p can be estimated to minimize E_n by these values of parameters D_T, k and D_B. The distance of radio propagation D_T can be either constant or adjustable depending on the characteristics of each sensor node. If the distance of radio propagation is constant, $D_T = R_T$; whereas it is adjustable, $D_T = D_N$. The value of k depends on the geographical features of sensing area. In free space model, the value of k is 2 [HF46]. In two ray ground model, value of k is 4 [TSR]. The value of D_B depends on the positions of base station and sensed data. We consider two conditions of the base station position: at the center of sensing area or the corner of sensing area. D_B in this two conditions are represented as D_{B_center} and D_{B_corner} respectively. Their PDF are as Eq. 4-15 and 4-16.

$$f(D_{B\_center}) = \frac{8 D_{B\_center}}{l^2} \tag{4-15}$$

where $0 \le D_{B\_center} \le \frac{l}{2}$.

$$f(D_{B\_corner}) = \frac{2 D_{B\_corner}}{l^2} \tag{4-16}$$

where $0 \le D_{B\_corner} \le l$.

Table 4.1. Eight scenarios with different values of parameters.

Scenario 1	$D_T = R_T$	$k = 2$	D_{B_center}
Scenario 2			D_{B_corner}

Scenario 3		$k=4$	D_{B_center}
Scenario 4			D_{B_corner}
Scenario 5	$D_T = D_N$	$k=2$	D_{B_center}
Scenario 6			D_{B_corner}
Scenario 7		$k=4$	D_{B_center}
Scenario 8			D_{B_corner}

We define eight scenarios as shown in table 4.1 to formulate the energy consumption in WSNs. These expectations of energy consumption are presented in table 4.2.

Table 4.2. The expended energy consumptions in eight scenarios.

Scenario 1	$E[E_n] = (\alpha_{amp} {R_T}^2 + \alpha_t + \alpha_r) \times \frac{2(\sqrt{3}-1)\pi \times l \times {R_S}^2}{9{R_P}^3}$
Scenario 2	$E[E_n] = (\alpha_{amp} {R_T}^2 + \alpha_t + \alpha_r) \times \frac{4(\sqrt{3}-1)\pi \times l \times {R_S}^2}{9{R_P}^3}$
Scenario 3	$E[E_n] = (\alpha_{amp} {R_T}^4 + \alpha_t + \alpha_r) \times \frac{2(\sqrt{3}-1)\pi \times l \times {R_S}^2}{9{R_P}^3}$
Scenario 4	$E[E_n] = (\alpha_{amp} {R_T}^4 + \alpha_t + \alpha_r) \times \frac{4(\sqrt{3}-1)\pi \times l \times {R_S}^2}{9{R_P}^3}$
Scenario 5	$E[E_n] = 2(\sqrt{3}-1)\pi \times l \times {R_S}^2 \times \left(\frac{\alpha_{amp}}{3\sqrt{3}R_P} + \frac{\alpha_t + \alpha_r}{9{R_P}^3} \right)$
Scenario 6	$E[E_n] = 4(\sqrt{3}-1)\pi \times l \times {R_S}^2 \times \left(\frac{\alpha_{amp}}{3\sqrt{3}R_P} + \frac{\alpha_t + \alpha_r}{9{R_P}^3} \right)$
Scenario 7	$E[E_n] = \frac{2}{9}\pi \times l \times {R_S}^2 \times \left(\frac{(3\sqrt{3}-1)R_P}{3} \times \alpha_{amp} + \frac{\sqrt{3}-1}{{R_P}^3} \times (\alpha_t + \alpha_r) \right)$
Scenario 8	$E[E_n] = \frac{4}{9}\pi \times l \times {R_S}^2 \times \left(\frac{(3\sqrt{3}-1)R_P}{3} \times \alpha_{amp} + \frac{\sqrt{3}-1}{{R_P}^3} \times (\alpha_t + \alpha_r) \right)$

The expectation of E_n will be exponential decreased by the increasing the value of R_P. In other words, increasing the sensor nodes' probing range will minimize efficiently the power

consumption in probing environment WSNs. By Eq. 4-9, when the radius of sensor nodes' probing range is $1/\sqrt{3}$ of the radius of their transmission range, WSNs can minimize the power consumption on the maintainability of its scalability. Fig. 4-4 shows the relationship between the power consumption and R_P by these parameters listed in table 4.3.

Table 4.3. The values of energy consumption parameters

Parameter	Value
R_S	50m
R_T	80m
n	400
l	300m
α_{amp}	100pJ/bit/m^2 (Free Space Model) 0.013pJ/bit/m^2 (Two Ray Ground Model)
α_t	50nJ/bit
α_r	50nJ/bit

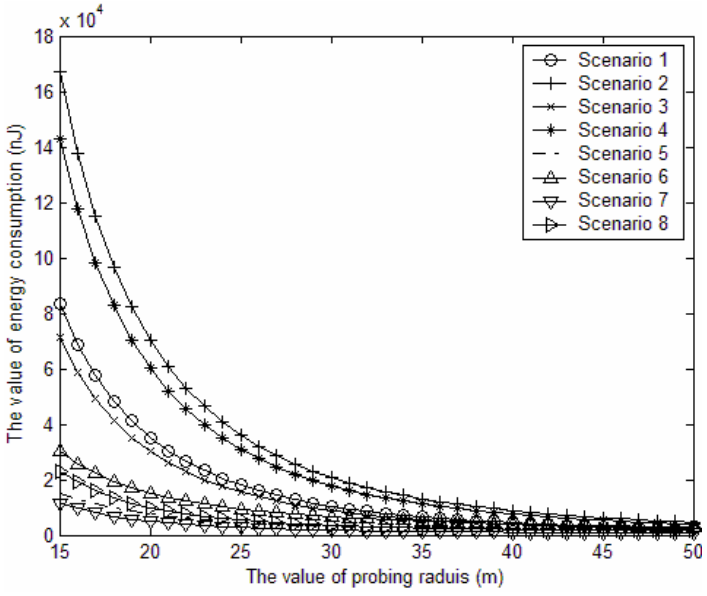

Figure 4.2. The energy consumption in the hexagonal working range model.

4.3. The Sensing Rate Analyses and Formulae

The power consumption of probing environment WSNs can be reduced as the result of increasing sensor nodes' probing range. Unfortunately, the sensing ranges of fewer working nodes can not cover the whole sensing area. It will lead to the dead spaces and reduce the sensing rate of WSNs. Therefore, we make efforts to formulate the influence of sensor nodes' probing range on the both power consumption and sensing rate of WSNs. The sensing rate of WSNs can be evaluated by the cover rate of sensing ranges as E.q. 4-1. This cover rate is irregularly changeable as a result of the WSNs topology changing. It is difficult to evaluate the actual cover rate. By our network model, we attempt to define some mathematical formulae in the relationship between the probing range and the sensing rate.

In our network model, as shown in Fig. 4.2, dead spaces will occur when D_N is not less than $\sqrt{3}R_S$, and the dead spaces are also distribute over the sensing area uniformly. By E.q. 4-1, the mathematical relationship between D_N and the sensing rate SR can be defined in Eq. 4-17.

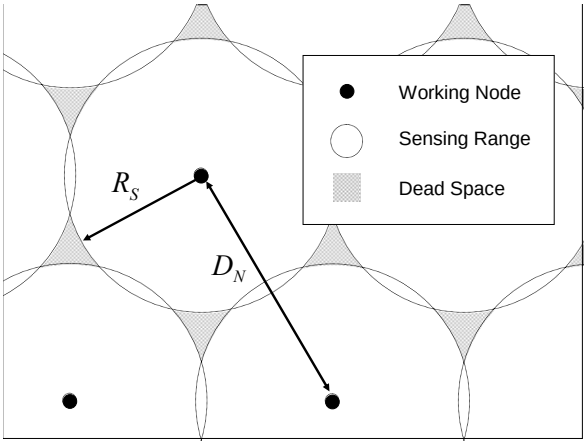

Figure 4.3. The dead space in a hexagon model

$$SR = \begin{cases} 1, & D_N \le \sqrt{3}R_S \\ 1 - \dfrac{2 \times N_W \times G(D_N, R_S)}{R}, & \sqrt{3}R_S < D_N < 2R_S \\ \dfrac{N_W \times \pi \times {R_S}^2}{R}, & D_N \ge 2R_S \end{cases} \quad (4\text{-}17)$$

where $G(D_N, R_S) = \frac{\sqrt{3}}{4}{D_N}^2 - \frac{1}{2}\pi{R_S}^2 + 3 \times ({R_S}^2 \cos^{-1}\frac{D_N}{2R_S} - \frac{1}{4}D_{N\_hex}\sqrt{4{R_S}^2 - {D_N}^2})$

By Eq. 4-7 and 4-17, *SR* can be decided by the factors R_S and D_N as shown in Eq. 18. Because that all sensor nodes are homogeneous, R_S can be defined as a constant value. Therefore, we can calculate the expectations of *SR* by the PDF of D_N shown in Eq. 4. The expectations of *SR* , *E(SR)*, is shown in Eq. 19-23.

$$SR = \begin{cases} 1, & D_N \le \sqrt{3}R_S \\ 1 - \dfrac{4 \times G(D_N, R_S)}{\sqrt{3}{D_N}^2}, & \sqrt{3}R_S < D_N < 2R_S \\ \dfrac{2 \times \pi \times {R_S}^2}{\sqrt{3}{D_N}^2}, & D_N \ge 2R_S \end{cases} \quad (4\text{-}18)$$

where $G(D_N, R_S) = \frac{\sqrt{3}}{4}{D_N}^2 - \frac{1}{2}\pi{R_S}^2 + 3 \times ({R_S}^2 \cos^{-1}\frac{D_N}{2R_S} - \frac{1}{4}D_{N\_hex}\sqrt{4{R_S}^2 - {D_N}^2})$

$$E(SR) = F_1(\sqrt{3}R_P) - F_1(R_P) \quad where\ R_P \le R_S \quad (4\text{-}19)$$

$$E(SR) = F_1(\sqrt{3}R_S) - F_1(R_P) + F_2(\sqrt{3}R_P) - F_2(\sqrt{3}R_S) \quad where\ R_S < R_P < \frac{2}{\sqrt{3}}R_S \quad (4\text{-}20)$$

$$E(SR) = F_3(\sqrt{3}R_P) - F_3(2R_S) + F_2(2R_S) - F_2(\sqrt{3}R_S) + F_1(\sqrt{3}R_S) - F_1(R_P)$$
$$where\ \frac{2}{\sqrt{3}}R_S < R_P \le \sqrt{3}R_S \quad (4\text{-}21)$$

$$E(SR) = F_3(\sqrt{3}R_P) - F_3(2R_S) + F_2(2R_S) - F_2(R_P) \quad where\ \sqrt{3}R_S < R_P \le 2R_S \quad (4\text{-}22)$$

$$E(SR) = F_3(\sqrt{3}R_P) - F_3(R_P) \quad where\ R_P > 2R_S \quad (4\text{-}23)$$

There functions F_1, F_2 and F_3 are shown as Eq. 24-26.

$$F_1(D_N) = \int 1 \times f(D_N)d(D_N) = \frac{{D_N}^2}{2{R_P}^2} \quad (4\text{-}24)$$

$$F_2(D_N)=\int(1-\frac{4G(D_N,R_S)}{\sqrt{3}D_N^{\,2}})\times f(D_N)d(D_N)$$
$$\cong\frac{2\pi R_S^{\,2}}{\sqrt{3}R_P^{\,2}}\ln(D_N)-4\sqrt{3}\frac{R_S^{\,2}}{R_P^{\,2}}(\frac{\pi}{2}\ln(D_N)-\frac{D_N}{2R_S}-\frac{D_N^{\,3}}{144R_S^{\,3}}-\frac{3D_N^{\,5}}{6400R_S^{\,5}}) \quad (4\text{-}25)$$
$$+\frac{\sqrt{3}}{R_P^{\,2}}(\frac{D_N}{2}\sqrt{\frac{R_S^{\,2}}{4}-D_N^{\,2}}+\frac{R_S^{\,2}}{8}\sin^{-1}(\frac{2D_N}{R_S}))$$

$$F_3(D_N)=\int\frac{2\pi R_S^{\,2}}{\sqrt{3}D_N^{\,2}}\times f(D_N)d(D_N)=\frac{2\pi R_S^{\,2}}{\sqrt{3}R_P^{\,2}}\ln(D_N) \quad (4\text{-}26)$$

We present the relationship between the variable of $E(SR)$ with R_P as shown in Fig. 4-4. When R_P is not more than R_S, *E(SR)* is 1 and the value will be exponential decreased by the increasing of R_P.

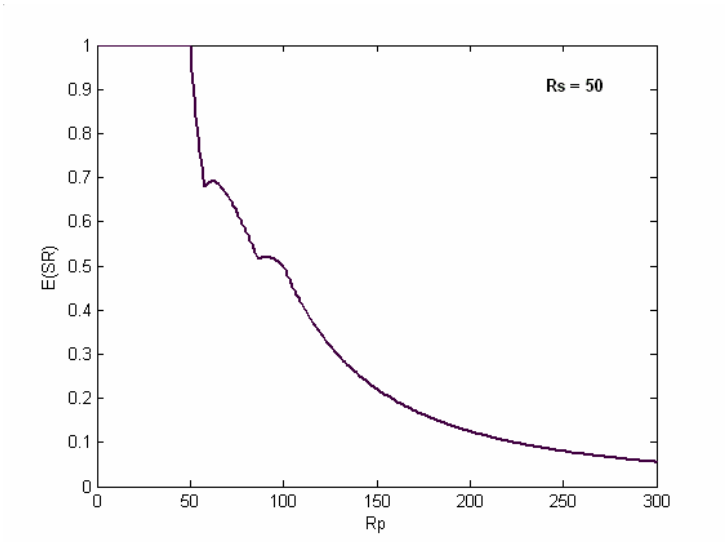

Figure 4.4. The variation of expectative sensing rate

4.4. The operation of PRAM

The main function of PRAM is to examine the required *SR* in WSNs by control the value of R_P. In the session 4.3, we have formulated the relationship between the expectations of *SR* and R_P in E.q. 4-19,20,21,22, and 23. The appropriate value of R_P in the condition to satisfy the expectative *SR* required from applications can be acquired by these formulae. The

flow chart of PRAM is shown in Fig. 4.5.

Step 1. Input the values of *E(SR)* and R_S
Step 2. Find the maximum of R_P which satisfies E.q. 4-23.
If R_P is existent **Then** go to ***Step 8***.
Step 3. Find the maximum of R_P which satisfies E.q. 4-22.
If R_P is existent **Then** go to ***Step 8***.
Step 4. Find the maximum of R_P which satisfies E.q. 4-21.
If R_P is existent **Then** go to ***Step 8***.
Step 5. Find the maximum of R_P which satisfies E.q. 4-20.
If R_P is existent **Then** go to ***Step 8***.
Step 6. Find the maximum of R_P which satisfies E.q. 4-19.
If R_P is existent **Then** go to ***Step 8***.
Step 7. $R_P = R_S$
Step 8. **If** R_P more than $\frac{1}{\sqrt{3}} R_T$ **Then** $R_P = \frac{1}{\sqrt{3}} R_T$
Step 8. Output R_P

Figure 4.5. The Flow Chart of PRAM

In these steps 2-6 of PRAM, we try to find the maximum value of R_P to result in the desired expectation value of *SR*. Because the expectation of E_n will be exponential decreased by the increasing of R_P, the desirable probing range can be presented to minimize the energy consumption based on the premise that the required sensing rate can be satisfied. If the value of R_P is not existent in steps 2-6, its value will be set to R_S, it is the maximum value to result in the expectation value of *SR* is 1. Therefore, the operation of PRAM can calculate the appropriate value of R_P to satisfy the expectative *SR* required from applications and minimize the power consumption in order to extend the lifetime of WSNs.

4.5. Simulation

In this section, we demonstrate how PRAM improves the performance of PEARS in

satisfy the applications sensing rates. We use ns-2 simulator with the CMU wireless extension to validate the performance of PRAM. Some relational parameters are listed in table 4. We assume the sensing rates of application requested are 1, 0.7, and 0.5. By the operation of PRAM, the appropriate values of R_P can be obtained which are 50, 57.4 and 86.7. As shown in Fig. 4.8, we present the variations of sensing rate in four different conditions: non-pease, R_P = 50, R_P = 57.4, and R_P = 86.7.

Table 4. 4. The parameters of simulation network

Description	Parameter	Value
Sensing Area	A_{sS}	50*50 (m^2)
Energy of each sensor node	E_S	100000 dbm
Number of sensor nodes	N_S	2000
Sensing range radius	R_S	5 (m)
Transmission range radius	R_T	8 (m)

As shown in Fig. 4.8, when the requested sensing rates are 1, 0.7, and 0.5, the life times will be about 4, 7, and 12 times than non-peas environment. Simulation results show the values of probing radius obtained by PRAM can satisfy the sensing rates required by applications and extend the life times of sensor network.

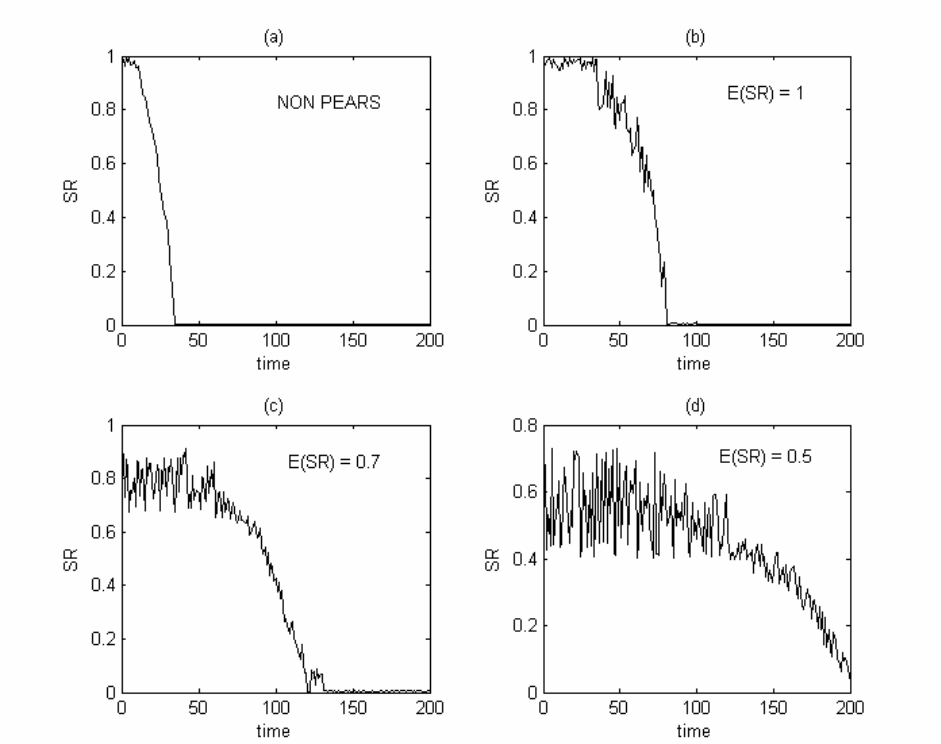

Figure 4.6. The sensing rates in different probing ranges.

Chapter 5

A New Energy-Proportional Routing Approach in Sensor Networks

This chapter proposes an energy-proportional routing (EPR) algorithm, which effectively extends the lifetimes of sensor networks. The algorithm makes no specific assumption on network topology and hence is suitable for improving sensor networks with clustering. To optimally utilize energy, clusters that conserve energy are ideal candidates as intermediate units for forwarding data from others. To balance the load, first, the proposed algorithm predicts energy consumption of each node in each round. Then the algorithm controls the energy consumption of each unit as close as possible to the threshold representing the energy utilization mean value among clusters. Finally the algorithm checks satisfaction of the energy constraints in terms of distances and predicted data amounts. The proposed algorithm performs routing by determining whether a cluster head or a node should either undertake forwarding tasks or transmit data to intermediate hops. In this way, energy dissipation is evenly distributed to all units and the lifetime of the whole wireless sensor network is ultimately extended. The algorithm applies hierarchically to different levels of network topology. In addition to experiments, the mathematical proofs of lifetime extension by the proposed routing algorithm are given in accordance with three widely accepted

criteria – total energy dissipation, the number of live nodes in each round and the throughput (data amount per round).

In the field of sensor networks, energy-awareness schemes are more and more complex and important [1-9]. Among the sensor network clustering algorithms [WA02, PC98, HI03, IW02, GM03, SK02], the generalized and improved LEACH [WA02] from [WC00, WS00, WH00] is a typical example of an effective clustering scheme for energy reduction purposes. In [WA02], sensor nodes are partitioned into clusters each of which has a cluster head responsible for aggregating data from its members. The cluster head then compresses the aggregations and sends the compressions to the base station. Based on the distributive algorithm, the nodes are randomly selected as cluster heads in accordance with the probability distribution proposed in [WA02]. After the LEACH algorithm, successive ideas for energy-efficient clustering and routing algorithms are proposed [SK02, SL02, OS04, OY04, SD05]. In [SK02, SL02], the PEGASIS algorithm, starting at the farthest node, a chain is formed greedily so that data from each node arrives at the leader node and the leader aggregates the data for sending to the base station. The leader in PEGASIS is the top confluent node that aggregates multiple chains' data. The leader passes a token to the end node of a branch path to aggregate data along that path. Other confluent nodes exist in different levels of hierarchy. Only confluent nodes at a level will be active in the next level. We can regard the group of a confluent node along with its sub-chains before it as a special type of cluster in which multi-hop intra-cluster routing is performed and hence we regard confluent nodes as cluster heads such that inter-cluster routing is performed.

In [OS04, OY04], the HEED algorithm periodically selects cluster heads according to a hybrid of the node residual energy and the cost such as node proximity to its neighbors or node degree. At the beginning, tentative cluster heads are randomly selected among nodes with higher residual energy. The member nodes within the communication range of a cluster

head join the cluster head according to the cost called average minimum reachable power. Cluster nodes iteratively double its probability to be a cluster head until the probability reaches 1. A tentative cluster head becomes a final cluster head when the probability reaches 1. The HEED algorithm primarily contributes to clustering and there is not specific routing algorithm proposed for HEED in [OS04, OY04].

The BCDCP algorithm [SD05], by selecting among the nodes with larger energy level than the average, the most distant pair of nodes, say $s1$ and $s2$, form subsequent two clusters and group each of the remaining nodes in the current cluster with either $s1$ or $s2$, whichever is the closest. This binary splitting continues until enough clusters are formed. After the clusters are formed, the multi-hop routing among the clusters uses the minimum spanning tree approach then randomly chooses a cluster head to aggregate and forward all the data to the base station.

We discuss intra-cluster and inter-cluster communications of related works [OS04, OY04, SD05] as follows. Elegant methods of clustering and routing were proposed in [WA02, PC98, HI03, IW02, GM03]. Clustering algorithms such as those in [OS04, OY04, SD05] group sensor nodes with cluster heads regarding either the least energy costs or the shortest distances. In [SK02, SL02], the PEGASIS takes greedy method, which means selecting the node with the least energy cost as the next hop for forwarding. For inter-cluster communication, the BCDCP [SD05] uses the minimum spanning tree as the routing approach regarding again the least total energy cost. While assuming packet length and data amounts are fixed, these works perform very low-cost clustering. However, the least energy cost does not mean the longest lifetime when data amounts and residual energy are not evenly distributed especially among heterogeneous sensors. To balance energy loads, in these articles sensor nodes either take turns to be a cluster heads or according to a random scheme to be selected as cluster heads. For examples, sensor nodes in PEGASIS [SK02, SL02] take

turns to be confluent node of different levels and BCDCP [SD05] random selects one among cluster heads to forward the final fused data to the base station. Taking turns or random scheme makes the cluster heads share energy loads in the whole lifetime of the sensor network. However, this fairness does not mean longer lifetime extension if data amounts and residual energy of clusters are quite different. The unbalance situation could happen as follows. Some clusters or nodes could potentially be busy transmitting data for an extended period while others were not. For inter-cluster communication, those clusters that have been busy transmitting data will quickly die out due to very low residual energy left. The remaining clusters, in contrast, having had less data to transfer, produce few aggregations. Consequently, the quality of the sensor network decays dramatically to an unacceptable level and the lifetime of the network is reduced. The same situation happens in intra-cluster communication when member nodes have variable data amounts and quite different transmission distances to their destinations.

This chapter proposes an *Energy-proportional Routing* (EPR) algorithm to overcome the above problems. When a source node transmits the gathered data to a destination e.g., the base station, via intermediate nodes, the intermediate nodes can evenly share the responsibility of the *load* in a round. We call the concept *energy-proportional balance,* which is different from the balance concepts in [9-13]. The EPR algorithm can be hierarchically applied both to intra- and inter-cluster communications. For intra-cluster communication, the EPR replaces the least energy cost with the optimal energy proportion for cluster head election and communication. The balance concept is also different from [GM03] where the clusters are formed according to the nodes' geometrical deployment. The balancing in [GM03] is based on minimal variance of cardinality of clusters since the assumption in [GM03] is that all sensor nodes produce data at the same rate. For inter-cluster communications, the operation steps of the proposed algorithm are as follows. First, sensor

nodes are formed into clusters such as those in many state-of-art clustering algorithms for sensor networks [WA02, PC98, HI03, IW02, GM03]. Second, every cluster head predicts the amount of data to be transmitted according to the Markov model. This prediction is useful in calculating local energy utilization for each cluster head. In some cases, the data amount of a cluster is known without prediction before communication. Finally, for those cluster heads having higher energy dissipation than the energy mean value, we adopt a novel routing algorithm to direct their data to those clusters having been less active for an extended period and having much more energy remaining. In this way, total energy dissipation of the sensor network is kept evenly distributed and the expected lifetime is extended.

5.1. Energy Proportional Balance in Sensor Networks

In order to understand the relation between the residual energy of a sensor node and the cost (the dissipated energy from the sensor node to the other sensor nodes), we define data capacity to show this relation in Eq. 5-1. It actually shows the maximal amount of data that can be forwarded.

$$D_{ij,total} = \frac{E_i}{E_{Tx}(1, d_{ij})} = \frac{E_i}{\alpha_t + \alpha_{amp} d_{ij}^2}, \tag{5-1}$$

where $D_{ij,total}$ is the maximum amount of data to be transmitted from node i to node j, E_i is the remaining energy in Joules of node i, and $E_{TX}(1, d_{i,j})$ is the additional estimated energy dissipation per bit when the bit is transmitted from node i to node j. According to the radio frequency transmitting model for energy widely accepted in [WA02, PC98, HI03, IW02, GM03], transmitting k bytes across distance d will consume $E_{TX}(k, d) = k\alpha_t + k\alpha_{amp}d^2$.

To predict sensing data amount rather than to predict energy consumption such as in [RB02] of a node in each round, we apply the Markov model to save computation overhead since it is much simpler. The computation of prediction itself dissipates energy. Therefore,

low complexity is an important requirement for the prediction. The proposed prediction steps are as follows: First, we divide the period of a round into T phases each of which is identified with a time stamp. From one time-stamp to the next one, the state of a sensor node will change (state i changes into state s). During a round, a node's state transits at each time stamp t. By using the Chapman Kolmogorov equations, the t-step transition probabilities are represented as

$$P_{is}^{(t)} = \sum_{j=1}^{M} P_{ij}^{(r)} P_{js}^{(t-r)}, 0 < t < T \tag{5-2}$$

Therefore, we calculate the summation of all probability $P_{is}^{(t)}$ over T phases to obtain the number of time steps that a node stays in state s in a round. Suppose a node at state s each time transmits collected k_s-byte of data to its cluster head. We obtain the total predicted data amount in a round that a node n at state s transmits as:

$$D_n^{(s)} = k_s \sum_{t=1}^{T} P_{is}^{(t)} \quad . \tag{5-3}$$

Next, to obtain the predicted data amount of a node, we summate the values $D_n^{(s)}$ for all state s in {1, 2, …, M}. Suppose a cluster is composed of N sensor nodes, the predicted data amount of a cluster is as Eqs. 5-3, 5-4.

$$D_{i,predict} = \sum_{n=1}^{N} \sum_{s=1}^{M} D_n^{(s)} \quad , \tag{5-4}$$

Here we assume that there are four states (M = 4) in the proposed algorithm. The four states and their respective k_s's are defined as follows:

State 1: sensing off, radio off, $k_s = 0$;
State 2: sensing on, radio off, $k_s = 0$;

State 3: sensing on, radio receiving, $k_s = 0$;
State 4: sensing on, radio transmitting, $k_s = k$.

These states are sufficient and necessary for predicting the amount of data to be transmitted. In inter-cluster communication, only in State 4 can a cluster transmit data to an intermediate cluster head or base station while in the other states it keeps sensing or receiving. When entering state 4, the data packet of length k bytes is sent. Note that the probabilities of transitions among states depend on the past history of sensor nodes. Consequently, the probabilities are updated per round in order to be adaptive to the historical statistics. We update the probability, used by Eqs. 5-3, 5-4, in the beginning phase of each round.

We find that the prediction method is very important. The performance of the proposed algorithm depends on the method of prediction. If the method of prediction does not precisely predict the future amount of data for transmission in each node, energy saving is limited. However a trade-off arises in that the time complexity of the prediction algorithm also affects the lifetime of sensor network. While calculating a new routing path, all nodes must be awake and they must receive topology information from the base station within each period. If we execute complex computations in order to acquire precise predictions, it consumes more energy. Therefore, we adopt a simple and widely used method – the Markov model to predict the data transmissions. There are, of course, other precise prediction algorithms. For example, fuzzy algorithms, generic algorithms, and neural network algorithms are all good candidates for predictions. However, they are not suitable for sensor networks because they waste too much time in learning and obtaining rules.

Before introducing the energy-proportion threshold, we introduce how we define the utilization ratio of sensor nodes in order to observe the conditions of all sensor nodes including cluster heads while working. The equation for the utilization ratio is as follows:

$$U_{ij} = \frac{D_{i,predict}}{D_{ij,total}} = \frac{D_{i,predict}\left(\alpha_t + \alpha_{amp} d_{ij}^2\right)}{E_i}, \quad (5\text{-}5)$$

where $D_{i,predict}$ is the predicted amount of data of the node i obtained in E.q. 5-4, and $D_{ij,total}$ obtained in Eq. 5-1 is the capacity from node i to node j. We define a threshold value to determine whether a node is *energy proportionally balanced* or not. Equation Eq. 5-6 is for calculating the threshold.

$$\omega_{th} = \frac{\sum_{i=1}^{N} U_{i0} E_i}{\sum_{i=1}^{N} E_i}, \quad (5\text{-}6)$$

where E_i is the residual energy of the i-th node, and U_{i0} is the utilization ratio of transmission from the i-th node to its destination such as the base station. By (1)-(5), the threshold value of a round is the proportion of total predicted energy consumption in the total remained energy. That is,

$$\omega_{th} = \frac{\sum_{i=1}^{N} E_{i,predicted}}{\sum_{i=1}^{N} E_i}, \quad (5\text{-}7)$$

where summation of $E_{i,predicted}$ is the total predicted energy consumption for transmission and receiving (if with relaying). In fact, the threshold is the average energy utilization proportion among sensor nodes when accounting for intra-cluster communication. When accounting for inter-cluster communication, it is the average energy utilization proportion among cluster heads. Therefore, we arrive at the following trivial proposition to explain how the predicted data amount and energy consumption relates to distances.

Proposition 1. The total predicted energy of N-cluster sensor network in a round is the

product of the energy-proportional threshold and the total energy remaining. That is,

$$\sum_{i=1}^{N} D_i(\alpha_t + \alpha_{amp} d_{i0}^2) = \omega_{th} \sum_{i=1}^{N} E_i \quad . \tag{5-8}$$

where D_i is the predicted data amount. Note that this proposition also holds when we consider the intra-cluster communication energy consumption in an N-sensor cluster.

An example for determining and applying the threshold in inter-cluster communication is as follows. Suppose there is cluster heads *A*, *B*, *C*, *D* and *E* with a common destination node *O* such as the base station. Suppose applying clustering and routing that the utilization ratios of cluster heads *A, B, C, D, E* are 22.22%, 62.5%, 13.95%, 28.31%, and 25.% respectively, while the residual energy of cluster heads *A, B, C, D, E* are 2 joules, 1.5 joules, 2 joules, 0.5 joules, and 1 joule respectively. We then have 29.3% as the mean utilization of energy by using Eq. 5-6. Therefore, for load balancing, cluster head *B* should neither directly send its aggregation to the base station nor serves a confluent node for forwarding since its utilization ratio is much higher than the threshold. The cluster heads *A, C*, *D*, and *E* who have lower utilization ratios than the threshold 29.3% are candidates for sharing load of cluster head *B*. The proposed EPR algorithm then route transmission paths of the network by assigning *A, C*, *D*, and *E* as intermediate nodes that forward data from node *B*. Hence, the utilization ratios of *A, C*, *D*, and *E* will increase while *B*'s will decrease until they are very close to ω_{th} 29.3%. Since the EPR consider the total energy-proportional balance among clusters, rather than either merely simple balance of energy consumption or communication distance, the network lifetime is extended even in scenarios with quite different parameters. For this example, cluster *B* will not quickly die out of energy and the lifetime of the network is extended no matter how data amounts and residual energy are distributed. For intra-cluster communication, if we replace the role of cluster heads *A*, *B*, *C*, *D*, and *E* with common

sensor nodes in a cluster and to replace the base station as the cluster head, this example also show the application of the EPR in intra-cluster communication.

In comparing the energy-proportional balance to the related works' balance issues, we explain the differences as the following paragraphs. In the clustering process in the BCDCP [SD05], the most two distant sensor nodes in a subgroup are selected as two cluster heads then the other sensor nodes select the least distant cluster head to further partition the subgroup into sub-twos. If the sub-twos have quite different cardinalities, balancing regarding the cardinality is performed. Once enough clusters are formed, the clustering process stops. Though cluster members are suppose to have relative short distance to their cluster head. However, the distributions of residual energy, data amounts, and communication distances in the cluster could have large variances such as in the above example. If the variances sustains for an extended period as in the above example, the lifetime of using EPR in the sensor network will be extended with additional rounds comparing to the original routing. The difference will be more obvious if the scale of the sensor networks is getting larger. For the inter-cluster communications in the BCDCP algorithm [SD05], minimum spanning tree regarding energy cost is proposed for the purpose. There are three ways to approach the energy-proportional balance for BCDCP. First, it is easy to apply the EPR to the tree nodes (or cluster head) with branches (or descendent cluster heads) if there exists other minimum spanning trees. Second, when determining the minimum-spanning tree, the minimum cost is based on the most energy-proportional balance rather than on the least energy cost. Finally, to forward the final fused data from other clusters to the base station in each round, rather select the cluster that will cause the least *total* energy proportion than take turns.

For the clustering process in HEED, the sensor nodes with more residual energy will be elected cluster heads. The grouping of clusters is based the least hybrid energy cost. For

sensor nodes with variable power level, the cost estimation uses so called average minimum reachability power (AMRP) that is the mean power level of the cluster members. There are two ways to approach energy proportional balance for the clustering. First, since adopting AMRP for clustering still suffers from unbalance problem if the proportions of energy to be consumed in the residual energy are quite different, we can replace the AMRP with the least energy proportion as cost estimation. Second, apply the EPR algorithm for intra-cluster communication. For inter-cluster communication, since there is no specific routing proposed in HEED, we also can apply the EPR routing.

For PEGASIS chaining, a node searches the nearest sensor for data forwarding. Once the next sensor contains little residual energy while itself produces large amount of sensed data, it is not suitable to undertake forwarding tasks. Rather than starting at the furthest node, starting at the node with largest utilization ratio will extend the network lifetime. Moreover, the node with large utilization ratio should neither act as the leader nor a confluent node at any hierarchical level of grouping. Thus to approach the energy-proportional balance, rather than take turns we should elect the confluent nodes that have enough residual energy and thus have relative lower energy consumption proportion.

From the above discussions, we know that the energy-proportional balance tackles unbalance problems in cluster cardinalities, nodes' residual energy, communication distances, and data amounts concurrently.

5.2. Operations of the EPR Algorithm

In what follows, we are presenting the operations of inter-cluster communications with the energy-proportional routing algorithm. The same steps can also be applied to the hierarchy of intra-cluster communications by replacing the base station and the cluster head nodes with cluster head and common nodes respectively in a cluster.

Shown in Fig. 5.1 is the EPR algorithm where we assume there are N clusters (N nodes in intr-cluster communication) in initial rounds. To begin with, we compute the average utilization (i.e., Line 3 in Fig. 5.1). Then, we divide the clusters into two groups by comparing the average utilization (i.e., Line 4). The two groups are stored in two respective lists S_L, the group of greater utilization, and S_S, the group of less utilization. We sort the members in the lists according to the utilization ratio in decreasing order. In the algorithm, the *Max()* operation selects the first cluster head L with the maximum utilization from the list S_L (i.e., Line 7). The *Min()* operation selects the cluster head s with the minimum value of utilization to be a relaying hop from the group S_S (i.e., Line 11). In the next stage, as shown in Line 13 of Fig. 5.1, we forward the data of cluster heads L□s of list S_L to cluster head s so that utilization of s is increased until s reaches the threshold (that is, the average utilization). If it reaches the threshold as checked at Line 15, we remove it from the group S_S and add it to the queue called *ReadyQueue* (Line 18). If utilization ratio of L is still greater than ω_{th} and thus still has data for forwarding, we perform the same procedure to select the next forwarding candidate from list *Ss* until L completely allocates its own data to the other cluster heads for forwarding. We can see this from the while loop of the algorithm (line 9 to line 21). It must also satisfy Corollary 2, as checked at Line 23, to ensure that the total dissipated energy of forwarding is less than that by directly transferring. If the cluster head L satisfies the equation, we remove it from the group of high utilization (i.e. relaying method). Otherwise, referring to Line 27, we restore the cluster head to their original status as giving up forwarding and directly send its data to the destination (base station). When either the group of high utilization or the group of low utilization is empty, we finish the algorithm. By summarizing the above time complexity, the algorithm takes O(N) time to complete.

```
Algorithm Energy-proportional Routing
Input: AliveNodes: all alive nodes at each round
Output: R: routing table for every cluster or node
procedure EPR(r: round)
```

```
variables
   i, j: cluster head nodes.
   S_E: the list of members whose utilization equals the average utilization.
   S_L: the list of members whose utilization is greater than the average.
   S_S: the list of members whose utilization is less than the average.
   Av_Util: The average energy-proportion.
Begin

01 if(AliveNodes≠∅){//***
02   predictData(AliveNodes);
03   Av_Util ← Compute_average(AliveNodes);
      //Split AliveNodes into S_L and S_S
      //      according to Av_Util
04   split(S_L, S_S, AliveNodes, Av_Util);
05   //To run main program
06   while((S_L ≠∅) and (S_S ≠∅)){//@@@
07     i ← Max(S_L); //choose L from S_L list
08     //Check if i reaches threshold
09     while(utilization(i) > Av_Util){//###
10     //allocation not complete yet; continue!
11       j ← Min(S_S); //choose j from S_S list
12       //forward k_ij bytes from i via j to BS
13       k_ij ← forward_data(j, i);
14       //Check if j reaches threshold
15       if(utilization(j) == Av_Util){
16         remove(S_S, j); //Remove j from S_S and
17         //insert it to RedyQueue and list S_E
18         insert(ReadyQueue, j);
19         insert(S_E, j);
20       }
21     }//###
22     //check whether constraint Eq.(9) is met
23     if(constraint(ReadyQueue)==TRUE){
24     //update routing table entry R[i,j]=k_ij
25       insert(R, k_ij, i, j);
26     }else{
27       restore(ReadyQueue, j, k_ij);
28     }
29     remove(S_L, i);
30   }//@@@
31 }//***
End
```

Figure 5.1. The EPR algorithm.

In traditional sensor networks such as those in [WA02, RB02, MA02, ST01, PC98], few articles discuss the computation power consumption for obtaining new routing paths since it is usually much less than the transmission power consumption. The proposed algorithm spends additional time to collect energy load information and performs the threshold comparisons for selecting intermediate nodes. These overheads depend on the distances of the nodes. Therefore the bottleneck of the proposed algorithm depends on the occupied area and the scale of the sensor network. However, in most cases such as those in [SK02, SL02, SD05], the base station can identify each node. If the base station can identify each node, during the setup phase the base station can undertakes most of the calculations including data amount

prediction, the EPR threshold calculation, and routing table generation and broadcasting. Therefore, the sensor nodes energy will be used rather in data transmission than in heavy-load computation.

The prediction of data amounts in Line 2 can be done in the base station since the base station can identify the nodes from the headers of the received packets. The execution of the EPR produces the routing table R. The base station performs execution of the EPR and broadcast the routing information to the sensors. The routing is prepared in the so-called setup phase in rounds of sensor networks and the execution wont delay the data communication in the next phase. All the sensed data are transmitted to the base station in each round in the communication phase. The proposed algorithm does not make any assumption on system parameters such as packet length, initial battery energy, and the amounts of data packets in each round. These parameters are assumed constant in traditional sensor networks.

5.3. Mathematical Analysis

In the following proposition, we show that if the forwarding of a cluster head does not save enough energy, we should give it up. Moreover, the proposition provides an important judgment constraint in the algorithm in Fig. 5.1.

Proposition 2. Assume that the total predicted data amount from cluster head i to base station is D_i. We partition D_i into k_1, k_2, …, k_m, which will be respectively transmitted to other clusters' heads 1, 2, …, and m for relaying. Define the effective distance of forwarding as:

$$\frac{1}{D_i}\sum_{j=1}^{m} k_j (d_{ij}^2 + d_{j0}^2) \tag{5-9}$$

In each round iff the total effective distance is at least $(\alpha_t+\alpha_r)/\alpha_{amp}$ smaller than the direct distance d_{i0} to the original destination (such as base station), the first life time factor,

decreasing the total energy dissipation is satisfied.

$$d_{i0}^2 - \frac{1}{D_i}\sum_{j=1}^{m} k_j (d_{ij}^2 + d_{j0}^2) \geq \frac{\alpha_t + \alpha_r}{\alpha_{amp}} \tag{5-10}$$

Equation 5-10 is derived as follows. When cluster head i directly transmits D_i amount of data to the base station, the total energy consumption is

$$E_{i0}(D_i) = D_i \alpha_{amp} d_{i0}^2 + D_i \alpha_r \tag{5-11}$$

When cluster head i transmits D_i amount of data to the base station via the other m intermediate cluster heads, the total energy consumption is

$$E_{i,via}(D_i, m) = \sum_{j=1}^{m} E_{ij} + \sum_{j=1}^{m} E_{j0}$$
$$= (\sum_{j=1}^{m} k_j \alpha_{amp} d_{ij}^2 + k_j \alpha_t) + (\sum_{j=1}^{m} k_j \alpha_{amp} d_{j0}^2 + k_j \alpha_t + k_j \alpha_r),$$
$$D_i = \sum_{j=1}^{m} k_j$$

In order that the adjusting method consumes energy less than or equal to the original cluster-based method, the following inequality must be satisfied:

$$E_{i,via}(D_i, m) \leq E_{i0}(D_i)$$

We reduce it to the following inequality:

$$D_i \alpha_t + D_i \alpha_{amp} d_{i0}^2 \geq 2\alpha_t \sum_{j=1}^{m} k_j + \alpha_{amp} \sum_{j=1}^{m} k_j (d_{ij}^2 + d_{j0}^2) + \alpha_r \sum_{j=1}^{m} k_j$$
$$\Leftrightarrow D_i \alpha_{amp} d_{i0}^2 - \alpha_{amp} \sum_{j=1}^{m} k_j (d_{ij}^2 + d_{j0}^2) \geq D_i \alpha_t + D_i \alpha_r$$
$$\Leftrightarrow d_{i0}^2 - \frac{1}{D_i}\sum_{j=1}^{m} k_j (d_{ij}^2 + d_{j0}^2) \geq \frac{1}{\alpha_{amp}} (\alpha_t + \alpha_r)$$

The proposed routing algorithm conserves energy since it always checks this inequality.

In addition to Proposition 2, we observe that lines 15-19 of the proposed EPR algorithm keep the utilization proportion of the relaying nodes lower than the threshold ω_{th}. Suppose in round ρ, there are $n_i[\rho]$ nodes j's that send their data $D_j[\rho]$ to node i for relaying, the total consumed energy including transmitting and receiving of cluster i is

$$E_{i,predicted} = E_{i,Tx} + E_{i,Rx} =$$
$$\left(D_i[\rho] + \sum_{j=1}^{n_i[\rho]} D_j[\rho] \right)(\alpha_{ti} + \alpha_{amp} d_{i0}^2) + \alpha_{ri} \sum_{j=1}^{n_i[\rho]} D_j[\rho]$$

where $D_i[\rho]$ is the predicted data amount locally at cluster i and the summation $\sum_{j=1}^{n_i[\rho]} D_j[\rho]$ is the total received data amount from node j's for relaying.

As shown in Fig. 5.1, the EPR algorithm ensures that this energy consumption is lower than the predicted average. That is, it is lower than

$$E_{i,predicted} = \omega_{th}[\rho] E_i[\rho] \tag{5-12}$$

In this paper, there are three criteria used for evaluating whether a lifetime is extended or not. The first criterion is "less total energy dissipation." Equation 5-12 has proven this since in the proposed algorithm, the equation 5-12 constrains the routing. In this way, we ensure that every cluster head distributes its data to intermediate hops for relaying only when this relaying saves energy. The second criterion is "a greater number of nodes alive in each round" which is proven in Theorem 1. Initially, in the first few rounds, there could be no dead nodes but we can see the effect of the algorithm preventing dying out of the nodes in later rounds. The last criterion is "more throughput at each round" which is proven in Corollary 1.

Theorem 1. (*Number of alive nodes in each round*) In a clustered sensor network, after enough number of rounds r, the number of nodes alive using the EPR algorithm is greater

than would be the case in the absence of such an algorithm.

Proof: We prove the theorem by showing that the total integrated energy consumption of a cluster head i over each round ρ that results from using or not using the proposed algorithm is different.

For cluster-head i, suppose in the ρ-th round the data amount is $D_i[\rho]$. Then, till round r the data amount is discrete time signal $D_i[1]$, …, $D_i[r]$. The cluster head has two possible playing roles. The first role is a cluster head which distributes its data to other cluster heads j's rather than directly transmit its data to the base station. Another role is a cluster head, which both forwards other clusters' data and transmits its own data to the base station. Since each round is independent of the others, without loss of generality we re-number the rounds with integers 1 to r_0 that cluster head i plays the first role. In the other rounds that i performs as a relaying node, we re-number the rounds with integers r_0+1 to r.

Playing the first role, cluster head i needs to transmit its data to other cluster heads j's and the required energy E_{role1} in a round ρ is $\sum_j E_{ij}^{(Tx)}[\rho]$, and the integrated energy playing the first role from round 1 to r_0 is

$$E_{role1}(i,r) = \sum_{\rho=1}^{r_0}\sum_j E_{ij}^{(Tx)}[\rho] < \sum_{\rho=1}^{r_0}\omega_{th}[\rho]E_i[\rho] \tag{5-13}$$

where $E_{ij}^{(Tx)}[\rho] = D_i[\rho](\alpha_{ti} + \alpha_{amp}d_{ij}^2)$ is the energy consumption of transmissions from i to j's and the transmission energy at each round ρ must keep the utilization lower than ω_{th}, that is, the transmission energy must lower than $\omega_{th}[\rho]E_i[\rho]$.

Playing the second role, cluster head i needs to both forward $D_j[\rho]$ amount of data from others, j=1,…, $n_i[\rho]$ and send it's own $D_i[\rho]$ to the base station. Since the algorithm always keeps the utilization ratio of i smaller than the threshold ω_{th}, consequently the required

energy $E_{i,role2}$ is as follows and by Proposition 1 the inequality holds.

$$E_{role2}(i,r) = \left[\sum_{\rho=r-r_0+1}^{r} \left(E_{i0}^{(Tx)}[\rho] + E_i^{(Rx)}[\rho] \right) \right]$$
$$< \sum_{\rho=r-r_0+1}^{r} \omega_{th}[\rho] E_i[\rho] \qquad (5\text{-}14)$$

where

$$E_{i0}^{(Tx)}[\rho] = \left(D_i[\rho] + \sum_{j=1}^{n_i[\rho]} D_j[\rho] \right)(\alpha_{ti} + \alpha_{amp} d_{i0}^2),$$
$$E_i^{(Rx)}[\rho] = \alpha_{ri} \sum_{k=n_i[\rho]+1}^{N} D_k[\rho],$$

are respectively the energy consumptions of transmission from i to the base station and receiving from all others at i, and $E_i[\rho]$ is the remained energy of cluster head i at beginning of round ρ.

Till round r, let cluster i's integrated energy consumptions of using and not using the proposed algorithm be $E_{after}(i, r)$ and $E_{before}(i, r)$. Thus we obtain:

$$E_{before}(i,r) - E_{after}(i,r)$$
$$= E_{before}(i,r) - \left[E_{role1}(i,r) + E_{role2}(i,r) \right]$$
$$> E_{before}(i,r) - \sum_{\rho=1}^{r} \omega_{th}[\rho] E_i[\rho]$$

By Proposition 1, equations 5-12 and 5-14 we have

$$E_{before}(i,r) = \sum_{\rho=1}^{r} D_i[\rho](\alpha_{ti} + \alpha_{amp} d_{i0}^2) = \sum_{\rho=1}^{r} \omega_{th}[\rho] E_i[\rho]$$

Consequently, the energy saving is assured by

$$E_{before}(i,r) - E_{after}(i,r) > 0$$

Therefore, without using the algorithm cluster *i* will quickly be out of energy. For the sensor network, after enough rounds nodes are dying out because they are out of energy. Q.E.D.

In Theorem 1, though the cluster heads could be selected according to some algorithm, the topology among clusters does not change until there are nodes dying out. Therefore, for any cluster *i*, suppose the opportunity that a node in it to become a cluster head is fair, the total energy consumption in cluster *i* is still large without use of the proposed algorithm. Finally, we prove the satisfaction of the larger throughput criterion.

Corollary 1. (*Throughput*) In a clustered sensor network, after enough number of rounds *r*, the throughput of using the EPR algorithm is greater than if not using the algorithm.

By Theorem 1, the argument is trivial. In the first rounds, since there are no dead nodes, the throughputs of using and not using the proposed algorithm are the same. However, after enough rounds, nodes begin to die out because of their large utilization ratio, and the throughput degrades.

5.4. Experiments and Simulations

We start with experiments showing the effect of the variation of data amounts. Differences in data amounts produce differences in the residual energy of sensor nodes after rounds. The variance of energy utilization ratio becomes obvious. The experiments include simulations with and without such variance and the results show that the variance makes the traditional algorithms fail to extend the network lifetime. We do not need to implement the whole networks adopting algorithms in [SK02, SL02, OS04, OY04, SD05] otherwise we cannot see the exact effect of the variance in intra-cluster communications. After showing the effects of the variance, we simulate the whole network and make comparisons with LEACH-C, where we can see how the EPR improves LEACH-C in the inter-cluster communications.

5.4.1. Effect of the energy-proportion variance

If the variance of the data distribution among sensor nodes is large enough, a node with large energy utilization ratio will quickly die due to out of energy. Especially, the node is in a sub-chain of a long chain or on a tree branch path. The minimum total energy cost approach will fail to extend the lifetime due to the cost does not take the variance of energy proportion into account. We perform the experiment in a cluster, which is produced by some kind of clustering algorithm. To see the effect of the energy proportion variance on intra-cluster communication, we assume that the cluster head has unlimited energy and hence according to algorithms in [SK02, SL02, OS04, OY04, SD05], the cluster head won't be displaced. When we replace the member nodes and the cluster head with clusters and the base station respectively, the experiments also show that inter-cluster communications also suffer the unbalance problem caused by variance of energy proportion. Figure 2 shows results of the experiment without the variance and the parameters are fixed as in [SD05]. The packet length is fixed at 500 bytes and the number of frames is fixed at 40. Figure 3 shows the results with variance of frame amounts uniformly distributed from 10 to 70. Both experiments use 10 sensor nodes uniformly distributed within a 25m×25m square, which implies that there would be 160 sensors when the total network is deployed in a 100m×100m square. The results are the average from 50 different cluster topologies. The other settings are chosen to be the same as in [13].

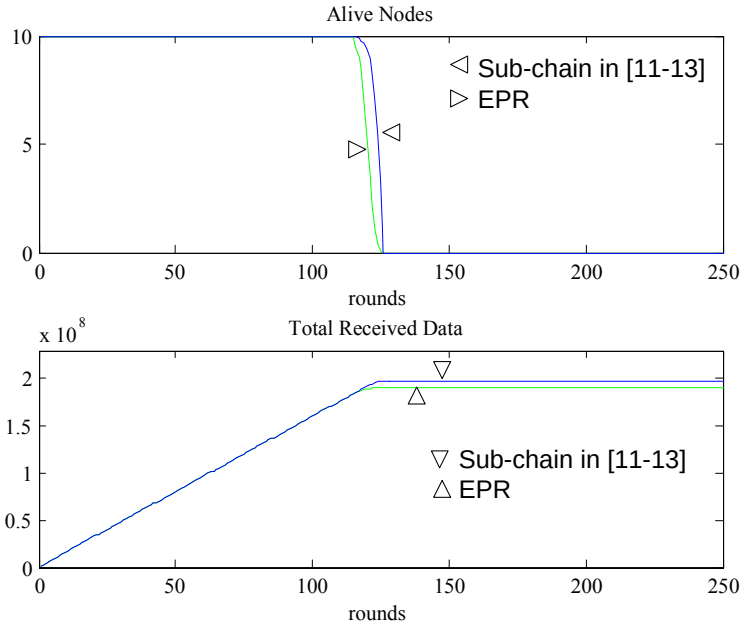

Figure 5.2. Simulation results without data amount variance.

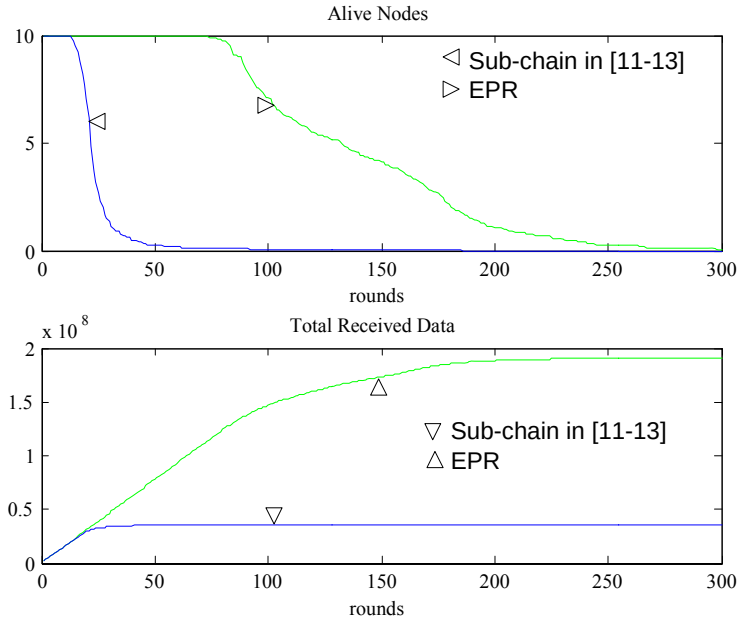

(a)

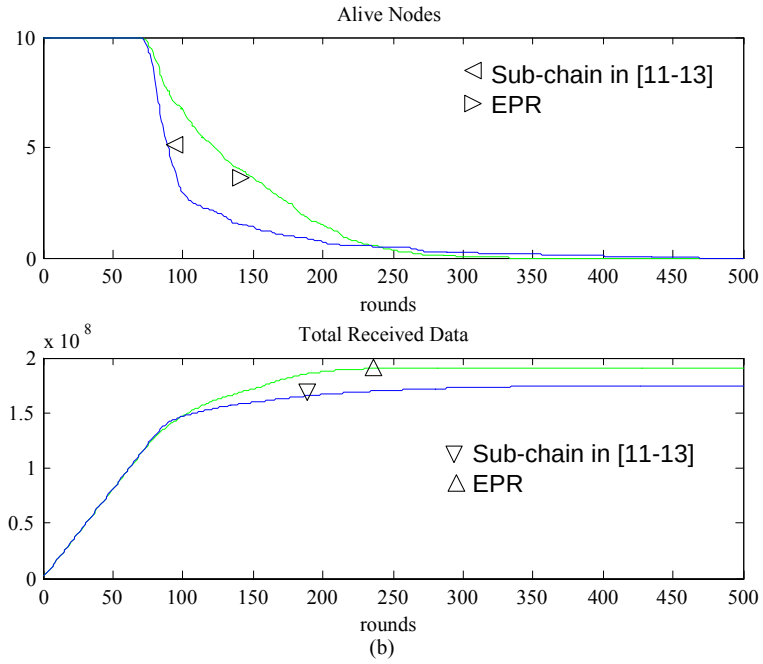

Figure 5.3. Simulation results with data amount variance: (a) the nodes along the chain need to forward data from others and (b) every node transmits a variable amount of data at a time only when it receives a token.

The experiments shown in Fig. 5.2 and Fig. 5.3 are also applicable to the inter-cluster communications if the sub-chain is in a branch of a minimum-spanning tree in [SD05]. In Fig. 5.3(a) we find that the shortest chain or the minimum-spanning tree approach no longer estimates minimum cost if the data amounts vary and the nodes quickly die due to not energy-proportional balanced. In Fig. 5.3(b), the base station uses token to instruct sensor nodes to transmit data in different time slots, the network works better. However it still suffers the unbalanced problem if without EPR routing.

5.4.2. The simulation of the whole sensor network

We compare the performance of the proposed algorithm with that of the LEACH-C [WA02] – the most typical example of clustered sensor networks. To show the improvements in inter-cluster communication, the clustering used in EPR is the same as LEACH-C while the routing among clusters is different. Note that, the proposed algorithm is a generic solution to those who do not take the *energy -proportional balance* into account. We use the network

simulator NS2 to help us in the experiments. We put 100 nodes into an area of 100×100 square meters. We put the base station at the position (0, 0). The initial energy of each node is 2 joules. We set the time period of a round as 10 seconds and set the data rate of each node as 1 Mbps. In Fig. 5.4 (a), (b) and (c), we perform the experiment that large quantities of sensing data are generated in specific areas and while little sensing data is generated in others. The cluster heads transmit data to the base station directly in the LEACH-C algorithm and the sensors nodes die out quickly. In contrast, our algorithm handles this situation well and lifetime is extended about 30%.

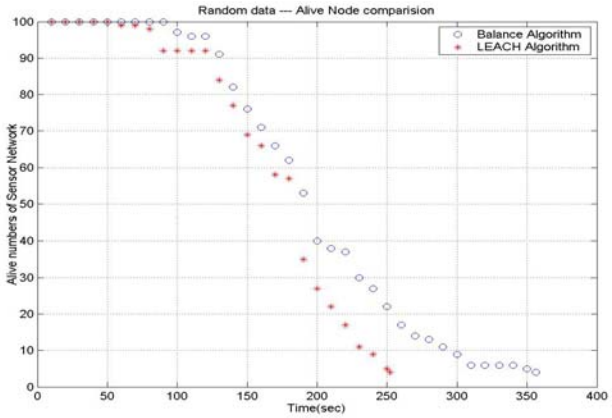

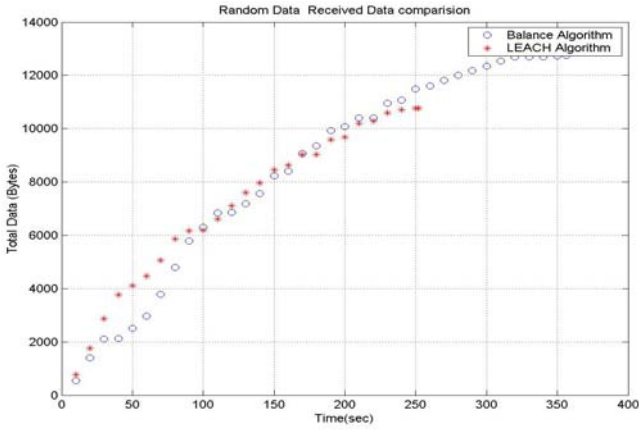

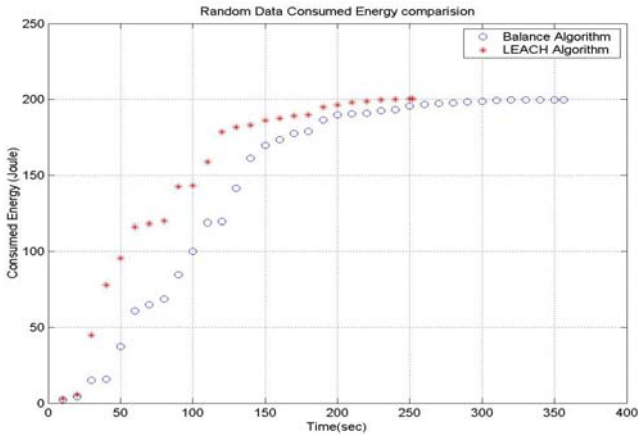

Figure 5.4. The experiment generating random lengths of sensing data: (a) Alive nodes in sensor network, (b) total received data by the base station, and (c) total dissipated energy of sensor network.

Chapter 6

Conclusions

In this dissertation, we have outlined our proposal for a new distributed regional location management scheme called MORR to reduce the total signaling cost of a mobile node on the mobile Internet. MORR adjusts the optimal radius value of a regional domain and attempts to locate the optimal GFA in order to reduce potential signaling costs. We developed a novel network model and formulated the moving behavior of mobile nodes within this model. Then the historical moving patterns of a mobile node were recorded and stored in the defined data structure of a mobile node to manage the mobile node registration in order to determine the optimal GFA. In our analysis, the results demonstrate that the total signaling cost is greatly reduced by the proposed MORR. The superior performance of our scheme is noticeable both when the mobile node is in GM mode and in RM mode.

Then, we have derived the relationship between transmission power and interference range by mathematical models. We also have proposed some mathematical models to present the relationships between transmission power and interference area. By these models, we estimated the probability of transmission success and calculate the expected value of energy consumption. In addition, we have proposed APCM mechanism to evaluate the optimal transmission power level to minimize the whole of energy consumption and satisfy the quality of service in Ad hoc wireless networks. As shown in the simulations, up to 32 percent energy can be conserved, packet loss rate will be reduced 6 percent and enhances the utilization of energy to 22 percent.

This dissertation has provided a probing radius adjusting mechanism “PRAM” to control the trade-off between energy efficiency, network scalability and sensing rate. By this mechanism, the desirable probing range can be presented to minimize the energy consumption based on the premise that the required sensing rate and scalability of WSNs can be satisfied. Simulation results show PRAM can adjust exactly the value of probing range to satisfy the required sensing rate and extend substantially the life time of sensor networks.

A new routing algorithm also has been proposed in this dissertation, and for the algorithm we have performed mathematical analyses and experiments. Both theoretical and experimental results confirm that the proposed EPR algorithm is useful to improve conventional clustered sensor networks in common cases where amounts of data are not evenly distributed. We have proved that high local utilizations do not mean high global utilization. We reduced local utilizations of clusters to achieve promotion of global utilization of energy. Three criteria are used in the mathematical analyses and experiments to evaluate lifetime extension: less total energy consumption, more alive nodes in rounds, and more throughputs. We proposed the algorithm in order to ensure that the three criteria are met. By the mathematical analysis, we believed that the idea of energy-proportional balance is generically useful in clustered sensor networks.

Bibliography

[AA94] Alexander Marlevi, Anders Danne and George Liu, "Method and Apparatus for Detecting and Predicting of Mobile Terminals," *Ericsson Patent*, No. 027500-969, Oct. 1994.

[AA97] D.O. Awduche and E.Agu, "Mobile Extensions to RSVP," *Proceedings of ICCCN' 97*, Las Vegas, NV, Sep. 1997, pp. 132-136.

[AA98] A. Valko, A. Campbell, and J. Gomez, "Cellular IP," *Internet Draft*, draft-valko-cellularip-00.txt, November 1998.

[AC96] B.A. Akyol and D.C. Cox, "Routing for Handoff in a Wireless ATM Network," *IEEE Personal Communications Magazine*, Oct, 1996, pp. 26-33.

[AD01] A. Manjeshwar and D. P. Agarwal, "TEEN: a routing protocol for enhanced efficiency in wireless sensor networks", *1st International Workshop Parallel Distributed Computing Issues Wireless Networks Mobile Computing*, April 2001.

[AD02] A. Cerpa, D. Estrin, "ASCENT: Adaptive Self-Configuring sEnsor Networks Topologies" *INFOCOM 2002*, vol. 3, June 2002, pp. 23-27.

[AGG96] D.O. Awduche, A. Ganz, and A. Gaylord, "An optimal search strategy for mobile stations in wireless networks," *Proceedings of ICUPC'96*, Cambridge, MA, Sep. 1996, pp. 946-950.

[AL97] A. Kamerman and L. Monteban, "WaveLAN-II: A High-Performance Wireless LAN for the Unilicensed Band," *Bell Labs Technical Journal*, vol. 2, no. 3, summer 1997, pp. 118-133.

[AM02] A. Manjeshwar and D. P. Agarwal, "APTEEN: a hybrid protocol for efficient routing and comprehensive information retrieval in wireless sensor networks", *2st International Workshop Parallel Distributed Computing Issues Wireless Networks*

Mobile Computing, April 2002.

[AR99] A. Chandrakasan, R. Amirtharajah, S. H. Cho, J. Goodman, G. Konduri, J. Kulik, W. Rabiner, and A Wang, "Design Considerations for Distributed Microsensor Systems," *IEEE Custom Integrated Circuits Conference (CICC '99)*, May 1999. pp. 279-286.

[AT99] A. B. McDonald, and T. F. Zanti, "A mobility-based framework for adaptive clustering in wireless ad-hoc networks", *IEEE Jounal on Selected Areas Communication*, vol. 17, Aug. 1999, pp. 1466-1487.

[BA93] B.R. Badrinath, A. Arup and T.Imielinski, "Structuring Distributed Algorithms for Mobile Hosts," *Technical Report*, Department of Computer Science, Rutgers University, June, 1993.

[BCS98] S. Basagni, I. Chlamtac, V.R. Syrotiuk, and B. A. Woodward, "A Distance Routing Effect Algorithm for Mobility (DREAM)," *Proceedings of ACM/IEEE MOBICOM'98*, Dallas, TX, Oct. 1998, pp. 76-84.

[BK02] B. Chen, K. Jamieson, H. Balakrishnan, and R. Morris, "Span: An Energy-Efficient Coordination Algorithm for Topology Maintenance in Ad Hoc Wireless Networks," *ACM Wireless Networks Journal*, vol. 8, no. 5, Sept. 2002, pp. 481-494.

[BM98] B. Erol, M. Gallant, G. Cote, and F. Kossentini, "The H.263 Video Coding Standard: Complexity and Performance," *Proceedings of Data Compression Conference (DCC '98)*, April 1998. pp. 259-268.

[Bult96] Bult, K., et al., "Low Power Systems for Wireless Micro-sensors," *International Symposium on Low Power Electronics and Design '96*, Aug. 1996. pp. 17-21.

[CE95] M. S. Corson and A. Ephremides, "A distributed routing algorithm for mobile wireless networks," *ACM-Baltzer Journal of Wireless Networks*, Jan. 1995, vol. 1, pp. 61-81.

[CE02] C.E. Perkins, "IP Mobility Support for IPv4," *Request for Comments* (RFC) 3344, Internet Engineering Task Force, August 2002.

[CH99] C. Yung, H. Fu, C. Tsui, R. Cheng, and D. George, "Unequal Error Protection for Wireless Transmission of MPEG Audio," *Proceedings of IEEE International Symposium on Circuits and Systems (ISCAS '99)*, June 1999, vol. 6, pp. 342-345.

[CJ95] C. L. Fullmer and J.J. Garcia-Luna-Aceves, "Floor Acquisition Multiple Access (FAMA) Packet-Radio Networks," *ACM Computer Communication Review*, vol. 25, no. 4, Oct. 1995.

[CK01] C. E. Jones, K. M. Sivalingam, P. Agrawal, and J.-C. Chen, "A Survey of Energy Efficient Network Protocols for Wireless Networks," *ACM Journal on Wireless Networks*, vol. 7, no. 4, July 2001, pp. 343–358.

[CP99] Charles Perkins, "Ad hoc on demand distance vector (aodv) routing," *Internet-Draft, draft-ietf-manet-aodv-04.txt*, Oct. 1999,Work in progrss.

[CS98] S. Choi and K.G. Shin, "Predictive and Adaptive Bandwidth Reservation for Hand-Offs in QoS-Sensitive Cellular Networks," *Proceedings of ACM SIGCOMM' 98*, Vancouver, BC, Oct. 1998, pp. 155-166.

[CS99] C. S. Raghavendra and S. Singh, "PAMAS — power aware multi-access protocol with signaling for ad hoc networks", 1999. *ACM Computer Communication Revision Available at: http://citeseer.nj.nec.com/460902.html*.

[CT01] C. -K. Toh, "Maximum battery life routing to support ubiquitous mobile computing in wireless ad hoc networks", *IEEE Communication Management*, vol. 39, June 2001, pp. 138–147.

[DL91] D. LeGall, "MPEG: A Video Compression Standard for Multimedia Applications," *Communications of the ACM*, April 1991, pp. 46-58.

[DS91] D. Duchamp, S. K. Feiner and G. Q. Maguire, Jr, "Software Technology for Wireless

Mobile Computing," *IEEE Network Magazine*, Nov. 1991.

[EA02] E. Gustafsson, A. Jonsson and C. Perkins, "Mobile IPv4 Regional Registration," *Internet Draft*, draft-ietf-mobileip-reg-tunnel-06.txt, March 2002.

[EB94] Charles E. Perkins and Pravin Bhagwat, "Highly dynamic destination-sequenced distance-vector routing (DSDV) for mobile computers," *Proceedings of the ACM SIGCOMM*, Aug. 1994, pp. 234–244.

[EN02] E.-S. Jung and N. H. Vaidya, "An Energy Efficient MAC Protocol for Wireless LANs," *Proc. IEEE INFOCOM '02*, vol. 3, New York, NY, USA, June 2002, pp. 1756-1764.

[ES02] E.-S. Jung and N. H. Vaidya, "A Power Control MAC Protocol for Ad Hoc Networks," in *Proc. ACM MOBICOM*, Atlanta, Georgia, Sept. 2002, pp. 36-47.

[ETSI96] ETSI, "High Performance Radio Local Area Network (HIPERLAN)," Draft Standard ETS 300 652, March 1996.

[FJ03] F. Ye, G. Zhong, J. Cheng, Songwu Lu, and Lixia Zhang "PEAS: a robust energy conserving protocol for long-lived sensor networks" *23rd IEEE International Conference on Distributed Computing Systems (ICDCS 2003)*, May 2003, pp. 19-22.

[FL75] F. Tobagi and L. Kleinrock, "Packet Switching in Radio Channels: Part II - The Hidden Terminal Problem in Carrier Sensing Multiple Access and Busy Tone Solution," *Communications, IEEE Transactions* on [legacy, pre - 1988], vol. 23, issue 12, Dec. 1975, pp. 1417-1433.

[FR00] F. Aurenhammer and R. Klein "Voronoi Diagrams." *Ch. 5 in Handbook of Computational Geometry* (Ed. J.-R. Sack and J. Urrutia). Amsterdam, Netherlands: North-Holland, 2000, pp. 201-290.

[GE94] George Liu, "Exploitation of Location-dependent Caching and Prefetching Techniques for Supporting Mobile Computing and Communications," *The 6th*

International Conference on Wireless Communications, Calgary, Canada, July 11-13, 1994.

[GG95] George Liu and Gerald Q. Maguire Jr, "Efficient Mobility Management Support for Wireless Data Services," *Proceedings of 45th IEEE Vehicular Technology Conference (VTC'95)*, Chicago, Illinois, July 26-28, 1995.

[GL95] G. Liu and G. Maguire, "A Predictive Mobility Management Algorithm for Wireless Mobile Computing and Communications," *Proc. of the IEEE International Conference on Universal Personal Communications (ICUP'95)*, Tokyo, Japan, Nov. 6-9, 1995.

[GM94] George Liu, "Mobility Agent Techniques for Supporting Wireless Data Services," *Ericsson Tech*. Report T/B 94:542.

[GM98] G. Asada, M. Dong, T. S. Lin, F. Newberg, G. Pottie, W. J. Kaiser, and H. O. Marcy, "Wireless integrated network sensors: Low power systems on a chip", *Proceedings of the 1998 European Solid State Circuits Conference*, The Hague, The Netherlands, September 1998.

[GM99] J. J. Garcia-Luna-Aceves and E.L. Madruga, "A Multicast Routing Protocol for Ad-Hoc Networks," *Proceeding of IEEE INFOCOM'99*, New York, NY, Mar. 1999, pp. 784 – 792.

[GM03] G. Gupta, and M. Younis, **"**Load-Balanced Clustering of Wireless Sensor Networks,**"** *Proceedings of the Intl. Conf. on Communications*, Anchorage, AK, May 2003, vol.3, pp.1848-1852.

[GPL98] M. Gerla, G. Pei, S. J. Lee, and C. C. Chiang, "On-Demand Multicast Routing Protocol (ODMRP) for Ad Hoc Networks," *Internet Draft, draft-ietf-manet-odmrp-00.txt*, Nov. 1998, Work in progress.

[GY95] G. Y. Liu and G. Q. Maguire, "A Predictive Mobility Management Scheme for

Supporting Wireless Mobile Computing," Technical Report, Royal Institute of Technology, TRITA-IT R95-04, Feb. 1995.

[Has97] Z. J. Hass, "A new routing protocol for the reconfigurable wireless networks," *Proceedings of the IEEE ICUPC '97*, vol. 2.2, Oct. 1997, pp. 562-566.

[HI03] H. O. Tan, and I. Korpeoglu, "Power Efficient Data Gatherting and Aggregation in Wireless Sensor Networks," *Proceeding of Int. Conf. Management of Data*, vol. 32, no. 4, Dec. 2003, pp. 66-71.

[HJ98] H. Woesner, J.-P. Ebert, M. Schlager, and A. Wolisz, "Power-Saving Mechanisms in Emerging Standards for Wireless LANs: The MAC Level Perspective," *IEEE Personal Communications*, vol. 5, no. 3, June 1998, pp. 40-48.

[HS93] H. Xie, S. Tabbane, and D. J. Goodman, "Dynamic Location Area Management and Performance Analysis," Proc. *43rd IEEE Vehicular Technology Conf.*, 1993, pp. 536-539.

[HT46] H. T. Friis, "A Note on a Simple Transmission Formula," *Proc. Of the IRE*, vol. 41, May 1946, pp.254-256.

[HT99] H. Y. Tzeng and T. Przygienda, "On First Address-Lookup Algorithms," *IEEE J. Selected Areas in Comm.* (JSAC), vol. 17, no.6, June 1999, pp. 1067-1082.

[IW02] I. F. Akyildiz, W. Su, et. al. **"**A Survey on Sensor Networks**"**, *IEEE Communications Magazine*, Aug. 2002, pp.102-114.

[JA99] J. Chan and A. Seneviratne, "A Practical User Mobility Prediction Algorithm for Supporting Adaptive QoS in Wireless Networks," *IEEE International Conference on Networks*, pp. 104, Brisbane, Australia, Sept. 28 – Oct. 1, 1999.

[JA01] J. Gomez, A. T. Campbell, M. Naghshineh, and C. Bisdikian, "Conserving Transmission Power in Wireless Ad Hoc Networks," in *Proc. IEEE ICNP*, Riverside, California, Nov. 2001, pp. 24-34.

[JA03] J. Gomez, A. T. Campbell, M. Naghshineh, and C. Bisdikian, "PARO: Supporting Dynamic Power Controlled Routing in Wireless Ad Hoc Networks," *ACM Journal on Wireless Networks*, vol. 9, no. 5, Sept. 2003, pp. 443-460.

[JB99] Josh Broch, David B. Johnson, and David A. Maltz, "The dynamic source routing protocol for mobile ad hoc networks," *INTERNET-DRAFT, draft-ietf-manet-dsr-03.txt,*, Oct. 1999. Work in progress.

[JB00] J.-P. Ebert, B. Stremmel, E. Wiederhold, and A. Wolisz, "An Energy-efficient Power Control Approach for WLANs," *Journal of Communications and Networks* (*JCN*), vol. 2, no. 3, Sept. 2000, pp. 197-206.

[JB04] J. Deng, B. Liang, and P. K. Varshney, "Tuning the Carrier Sensing Range of IEEE 802.11 MAC," in *Proc. IEEE GLOBECOM*, vol. 5, Dallas, Texas, Nov. 2004, pp. 2987-2991.

[JD98] J. Broch, D.A. Maltz, D.B. Johnson, Y. Hu, and J. Jetcheva, "A performance comparison of multi-hop wireless ad hoc network routing protocols," *Proceedings of the ACM/IEEE International Conference on Mobile Computing and Networking*, Oct. 1998.

[JG93] J. Ioannidis and G. Q. Maguire Jr, "The Design and Implementation of a Mobile Internetworking Architecture," *USENIX Winter 1993 Technical Conference*, USENIX Association, Jan. 1993, pp. 491-502.

[JG00] J. E. Wieselthier, G. D. Nguyen, and A. Ephremides, "On the Construction of Energy-Efficient Broadcast and Multicast Trees in Wireless Networks," in *Proc. IEEE INFOCOM*, vol. 2, Tel-Aviv, Israel, March 2000, pp. 585-594.

[JG01] J. E. Wieselthier, G. D. Nguyen, and A. Ephremides, "Resource-Limited Energy-Efficient Wireless Multicast of Session Traffic," in *Proc. IEEE HICSS*, Island of Maui, Jan. 2001, pp. 3-6.

[JI95] J.S.M. Ho and I.F. Akyildiz, "Mobile User Location Update and Paging under Delay Constraint," *ACM-Baltzer J. Wireless Networks* (WINET), vol. 1, no. 4, Dec. 1995, pp. 413-415.

[JJ00] Gregory J. Pottie and William J. Kaiser, "Wireless integrated network sensors (WINS): Principles and practice," To appear, CACM, 2000.

[JL99] J. L. Sobrinho and A. S. Krishnakumar, "Quality-of-Service in Ad Hoc Carrier Sense Multiple Access Wireless Networks," *IEEE JSEC*, vol. 17, issue 8, Aug. 1999, pp. 1353-1368.

[JL00] J. Agre and L. Clare. "An Integrated Architecture for Cooperative Sensing Networks," *Computer*, May 2000, pp. 106-108.

[JM96] D. B. Johnson and D.A. Maltz, "Dynamic Source Routing in Ad Hoc Wireless Networks," *Mobile Computing* , edited by T. Imielinski and H. Korth, Chapter 5, Kluwer Publishing Company, Oct. 1996, pp. 153-181.

[JP99] J.-P. Ebert and A. Wolisz, "Combined Tuning of RF Power and Medium Access Control for WLANs," in *Proc. IEEE MoMuC*, San Diego, CA, Nov. 1999, pp. 74-82.

[JV01] J. P. Monks, V. Bharghavan, and W.-M. W. Hwu, "A Power Controlled Multiple Access Protocol for Wireless Packet Networks," in *Proc. IEEE INFOCOM*, vol. 1, Anchorage, Alaska, April 2001, pp. 219-228.

[JW02] J. Kulik, W. B. Heinzelman, and H. Balakrishnan, "Negotiation-based protocols for disseminating information in wireless sensor networks", *Wireless Networks*, vol. 8, March-May 2002, pp. 169-185.

[KM97] K. M. Sivalingam, M. B. Srivastava and P. Agrawal, "Low Power Link and Access Protocols for Wireless Multimedia Networks," in *Proc. IEEE VTC*, vol. 3, Phoenix, AZ, May 1997, pp. 1331-1335.

[KM02] K. Xu, M. Gerla, and S. Bae, "How Effective is the IEEE 802.11 RTS/CTS Handshake in Ad Hoc Networks," in *Proc. IEEE GLOBECOM*, vol. 1, Taipei, R.O.C, Nov. 2002, pp. 72-76.

[KV98] Y. B. Ko and N. H. Vaidya, "Location-Aided Routing (LAR) in Mobile Ad Hoc Networks," *Proceedings of ACM/IEEE MOBICOM '98*, Dallas, TX, Oct. 1998, pp. 66-75.

[LAN95] D. A. Levine, I. F. Akyildiz, and M. Naghshineh, "The Shadow Cluster Concept for Resource Estimation and Call Admission in Wireless ATM Networks", Proceedings of ACM MOBICOM '95, Nov. 1995, pp. 142-150.

[MA02] M. Bhardwaj and A. P. Chandrakasan, **"**Bounding the lifetime of sensor networks via optimal role assignments**"**, in *Proceedings of IEEE INFOCOM*, Jun. 23-27, New York, 2002, pp. 1587-1596.

[MH97] Mark Stemm and Randy H. Katz, "Measuring and reducing energy consumption of network interfaces in hand-held devices," *IEICE Transactions on Communications*, Aug. 1997, E80-B(8) PP. 1125–1131.

[MH00] M. B. Pursley, H. B. Russell, and J. S. Wysocarski, "Energy-Efficient Transmission and Routing Protocols for Wireless Multiple-hop Networks and Spread-Spectrum Radios," in *Proc. IEEE/AFCEA EUROCOMM*, Munich, May 2000, pp. 1-5.

[MH01] M. Kubisch and H. Karl, "Analyzing Energy Consumption in Wireless Networks by Relaying," Telecommunication Networks Group, Tech. Univ. Berlin, Berlin, Germany, Tech. Rep. TKN-01-006, June 2001.

[MG96] S. Murthy and J. J. Garcia-Luna-Aceves, "An Efficient Routing Protocol for Wireless Networks," *ACM/Baltzer Mobile Networks and Applications*, vol. 1, no, 2, Oct. 1996, pp. 183-197.

[MK97] M. Dong, K. Yung, and W. Kaiser, "Low Power Signal Processing Architectures for

Network Microsensors," *Proceedings International Symposium on Low Power Electronics and Design*, Aug.1997, pp. 173-177.

[MW00] M. Budagavi, W. Heinzelman, J. Webb, and R. Talluri, "Wireless MPEG-4 Video Communication on DSP Chips," *IEEE Signal Processing Magazine*, Jan. 2000, pp. 36-53.

[Niko03] Niko, "[MIP4] home registrations and regional registrations question," *http://www.ietf.org/mail-archive/working-groups/mip4/current/msg00190.html*, September 2003.

[OS04] O. Younis and S. Fahmy, "Distributed Clustering in Ad-hoc Sensor Networks: A Hybrid, Energy-Efficient Approach," *IEEE Transactions on Mobile Computing*, vol 3, no.4, Oct-Dec, 2004, pp. 366-379.

[OY04] O. Younis and S. Fahmy, "Distributed Clustering in Ad-Hoc Sensor Networks: A Hybrid, Energy-Efficient Approach," *Proceedings of IEEE INFOCOM*, Mar. 2004.

[PB94] C. E. Perkins and P. Bhagwat, "Highly Dynamic Destination-Sequenced Distance-Vector Routing (DSDV) for Mobile Computers," *Proceedings of ACM SIGCOMM '94*, Aug. 1994, pp. 234-244.

[PC97] V. D. Park and M. S. Corson, "A Highly Adaptive Distributed Routing Algorithm for Mobile Wireless Networks," *Proceedings of IEEE INFROCOM '97*. Oct. 1997.

[PC98] P. K. Agarwal and C. M. Procopiuc, **"**Exact and approximation algorithms for clustering,**"** P*roceedings of the Ninth Annual ACM-SIAM Symposium on Discrete Algorithms*, San Francisco, California, 25-27 Jan. 1998, pp. 658-667.

[PK90] P. Karn, "MACA - A New Channel Access Method for Packet Radio," in *Proc. ARRL Computer Networking Conference*, Sept.1990, pp. 134-140.

[PR99] C. E. Perkins and E. M. Royer, "Ad Hoc On-Demand Distance Vector Routing," *Proceedings of IEEE WMCSA '99*, New Orleans, LA. Feb. 1999.

[PT99] P. Johansson, T. Larsson, N. Hedman, B. Mielczarek, and M. Degermark, "Scenario-based performance analysis of routing protocols for mobile ad-hoc networks," *Proceedings of the ACM/IEEE International Conference on Mobile Computing and Networking*, Aug. 1999, pp. 195 – 206.

[RA93] R. Hager, A Klemets, G. Q. Maguire Jr, M.T. Smith, and Frank Reichert, "MINT - A Mobile Internet Router," *Proceedings of the IEEE Vehicular Technology Conference '93*, Institute of Electrical and Electronics Engineers, May 18-20, 1993.

[RB02] R. A. F. Mini, B. Nath, and A. A. F. Loureiro. **"**A probabilistic approach to predict the energy consumption in wireless sensor networks,**"** *IV Workshop de Comunicaçẽo sem Fio e Computaçẽo Móvel, Sẽo Paulo*, Brazil, Oct. 23-25 2002.

[RE00] Samir R. Das, Charles E. Perkins, and Elizabeth M. Royer, "Performance comparison of two on-demand routing protocols for ad hoc networks," *Proceedings of the IEEE Infocom(2000)*, March 2000.

[RL01] R. Wattenhofer, L. Li, P. Bahl, and Y.-M. Wang, "Distributed Topology Control for Power Efficient Operation in Multihop Wireless Ad Hoc Networks," in *Proc. IEEE INFOCOM*, vol. 3, Anchorage, Alaska, April 2001, pp. 1388-1397.

[RR00] R. Ramanathan and R. Rosales-Hain, "Topology Control of Multihop Wireless Networks Using Transmit Power Adjustment," in *Proc. IEEE INFOCOM*, vol. 2, Tel-Aviv, Israel, March 2000, pp. 404-413.

[RT98] R. Talluri, "Error-Resilient Video Coding in the ISO MPEG-4 Standard," *IEEE Communications Magazine*, June, 1998, pp. 2-10.

[RT01] R. Ramjee, T. La Porta, S. Thuel, K. Varadhan, and L. Salgarelli, "IP micro-mobility support using HAWAII," *Internet Draft,* draft-ietf-mobileip-hawaii-01.txt, July 2001.

[RS94] R. Nevoux and S. Tabbane, "Mobility Features for Personal and Terminal UMTS Communications," *The 6th International Conference on Wireless Communications*,

Calgary, Canada, July 11-13, 1994.

[SA00] S. Das, A. Misra, and P. Agrawal, "TeleMIP: Telecommunications-Enhanced Mobile IP Architecture for Fast Intradomain Mobility," *IEEE Personal Communications,* vol. 7, no. 4, Aug. 2000, pp. 50-58.

[SC98] S. Singh and C.S. Raghavendra, "Pamas - power aware multi-access protocol with signalling for ad hoc networks," *ACM Compute Communication Review*, July 1998.

[SC02] Lindsey, S.; Raghavendra, C.S.; "PEGASIS: Power-efficient gathering in sensor information systems," *Aerospace Conference Proceedings, 2002*. IEEE , Vol. 3 , vol.3. March 9-16, 2002, pp. 1125-1130.

[SD05] S. D. Muruganathan, D. C. F. MA, R. I. Bhasin, and A. O. Fapojuwo, "A Centralized Energy-Efficient Routing Protocol for Wireless Sensor Networks," *IEEE Radio Communications*, vol. 43, no 3, March 2005, pp. S8–S13.

[SJ94] S. Hoffpauir and J. Parker, "Impact of Terminal Mobility on the Intelligent Network," *The 6th International Conference on Wireless Communications*, Calgary, Canada, July 11-13, 1994.

[SK02] S. Lindsey, C. Raghavendra, and K. M. Sivalingam, "Data Gathering Algorithms in Sensor Networks Using Energy Metrics," *IEEE Transactions on Parallel and Distributed Systems*, vol. 13, no. 9, SEPT. 2002, pp. 924-935.

[SL02] S. Lindsey, C. Raghavendra, "PEGASIS: Power-Efficient Gathering in Sensor Information Systems," *IEEE Aerospace Conference Proceedings*, vol. 3, 2002, pp. 1125-1130.

[SM98] S. Singh, M. Woo, and C.S. Raghavendra, "Power-aware routing in mobile ad hoc networks," *Proceedings of the ACM/IEEE International Conference on Mobile Computing and Networking*, Oct. 1998, pp. 181–190.

[SN02] S. Tilak, N. B. Abu-Ghazaleh, and W. B. Heinzelman, "A taxonomy of wireless

micro-sensor network models", *ACM Mobile Computing Communication Revision*, vol. 6(2), 2002, pp. 28-36.

[SR01] S. Agarwal, R.H. Katz, S.V. Krishnamurthy, and S.K. Dao, "Distributed Power Control in Ad-hoc Wireless Networks," in *Proc. IEEE PIMRC*, vol. 2, San Diego, CA, Sept. 2001, pp. 59-66.

[SS98] S. Singh and C. S. Raghavendra, "PAMAS – Power Aware Multi-Access Protocol with Signalling for Ad Hoc Networks," *ACM Computer Communication Review*, vol. 28, no. 3, July 1998, pp. 5-26.

[ST01] S. Goel and T. Imielinski. **"**Prediction based monitoring in sensor networks - Taking lessons from MPEG," *Computer Communication Review*, no. 5, 2001, pp.82-95.

[ST02] S. Xu and T. Saadawi, "Revealing the Problems with 802.11 Medium Access Protocol in Multi-Hop Wireless Ad Hoc Networks," *Computer Networks: The International Journal of Computer and Telecommunications Networking*, vol. 38, issue 4, March 2002, pp. 531-548.

[Toh97] C. K. Toh, "Associativity-Based Routing for Ad-Hoc Mobile Networks," *Wireless Personal Communications Journal*, Special Issue on Mobile Networking and Computing Systems, Kluwer Academic Publishers, vol. 4, no, 2, Mar. 1997, pp. 103-139.

[TS02] T. S. Rappaport, "Wireless Communications: Principles and Practice," 2nd ed., New Jersey, Prentice-Hall, 2002.

[VA94] V. Bharghavan, A. Demers, S. Shenker, and L. Zhang, "MACAW: A Media Access Protocol for Wireless LAN's," in *Proc. ACM SIGCOMM*, vol. 24, no. 4, London, UK, Aug. 1994, pp. 212-225.

[VS99] V. Park and S. Corson, "Temporally-ordered routing algorithm (tora) version 1 functional specification," *INTERNETDRAFT, draft-ietf-manet-tora-spec-02.txt,*, Oct.

1999. Work in progress.

[VT99] V. Rodoplu and T. H. Meng, "Minimum Energy Mobile Wireless Networks," *IEEE JSEC*, vol. 17, no. 8, Aug. 1999, pp. 1333-1344.

[TSR] T. S. Rappaport, "Wireless Communications, Principles and Practice," *Prentice Hall PTR*, ISBN 0-13-093003-2.

[WA00] Heinzelman, W.R., Chandrakasan, A., Balakrishnan, H.; "Energy-efficient communication protocol for wireless microsensor networks", *the 33rd Hawaii International Conference on System Sciences*, Vol. 8, Jan. 4-7, 2000, pp. 80-89.

[WA02] W. B. Heinzelman, A. P. Chandrakasan, and H. Balakrishnan, "An Application-specific protocol architecture for wireless microsensor networks", *IEEE Transaction on Wireless Communication*, vol. 1, Oct. 2002, pp. 660-670.

[WC00] W. Heinzelman, A. Chandrakasan, and H. Balakrishnan, "Energy-Efficient Communication Protocol for Wireless Microsensor Networks," *Proceedings of Hawaii Conference on System Sciences*, Jan. 2000, pp.1-10.

[WH00] W. Heinzelman, "Application-Specific Protocol Architectures for Wireless Networks," *Ph.D. thesis, Massachusetts Inst. of Technology*, June 2000.

[WM99] W. Heinzelman, M. Budagavi, and R. Talluri,"Unequal Error Protection of MPEG-4 Compressed Video," *Proceedings of the International Conference on Image Processing (ICIP '99)*, Oct. 1999.

[WS00] W. Heinzelman, A. Sinha, A. Wang, and A. Chandrakasan, "Energy-Scalable Algorithms and Protocols for Wireless Microsensor Networks," *Proceedings of International Conference on Acoustics, Speech, and Signal Processing (ICASSP)*, June 2000, pp.3722-3725.

[WY03] W. Ma and Y. Fang, "Improved Distributed Regional Location Management Scheme for Mobile IP," *The 14th IEEE 2003 International Symposium on Personal, Indoor*

and Mobile Radio Communication Proceedings, Sep. 7-10, 2003, pp. 2505-2509.

[XI02] X. Jiang and I. F. Akyildiz, "A Novel Distributed Dynamic Location Management Scheme for Minimizing Signaling Costs in Mobile IP," *IEEE Transactions on Mobile Computing*, vol. 1, no. 3, July 2002, pp. 163-175.

[YC02] Y.-C. Tseng, C.-S. Hsu, and T.-Y. Hsieh, "Power-saving protocols for IEEE 802.11-based multi-hop ad hoc networks," in *Proc. IEEE INFOCOM*, vol. 1, New York, June 2002, pp. 200-209.

[YJ00] Ya Xu, John Heidemann, and Deborah Estrin, "Adaptive energy-conserving routing for multi-hop ad hoc networks," Submitted for publication, May 2000.

[YM95] Y. Takishima, M. Wada, and H. Murakami, "Reversible Variable Length Codes," *IEEE Transactions on Communications*, Feb. 1995, vol. 43(2), pp.158-162.

[ZB02] Z. J. Haas, J. Deng, B. Liang, P. Papadimitratos, and S. Sajama, "Wireless ad hoc networks," in the *Wiley Encyclopedia of Telecommunications*, John G. Proakis, Ed., New York: John Wiley & Sons, 2002.

[ZED93] L. Zhang, S. Deering, D. Estrin, S. Shenker and D. Zappala, "RSVP: A New Resource Reservation Protocol," *IEEE Network*, Sep. 1993.

[ZJ02] Z. J. Haas and J. Deng, "Dual Busy Tone Multiple Access (DBTMA) - A Multiple Access Control Scheme for Ad Hoc Networks," *IEEE Trans. Communications*, vol. 50, no. 6, June 2002, pp. 975-985.

Vita (簡歷)

姓名: 李冠榮 (Kuan-Rong Lee)

地址: 嘉義市公明路 4-1 號

電話: 05-2788306

Email: leekr@cad.csie.ncku.edu.tw

生日: 59 年 2 月 20 日

籍貫: 河南省滎陽縣

學歷: 國立成功大學資訊工程研究所 博士 (88/9 – 95/6)

國立成功大學資訊工程研究所 碩士 (82/9 – 84/6)

私立逢甲大學資訊工程學系 學士 (78/9 – 82/6)

省立嘉義高中 (74/9 – 77/6)

蘭潭國中 (71/9 – 74/6)

民族國小 (65/9 – 71/6)

經歷: 私立高苑科技大學電子系兼任講師

私立崑山科技大學電子系兼任講師

西門子行動通訊研發處工程師

Publication List (個人著作)

Journal Papers

1. **Kuan-Rong Lee**, Mong-Fong Horng and Yau-Hwang Kuo, “MORR: A Novel Regional Location Scheme Based on User Movement Behavior in Mobile IP,” IEICE Transaction on Information and Systems. Vol. E89-D. no. 2. Feb. 2006.
2. Chao-Lieh Chen, **Kuan-Rong Lee**, Jung-Hsing Wang, and Yau-Hwang Kuo, “Energy-proportional Routing for Lifetime Extension of Clustering-Based Wireless Sensor Networks,” Journal of Pervasive Computing and Communications (JPCC). (Accepted, 2006)
3. Po-Cheng Huang, **Kuan-Rong Lee**, Chien-Chung Su, Yaw-Huang Kuo, Mong-Fong Horng, Chien-Chou Lin, and Yu-Chang Chen, “Control Component Development of information Appliances on Networks," Journal of Information Science and Engineering (JISE). (Accepted, 2006)
4. S-C Lee, **Kuan-Rong Lee** and Yau-Hwang Kuo, “An Object Simulator for OO System”, Journal of Computers. Vol. 8, no. 2, 1996
5. **Kuan-Rong Lee**, Chao-Lieh Chen, and Yau-Hwang Kuo , “A Novel Probing Range Adjusting Mechanism in Energy-Efficient and Sensibility-Aware Probing Environment WSNs”, submitted to IEICE Transaction on Communication.

Conference Papers

1. **Kuan-Rong Lee**, Yau-Hwang Kuo, "A Novel Energy-Efficient Technology in Wireless Sensor Networks" International Symposium on Wireless Local and Personal Area Networks (part of IWCMC 2006), Vancouver, Canada. July 3-6, 2006
2. **Kuan-Rong Lee**, Yau-Hwang Kuo, "A Distributed Dynamic Regional Location Management Scheme Based on User Mobility Behavior to Minimizing Signaling Costs in Mobile IP", The 1st IFIP and IEEE International Conference on Wireless and Optical Communications Networks, WOCN 2004, June 7-9, 2004. Oman.
3. **Kuan-Rong Lee**, Yau-Hwang Kuo, "BORRM: A Behavior Oriented Regional Registration Mechanism on Mobile IP", IEEE International Conference on Computing, Communication and Control Technologies, Auguest 14-17, 2004. Texas, USA
4. Chao-Lieh Chen, Jung-Hsing Wang, **Kuan-Rong Lee** and Yau-Hwang Kuo, "An Energy-Proportional Routing Algorithm for Lifetime Extension of Clustering-based Wireless Seosor Networks", Proc. of the Workshop on Wireless, Ad Hoc, and Sensor Networks 2005. Taiwan
5. Mong-Fong Horng, Wei-Tsong Lee, **Kuan-Rong Lee** and Yau-Hwang Kuo, "An Adaptive Approach to Weighted Fire Queue with Qos Enhanced on IP Network", Proceeding of IEEE Tencon 2001, August 2001, Singapore, pp. 181-186, vol.1.
6. Yung-Cheng Chu. **Kuan-Rong Lee**, Jiang-Shong Ker, Yau-Hwang Kuo, "A Regional Registration Scheme Based on Personal Mobility Behavior for Mobile IP", 2004 Symposium on Digital Life and Internet Technologies, Jun. 2004
7. S-C Lee, **Kuan-Rong Lee**, Y. H. Kuo, "An Object Simulator for Object-Oriented Software Systems", Proc. of 6th Object-Oriented Technology Workshop, Taiwan, September 1995

系（別）: 成功大學資訊工程學系

題目: 在可移動式無線通訊網路中，行動管理、繞送與能源控制機制之研究

作者姓名: 李冠榮

學年度: 94 學年度